DT4GS

The Digital Twin for Green Shipping

D1.2: *DT4GS Modelling Framework for Ship operational Performance Optimisation Including Ship Efficiency Innovations*

Document Information

Grant Agreement No	101056799	**Acronym**	DT4GS
Full Title	Open collaboration and open Digital Twin infrastructure for Green Smart Shipping		
Call	HORIZON-CL5-2021-D5-01: Clean and competitive solutions for all transport modes		
Topic	HORIZON-CL5-2021-D5-01-13	**Type of action**	RIA
Coordinator	INLECOM GROUP		
Project URL	https://dt4gs.eu/		
Start Date	01/06/2022	**Duration**	36 months
Deliverable	D1.2	**Work Package**	WP 1
Document Type	R	**Dissemination Level**	PU
Lead beneficiary	FINC		
Responsible author	Nicolo Faggioni (FINC)		
Contractual due date	31/05/2023	**Actual submission date**	31/05/2023

Disclaimer and acknowledgements

Funded by the European Union

This project has received funding from the Horizon Europe framework programme under Grant Agreement No 101056799

Disclaimer

The content of this document reflects only the author's view. Neither the European Commission nor REA are responsible for any use that may be made of the information it contains.

While the information contained in the document is believed to be accurate, the authors or any other participant in the DT4GS consortium make no warranty of any kind with regard to this material including, but not limited to the implied warranties of merchantability and fitness for a particular purpose.

Neither the DT4GS Consortium nor any of its members, their officers, employees, or agents shall be responsible or liable in negligence or otherwise howsoever in respect of any inaccuracy or omission herein.

Without derogating from the generality of the foregoing neither the DT4GS Consortium nor any of its members, their officers, employees, or agents shall be liable for any direct or indirect or consequential loss or damage caused by or arising from any information advice or inaccuracy or omission herein.

Copyright message

Document information

Contributors	
Contributor Name	**Organisation (Acronym)**
Alessandro Caviglia	FINC
Nicolò Faggioni	FINC
Angeliki Deligianni	GLM
Dimitris Kaklis	DAN

Document history				
Version	**Date**	**%**	**Changes**	**Author**
0.1	22/08/2022	1%	ToC draft	A. Caviglia (FINC)
0.2	20/12/2022	30%	Preparation (unofficial)	N.Faggioni (FINC)
0.3	25/01/2023	50%	Introduction	N.Faggioni (FINC)
0.4	31/02/2023	80%	Partner chapters revision	N.Faggioni (FINC)
0.5	28/04/2023	100%	complete draft	N.Faggioni (FINC)

Quality Control (includes peer & quality control reviewing)			
Date	**Version**	**Name (Organisation)**	**Role & Scope**
01/05/2023	0.6	Antonis Antonopoulos (KNT) Arianna Fedi (RINAC)	Peer review
11/05/2023	0.7	Stathis Zavvos (VLTN)	Quality Review

Executive summary

This deliverable focuses on the assessment and reduction of fuel consumption in the maritime industry to promote sustainability and efficiency in the shipping sector. The work carried out explores a comprehensive approach that incorporates various methodologies and models across different aspects of ship operations.

The interactions between measures such as fuel consumption, rpm, draught, system degradation, and environmental conditions are complex, with often non-linear relationships. To address this complexity, engineering analysis and simulation models incorporating physics, empirical measurements, and data-driven elements are utilized.

By adopting effective assessment methods based on white and grey box approaches, ship operators can optimize fuel consumption through voyage optimization strategies. Route planning, weather routing, and the implementation of just-in-time models allow operators to take advantage of favourable conditions and minimize idle time. These practices reduce operational costs and minimize environmental impact.

The integration of hull and robotics inspection models plays a vital role in maintaining optimal ship performance. Regular inspections using advanced technologies enable the timely detection and resolution of potential issues, reducing fuel consumption caused by drag and mechanical inefficiencies. This proactive approach leads to substantial energy savings.

Condition-based monitoring, facilitated by sensor technologies and data analysis, provides valuable insights into a ship's performance. By promptly identifying and addressing equipment malfunctions or performance deviations, fuel-consuming inefficiencies can be mitigated, optimizing operational efficiency, and reducing overall fuel consumption.

The use of energy simulators offers ship operators a powerful tool to evaluate and analyse different energy management strategies. Through simulations, operators can identify the most fuel-efficient operating parameters, optimizing energy consumption and reducing the environmental impact of ship operations. Informed decision-making facilitates the implementation of sustainable practices and fuel consumption reduction.

Furthermore, the life cycle assessment model enables a comprehensive evaluation of a ship's environmental footprint throughout its entire life cycle. Considering all stages, from raw material extraction to end-of-life disposal, stakeholders can identify opportunities for improvement and implement sustainable practices that minimize fuel consumption and environmental impact.

In conclusion, this deliverable provides insights into the complexity of interactions affecting fuel consumption in the maritime industry. By incorporating various methodologies and models, it demonstrates the potential for fuel efficiency optimization through voyage assessment, proactive maintenance, energy management strategies, and comprehensive life cycle evaluation. Implementing these approaches will contribute to a more sustainable and efficient shipping sector.

Contents

List of figures

List of tables

Glossary of terms and acronyms used

Table 1 Glossary of acronyms and terms.

Acronym / Term	Description
ACU	Absorption Chiller Unit
DT	Digital Twin
EG	Exhaust Gas
EGE	Exhaust Gas Economizer
FOC	Fuel Oil Consumption
GIGO	Garbage In Garbage Out
HF	High frequency
HT	High Temperature
HVAC	Heating, Ventilation and Air Conditioning
LCA	Lifecycle Analysis
LL	Living labs
LT	Low Temperature
OFB	Oil Fired Boiler
OKC	Organic Kalina Cycle
ORC	Organic Rankine Cycle
SFOC	Specific Fuel Oil Consumption
WHR	Waste heat recovery
WP	Work package

1 Introduction

As digitalisation in the shipping industry has been maturing over the recent years, DT adoption will be dependent on establishing trusted and convincing DT application exemplars and ensuring that ship operators and other industry stakeholders can set up their own DTs based on their own business models, building their own confidential knowledge at reasonable cost. This requirement is at the heart of the DT4GS approach as illustrated in the figure below.

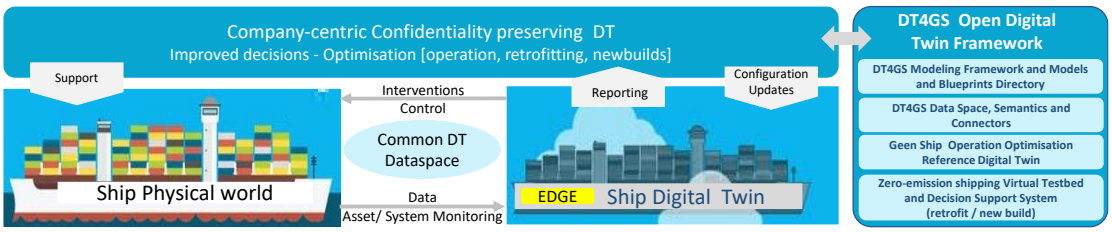

Figure 1 DT4GS approach

DT4GS will provide a virtual representation of ships and physical transport entities with a bi-directional communication links from sensing to actuation/control and data driven simulation and AI based decision support to people who will implement necessary actions. In DT4GS extra emphasis will be given to:

- DT applications onboard the ship utilising advanced IoT and edge computing infrastructure.
- Using labelled data for AI/ML training and to provide the ground truth for accurate predictions (supervised learning), and where there is need to learn from experience to provide the reward function (reinforcement learning).
- Creating a common point of reference in the digital world for shipping vessels, which different stakeholders can access and utilise and adapt in line with their own internal business needs.

To reach its goals, DT4GS is divided into 6 WPs, each with different goals, tasks, and deliverables. This document is linked to WP1, ''DT4GS modelling framework for ship operational performance optimisation including ship efficiency innovations'' which focuses on the methods to assess and reduce fuel consumption in ships, aiming to enhance fuel efficiency and sustainability in the maritime industry. The following discussion provide an overview of the key areas explored in this deliverable:

i. **Fuel oil consumption assessment:** This is based on analysis of high frequency data collected by the Living Labs. The data are fed to developed mathematical models that simulate the behaviour of ships in terms of required power. In particular, we aim to find the relations between ship's consumption data and the trim condition, hull status (fouling presence) and weather condition.
ii. **Navigation Management:** Navigation management concerns the areas of navigation, steering and routing, speed, displacement, trim, and the dynamic effects of ship motions, steering and weather. The following navigation optimisation models are covered: Route planning for optimal fuel consumption; Weather routing to avoid adverse conditions; Implementation of a just-in-time model to minimize idle time.
iii. **Hull Inspection Model using robotics:** Development of new hull inspection workflows utilising automation and robotics. This includes: Regular inspections of the ship's hull and underwater components; Application of robotics to advanced inspection techniques.
iv. **Condition-Based Monitoring:** Diagnostics models used for identifying wear and damage early on and avoid unplanned repairs. This includes: Continuous monitoring of critical components and systems; Utilization of sensors and data analytics techniques.

v. **Energy Simulator:** Simulating and analyzing different energy management strategies. Energy simulation models allow: Identifying the most fuel-efficient operating parameters; Informed decision-making and effective energy management. By knowing the devices installed onboard, in the engine room and by modelling the requested and delivered thermal fluxes of the individual devices, it is possible to evaluate the ship energy balance. The energy balance is an essential point to evaluate potential WHR solutions.
vi. **Life Cycle Assessment Model:** Evaluating the environmental impact throughout a ship's life cycle. The developed LCA models allow: Considering raw material extraction, construction, operation, and disposal; Identifying areas for improvement and implementing sustainable practices. By integrating these methodologies and models, ship operators and stakeholders can optimize fuel consumption, reduce environmental impact, and improve overall operational efficiency. This comprehensive approach aims to drive the maritime industry towards a more sustainable and economically viable future.

Considering the above, the objective of this deliverable is therefore the development of ship performance models that will be later incorporated in the developed digital twins by the living labs and provide comprehensive ship performance analysis before and after the installation of decarbonisation technologies.

1.1 Mapping DT4GS Outputs

The purpose of this section is to map DT4GS Grant Agreement commitments, both within the formal Deliverable and Task description, against the current document.

Table 2 Adherence to DT4GS Grant Agreement deliverable and work description.

DT4GS GA Component Title	DT4GS GA Component Outline	Respective Document Chapter(s)	Justification
DELIVERABLE			
D[1.2] [modelling framework for ship operational performance optimisation including ship efficiency innovations]	Modelling Framework Specification, Navigation Management and hull models, Integrated Machinery Performance management and remote-control models, Integrated ship energy production models, Robust Fuel consumption models, and Life Cycle assessment Models.	2, 3, 4, 7, 9	Modelling Framework Specification is covered in section 2.1. Hull models and Robust Fuel consumption models are covered in section 3. Navigation Management is covered in section 4. Integrated Machinery Performance management and remote control covered in Section 7. Life Cycle assessment Models are covered in Section 9.

TASK			
ST[1.2.1] [DT4GS modelling framework specification]	Utilise the EUROYARDS "CODE KILO" general architecture and business model of a Maritime Data Space for collaborative data / services sharing, and "ENGIMMONIA" for energy efficiency, focusing on Energy Management Systems that monitor onboard energy producers/users. The framework will include a metamodel to link ship subsystem models comprising of IoT sensors and decarbonisation technologies to impact KPIs, operational performance as well as sensing & control aspects, standardisation. The Framework will also comprise of semantic capabilities and gateways to external model libraries.	2, 7, 8	The EUROYARDS "CODE KILO" general architecture was used to inform the designs in Section 2. The section also discusses semantic capabilities and gateways to external model libraries. "ENGIMMONIA" for energy efficiency, focusing on Energy Management Systems was used to inform Section 7 (Integrated Machinery Performance Management and Remote Control). Metamodel to link ship subsystem models comprising of IoT sensors and decarbonisation technologies to impact KPIs, operational performance as well as sensing & control aspects, standardisation are addressed in Section 8.
ST[1.2.2] [Navigation Management]	This includes real-time predictive wind and solar energy spectra analysis linking with trim, route and speed optimisation algorithms, and environmental agents' model.	4, 5	Areas covered include route planning for optimal fuel consumption, and weather routing to avoid adverse conditions;

ST[1.2.3] [Hull and Robotic Inspection Models]	providing a holistic visualization of the vessel's structure and condition with the use of swarms of robots, mainly UAVs, parallel cable robots and underwater ROVs	6	Areas covered include regular inspections of the ship's hull and underwater components, and the integration of robotics and advanced inspection techniques;
ST[1.2.4] [Integrated Machinery performance management and remote control]	Create models for all on-board equipment and machinery, networks, and control systems to represent virtual engine rooms, connected to data on cost and the vessel's operating parameters to enable remote control of the vessel. Recommend ship system settings to save energy with equipment running at peak efficiency, based on predictions.	7	Areas covered include the continuous monitoring of critical components and systems, and the utilization of sensors and data analysis techniques.
ST[1.2.5] Integrated ship energy production, distribution, recovery & management]	Derive optimisation models to configure the WHR plant, and simulations to determine the effects of implementing additional Energy Recovery Units or new HVAC solutions, and to estimate the associated saving.	8	Areas covered include simulating and analysing different energy management strategies, identifying the most fuel-efficient operating parameters, informed decision-making and effective energy management.
ST[1.2.6] [Robust fuel consumption and CO2e emission Models]	CO_2 emissions will be monitored in relation to several industry-standard operations parameters. The Monitoring, Reporting, Verification (MRV) method.	3	Areas covered include LL data analysis by means of HF data available, and developing a mathematical model to emulate the behaviour of ships in terms of required power. In particular, the research study concerning to find the relations between

			ship's data and the trim condition, hull status (fouling presence) and weather condition; Thanks to the correct evaluation of power requested onboard for propulsion, energy generation and hotel load is possible to estimate the CO_2 emission with high precision.
ST[1.2.7] [Life Cycle Assessment]	model aligned with EPLCA to assess potential investments as well as operational, monetary and maintenance decisions. Holistic optimisation of the ship's design and operation lifecycle.	9	Areas covered include evaluating the environmental impact throughout a ship's life cycle, considering raw material extraction, construction, operation, and disposal, and identifying areas for improvement and implementing sustainable practices.
ST[1.2.8] Integrated modelling framework for ship performance improvement using JIT arrivals	The potential for energy savings across different ships and segments of the global fleet will be estimated by modelling the use of the SEAS JIT platform, simulating vessel energy performance in a year's voyages.	5	The implementation of a just-in-time model to minimize idle time is described in Section 5.

1.2 Deliverable Overview and Report Structure

In this section, a description of the Deliverable's Structure is provided outlining the respective sections and their content.

SECTION 2: High-level presentation concerning the holistic framework. Presenting the main models that have been in detail discussed in the next Sections.

SECTION 3: Fuel Oil consumption. To estimate the ship's consumption, models have been created with which it is possible to estimate the power required by the ship as the speed and boundary conditions change. Having obtained the required power, it is possible to estimate consumption through the characteristics of the engine installed on board. Finally, from the knowledge of consumption it was possible to estimate the greenhouse gases emitted.

SECTION 4 & 5: Navigation Management models. Knowing the relationship between ship speed and consumption, it is possible to determine the best route for consumption efficiency purposes using route planning models. In particular, the shortest route model that can generate way points is shown. The generated way points are then processed by a weather routing model that, based on the weather information, is able to modify the route appropriately. Finally, the route speed is validated through a just-in-time model that takes care of slowing down the ship if necessary to save fuel.

SECTION 6: Mathematical models are derived to evaluate the increase in resistance due to the presence of fouling. In addition, models for predicting fouling on board are provided. Finally, models for internal and external hull inspection are discussed.

SECTION 7: A system capable of performing condition-based monitoring is shown. Thus, it is a fully data-driven system that can determine whether a device is in a proper operating regime or not based on the data recorded on board.

SECTION 8: the structure of an energy simulator capable of evaluating the heat fluxes exchanged between various on-board devices was shown. This system has importance in the evaluation of alternative solutions for waste heat flux recovery (waste heat recovery system).

SECTION 9: Life Cycle Assessment. The aim is to provide a systematic analysis that helps to identify, quantify, interpret, and evaluate the environmental impact of different mitigation strategies through the vessel's life.

SECTION 10: Conclusions.

2 DT4GS Framework Specification

2.1 Framework Structure

Over the past 30 years in industry, continuous technological advancement has led to a constant improvement in the availability and quality of available and collectible data. In the maritime industry, one of the main goals is to build efficient products, then design hull shapes with lower hydrodynamic resistance without compromising stability and, above all, to study a propulsion system that allows compliance with environmental regulations. [1]

Technological development made it possible not only to optimize the initial design alone, designed to make the entire product more innovative, but above all to continue to monitor the ship during its operational life. This constant monitoring of the parameters considered vital makes it possible to precisely know the state of the ship by making available a large amount of data that allows its study and optimization under different points.

For example, the behaviour of a propulsion system is characterized by the interaction of several components that influence each other, which can be monitored and examined.

Continuous monitoring of the state of the system and the different diagnostics obtained allows the system's reliability to be improved and maintenance and operation expenses to be reduced. At the expense of a slightly higher cost compared to a ship without sensors installed on board, the economic advantage is higher as it requires a small number of sensors installed on board. [2].

In general, the steps for proper data analysis are:

- Preparation
- Modelling
- Evaluation

Data preparation includes a pre-processing step that can produce an ideal model. Modelling and data preparation go hand in hand, and, for this reason, it is an iterative process. The results of previous applications lead to a better approximation that will be closer and closer to the actual model. At the end of the process is the evaluation, which allows the estimation of the assumptions made during the analysis and provides the right considerations of the study performed. [3]

For this purpose, a Model-Based Design approach was used: a mathematical approach used for the development of complex control systems; it is a procedure based on:

- use of mathematical models
- design with simulation
- implementation with code generation

Using Model-Based Design, simulation models can be created so that users can easily evaluate whether the entire system will perform as expected. Simulation models require technical parameters that are essential for proper emulation of reality, which, in some cases, may be unknown or uncertain, resulting in drawbacks. Generating a simulation model and determining these parameters involves considerable effort in terms of time and resources.

Indeed, Model-based design is a method for designing systems in which a mathematical model is used to represent the behaviour of the system and to guide the design process. Moreover, can be a powerful tool

for understanding complex systems, but it also has its limitations due to the complexity of emulated phenomena.

Overall, model-based design is a widely used and powerful method for designing systems, and research in this area is active and rapidly evolving [4].

Model-based design is a method for designing systems in which a mathematical model is used to represent the behaviour of the system and to guide the design process.

The aim of the DT4GS project is to create a multipurpose platform able to perform an easy CO_2 evaluation by means a tailored digital twin.

Indeed, a digital twin can be created using a model-based design approach. The mathematical model used in the design process can be used to create a digital twin that can be used to simulate the behaviour of the physical system, analyse its performance, and optimize its design.

This virtual replica is connected to the physical asset through sensors, which provide data about the asset's performance. By comparing the data from the sensors with the predictions of the digital twin, it is possible to detect deviations from the expected behaviour and take corrective action to improve the performance of the physical asset.

Eventually, model-based design and digital twin are related concepts useful to design, simulate, analyse and optimize the performance of physical systems.

2.2 Challenges and Threats

Model-based design is a powerful method for designing systems, but it also has its limitations. One of the main constraints of model-based design is the availability and quality of data.

Data availability refers to the amount of data that is available to be used in the model. For a model to be accurate, it needs to be based on a sufficient amount of data. However, in many cases, the data required for a model may not be available or may be difficult to obtain. This can be a significant constraint in the model-based design process.

Data quality refers to the accuracy and relevance of the data that is used in the model. Inaccurate data or data that is not relevant to the system being modeled can lead to inaccurate predictions or unreliable models. Ensuring the quality of the data is a critical step in the model-based design process.

Another constraint of model-based design is the complexity of the system being modeled. Complex systems can be difficult to model accurately.

Moreover, it is important to validate the model's predictions in the real world. A model that accurately represents the system in the laboratory or simulation may not perform as well in the real world, due to unmodeled factors such as noise, disturbances, or variations in the system.

Eventually, the availability and quality of data, the complexity of the system, and the validation of the model's predictions are some of the constraints of model-based design. To overcome these constraints, it is important to have a robust data collection and management strategy, to use appropriate modeling techniques, and to validate the model's predictions through experiments or field tests.

In this context, the most critical stage is the initial creation of mathematical models based on the LL data. Indeed, a thorough analysis of the data is essential to check their quality. In fact, strict analysis is necessary to avoid the creation of unreliable models, avoiding garbage in garbage out (GIGO).

This can be achieved by using multiple sources of data, cleaning and preprocessing the data, and using appropriate data validation methods. Additionally, it is essential to have a good understanding of the system's underlying physics and dynamics to build accurate mathematical models.

Eventually, to avoid GIGO in model-based design, it is crucial to ensure that the input data used to build and validate the model is of high quality, accurate and relevant.

Of course, the problem of data goodness and availability is also present in the model feeding phase used to carry out the assessment during the ship's operation. But this is less impactful, as it is desirable that the first stage, during model creation, allows a hierarchy and pre-processing procedure to be established, which should continue to be adopted after model creation, so that model input is standardized.

For these reasons, a rigorous analysis was conducted on the availability and quality of available data. In particular, the analysis relied on high-frequency data to best characterize the models.

In this regard, several clarifications were requested from the LL partners to obtain a unified dataset among all partners and usable in the framework to be composed. Further updates on this topic will be presented in the future when a common guideline is established among all LL partners.

2.3 Employed Technologies

Several approaches to LL data management were considered. The first step was to decide which data to use to analyze the operational use of ships. In general, the available shipboard data has two different natures. The first type of data is contained in the "noon reports," in which various information on navigation and ship operation is transcribed once a day. In this case, the data are extremely rarefied, and much information is lost. The advantage of this approach is that all ships have this type of data available, so a model based on this type of data could easily be used by a large number of ship owners.

The other type of data provided by LL partners is high-frequency data; the sampling interval can vary from seconds to minutes, depending on the settings set on board. In this case, the amount of data allows accurate monitoring of the ship's status during operational performance. The downside of this approach is that because it is a large amount of data, it is not easy to manage; moreover, not all shipowners have systems for high-frequency acquisition of data from the field. This last statement is of little relevance as more and more ships are equipped with similar systems, given their marginal cost relative to that of construction.

For such reasons, HF data were chosen to analyze and evaluate the relationship between the required power and sailing operating conditions (such as trim, water conditions, and hull fouling condition).

Indeed, the idea is that by using HF data, a useful model can be created to increase or decrease the required power with respect to standard still-water conditions.

After choosing the dataset to refer to, the next step was to choose which approach to use to derive the mathematical models that would express the variation in power requirements as a function of sailing conditions.

In general, there are three approaches: White box, gray box, and black box approaches [5, 6, 7, 8]. Generally, they are used to describe the level of visibility or knowledge an individual or system has of a computer system or network. In particular, the definitions of these terms are the following:

- White Box: In this approach, the tester has complete knowledge of the internal workings of the software, including the code, algorithms, and logic.
  The focus is on testing individual functions, statements, and branches to ensure that they work as

intended. This approach requires a strong understanding of software development and programming concepts.

- Grey Box: In this approach, the tester has limited knowledge of the internal workings of the software, but not as much as in white box testing. The focus is on testing the functional and non-functional requirements of the software and how they are implemented. This approach requires some understanding of software development concepts and the ability to read and understand code.
- Black Box: In this approach, the tester has no knowledge of the internal workings of the software and only interacts with the inputs and outputs. The focus is on testing the software from the user's perspective and ensuring that it meets the specified requirements. This approach does not require any knowledge of software development or programming concepts, but rather a thorough understanding of the software's functional and non-functional requirements.

In summary, the main difference between the three approaches is the level of knowledge and involvement the tester has with the internal workings of the software being tested. White box testing focuses on the individual components, gray box testing focuses on the functional and non-functional requirements, and black box testing focuses on the user's perspective.

Initially, it was planned to follow the white box approach, specifically a dynamic approach to emulate all components of the propulsion chain (engine, axle, and propeller) [9, 10, 11]. Unfortunately given the large amount of data required to faithfully emulate each individual component, this approach was discarded due to the lack of necessary data and especially with the view that this model could be a generalized solution to the problem. Indeed, a hybrid approach was pursued in which white box and gray box models were employed.

In detail, the white box model is described by a workflow of different mathematical models selected from the literature and which will be shown in detail in the following paragraphs. As for the gray box model, it was decided to feed it with high-frequency data provided by ships.

As of today, in fact, it has been decided that these approaches represent the most suitable solution about the evaluation on the dependence between brake power demand and navigation conditions. Under this condition, key behaviors will be emulated through relationships known a priori and described by mathematical laws, these will be compared with the gray box model in which the ship's HF information is processed by organizing it due to a priori knowledge of the phenomenon being analyzed.

It should also be added that it is possible to develop a black box model fed by a training set of the ship's main data that allows the physical relationships of the model to be ignored, mapping only the actions and reactions of the system. In this case, the risk is that generality is lost, and a model developed on one ship is not usable for another. For these reasons this approach is only taken and included in the subsequent workflow but not described in detail because, at an early stage of the project, it is not used.

2.4 System Overview

The global maritime industry plays a critical role in facilitating international trade and transportation. However, the significant fuel consumption associated with ships poses both environmental and economic challenges. Addressing this issue is of paramount importance, and as such, there has been a growing emphasis on developing methods to assess and reduce fuel consumption in ships.

This deliverable explores a holistic approach to enhance fuel efficiency in maritime operations, encompassing various methodologies and models. The key focus areas include navigation management, hull and robotics inspection, condition-based monitoring, energy simulation, and life cycle assessment. By integrating these strategies, ship operators and stakeholders can optimize fuel consumption, minimize environmental impact, and improve overall operational efficiency.

The first area of focus is to develop a holistic approach that encompasses white box and grey box approaches and goes as far as assessing proper consumption and related CO_2 emissions. Accordingly, after assessing ship's consumption, route optimization can be carried out.

In detail, voyage optimization, which involves precise route planning, weather routing, and the implementation of a just-in-time model. Efficient route planning enables ships to navigate through favourable currents and weather conditions, minimizing resistance and fuel consumption. Weather routing systems utilize real-time weather data and sophisticated algorithms to provide optimal routes that avoid adverse weather conditions. The just-in-time model ensures that vessels arrive at ports precisely when their services are required, reducing idle time and unnecessary fuel consumption.

Another critical aspect is the hull and robotics inspection model. Regular inspections of a ship's hull, propellers, and other underwater components are vital to maintaining optimal performance and reducing fuel consumption. The integration of robotics and advanced inspection techniques allows for efficient and thorough assessments, minimizing downtime and ensuring the ship operates at peak efficiency.

Condition-based monitoring is an essential tool for assessing and optimizing fuel consumption. By utilizing sensors and data analysis techniques, critical components and systems aboard the ship can be continuously monitored, enabling proactive maintenance and early detection of potential issues. This approach ensures that fuel-consuming inefficiencies arising from faulty equipment or suboptimal performance are promptly addressed.

The deliverable also explores the use of energy simulators, which enable ship operators to simulate and analyse different energy management strategies. By simulating various scenarios, operators can identify the most fuel-efficient operating parameters, optimizing the ship's overall energy consumption. This approach allows for informed decision-making and effective energy management in real-world operations.

Lastly, the Life Cycle Assessment (LCA) model is introduced to evaluate the environmental impact of a ship throughout its entire life cycle. This comprehensive assessment considers factors such as raw material extraction, ship construction, operation, maintenance, and end-of-life disposal. By quantifying and analysing the environmental footprint at each stage, ship designers, operators, and regulators can identify areas for improvement and implement sustainable practices to minimize fuel consumption and environmental impact.

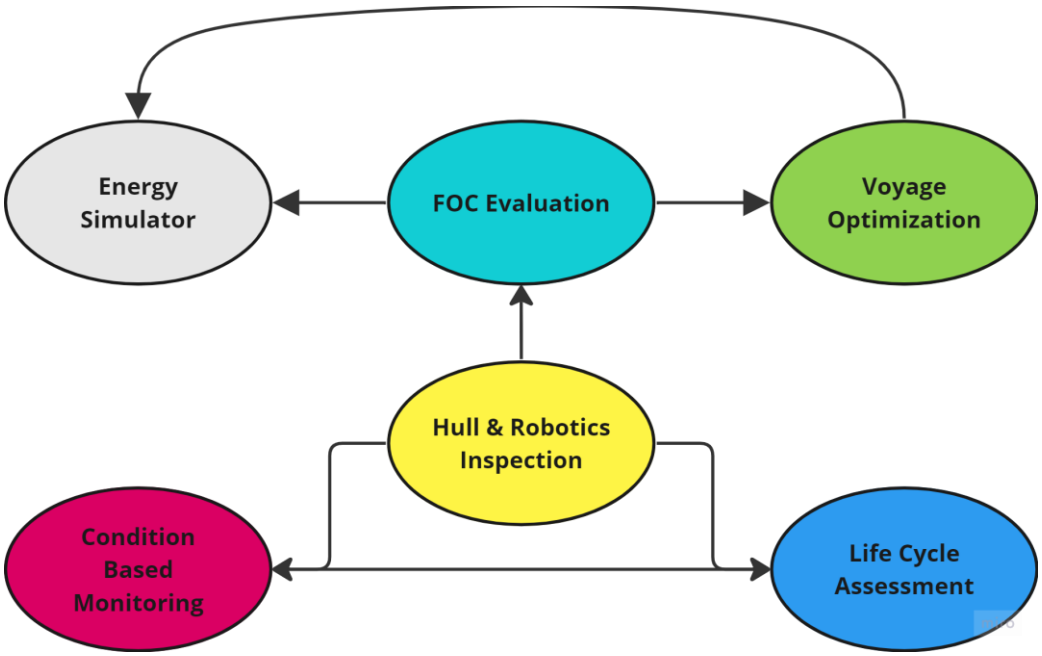

Figure 2. System overview, main topics

This deliverable presents a multifaceted approach to assess and reduce fuel consumption in maritime operations. By combining navigation management, hull and robotics inspection, condition-based monitoring, energy simulation, and life cycle assessment, ship operators can enhance fuel efficiency, reduce environmental impact, and optimize operational performance. Implementing these methodologies will contribute to a more sustainable and economically viable maritime industry in the future.

3 Fuel Oil Consumption Evaluation

3.1 Engine Power Estimation

In detail, what has been described in the following section is shown in Figure 3. This workflow describes the logical process of choosing the models to be used for the realization of a digital twin in order to evaluate the power demand and relative consumption of the ship. In particular, two main parts can be observed coexisting with each other.

The first, the one in which the process leading to the creation of the demand curve in terms of engine power and rotations per minute (RPM) is described, through a purely theoretical approach, is the one inside the green window located at the top.

In the second, located further down on the left of Figure 3, two modules are visible: the first "3d Grade polynomial Curve Fitting," which takes advantage of a grey box approach. The second "MLP regressor" is described by a black box model. As mentioned above, the latter model, based on a black box approach, is intended as food for thought since it has not been implemented at this stage of development.

The final output for both branches of the workflow is the demand in terms of power output to the engine and the relative propeller revolutions.

If you have simultaneously the HF data used for the Gray and Black Box models and the technical data to be used in the White Box model, you can make a comparison by looking at the differences between the demand curves of the theoretical models and those of the data-driven models.

Knowing the power and RPM of the engine, it is possible to estimate its consumption by knowing the engine consumption map, which is provided by the engine manufacturer. The consumption map contains information in terms of litres per hour or SFOC [g/kwh] of all engine operating points. Specifically, this information is contained in the form of iso-consumption curves.

Eventually, by knowing the required power for the voyage and the relationship that links power output and CO_2 emitted (depending on the type of motorization installed on board).

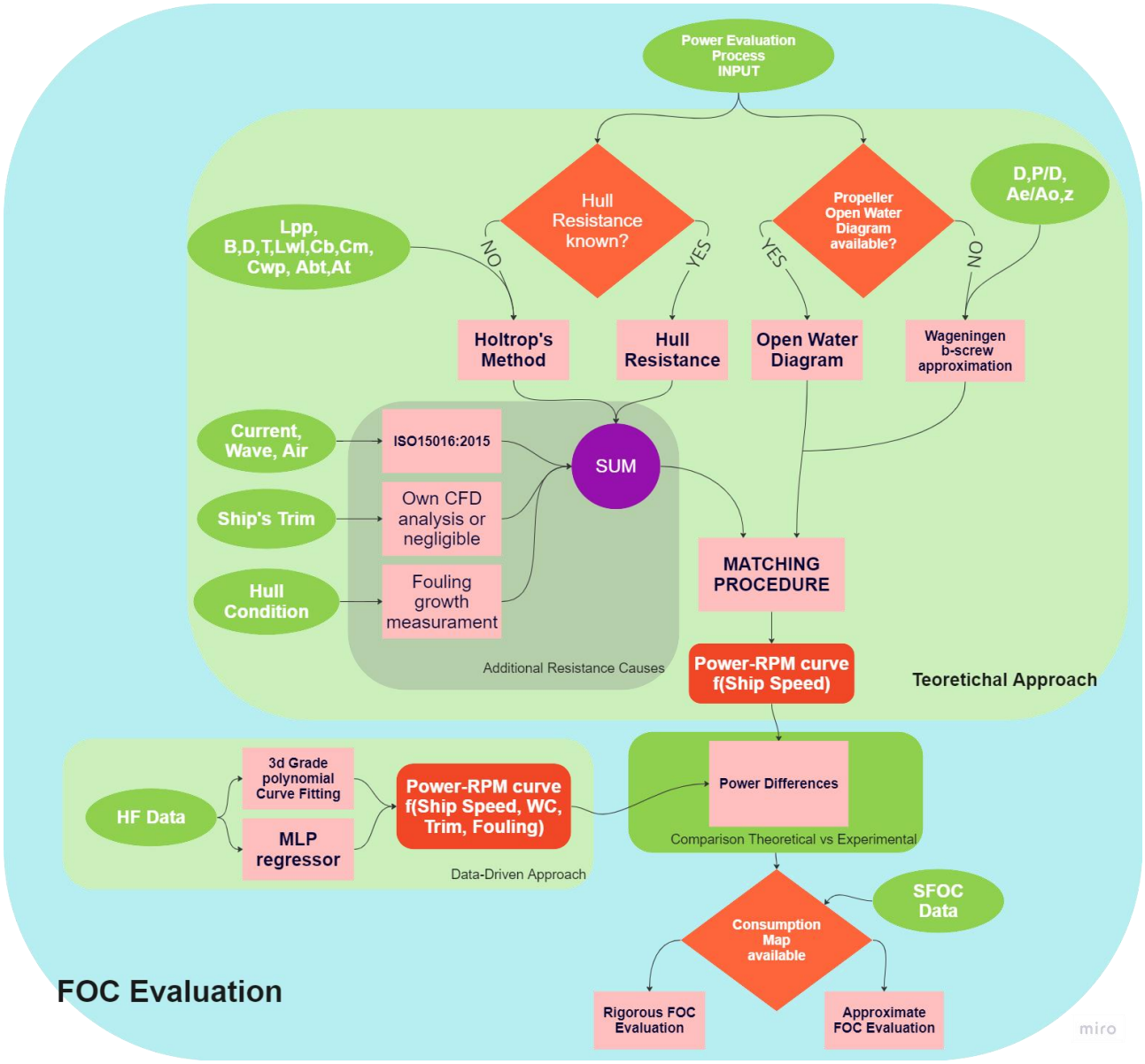

Figure 3. Brake power, engine rpm and FOC evaluation workflow.

3.2 Theoretical Approach Pipeline

The theoretical model is described with a model-based approach, in which the phenomena considered essential to assess the required brake power have been schematized mathematically.

This schematization was implemented to ensure a generalized model capable of encompassing most commercial ships. Paying attention to the amount of information needed to be able to use the theoretical model, trying to limit it as much as possible.

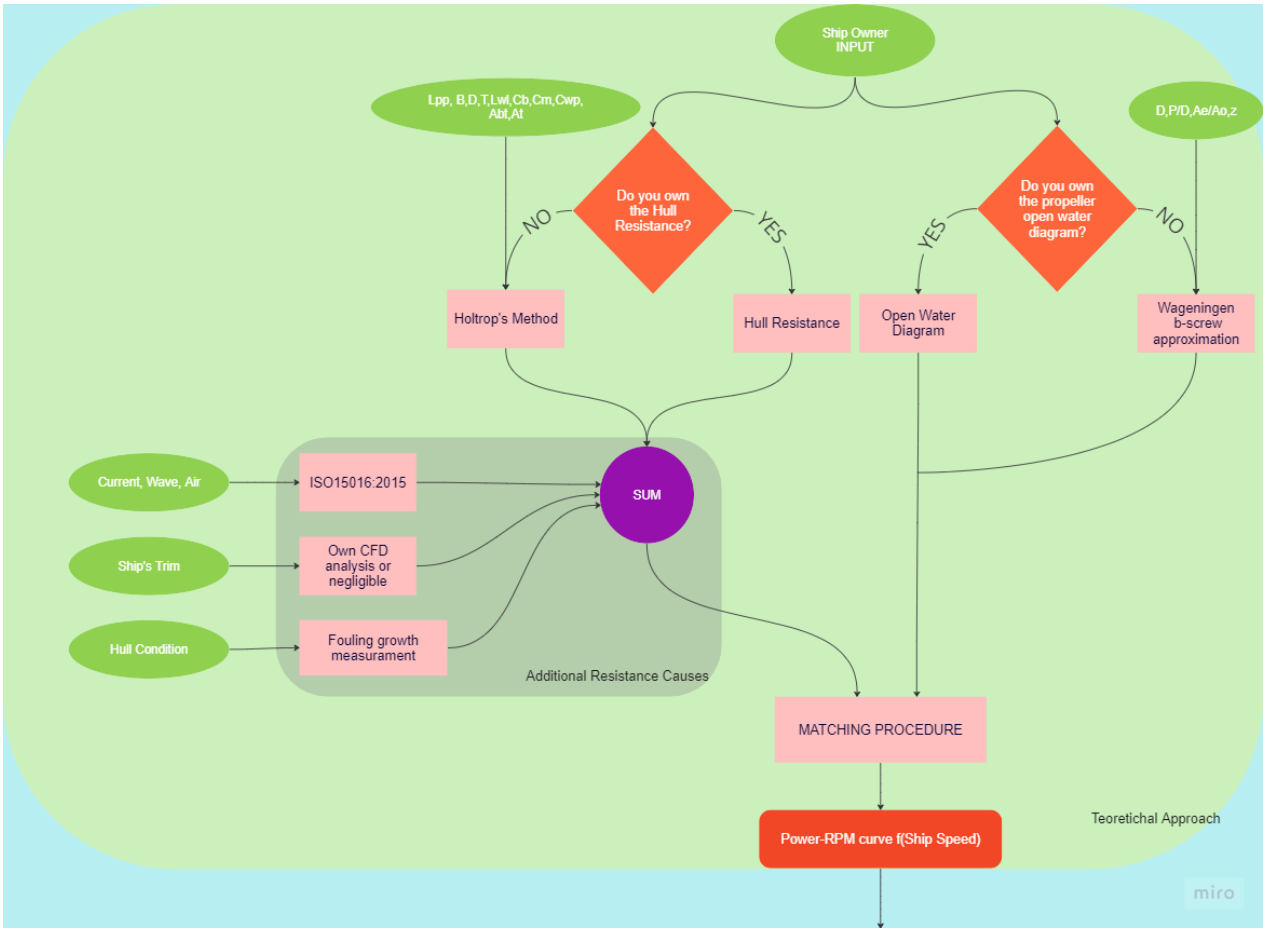

Figure 4. White box workflows

Two main branches can be distinguished within the mathematical model of Figure 4. The first, the left branch, concerns the evaluation of ship's hull resistance; the second, the right branch, establishes the methodology for determining the propeller operating conditions described by the open water diagram.

3.2.1 Hull Resistance Branch

This section describes how to determine ship hull resistance in still water.

The first block encountered within the pipeline establishes which model to use for the resistance assessment. In cases where the shipowner does not know the own hull resistance as a function of ship speed in still water, it can be determined using the method of Holtrop and Mennen [12, 13] by means of several dimension characteristics.

In detail, Holtrop and Mennen's method is a widely used empirical method to estimate the total resistance of a ship and is based on statistical analysis of extensive model test data.

The method estimates the total resistance of a ship as the sum of its frictional resistance and wave-making resistance. The frictional resistance is calculated using the ITTC friction line method, while the wave-making resistance is estimated using a set of equations based on Froude number and hull form coefficients.

The Holtrop and Mennen method takes into account a range of factors, including the length, beam, and draft of the ship, as well as its speed, displacement, and hull form coefficients. It also considers the effect of appendages such as rudders, skegs, and bilge keels. The accuracy of the method has been found to be good for a wide range of ship types and sizes, although it may not be as accurate for unusual hull forms

or for ships operating in unusual conditions. It is often used in the initial design stages of a ship to estimate its resistance and to evaluate the effect of changes in design parameters on resistance. Indeed, there are some constraints and limitations to this method that should be considered.

Limited accuracy for certain hull forms: The method is most accurate for conventional hull forms and may not be as accurate for unusual hull forms or complex geometry such as bulbous bows or stern flaps.

Limited applicability for high-speed vessels: The method is primarily designed for ships that operate at low to moderate speeds and may not be applicable to high-speed vessels such as fast ferries or planning boats.

Limited accuracy in rough seas: The method is based on model tests in calm water conditions and may not accurately predict resistance in rough seas or in waves.

Limited consideration of dynamic effects: The method does not take into account dynamic effects such as slamming, which can significantly affect resistance in some types of vessels.

Despite these constraints, the Holtrop and Mennen method remains a widely used and valuable tool for estimating ship resistance and optimizing ship design. It provides a useful starting point for further analysis and can help identify areas for further optimization and improvement.

At this point, the resistance to still water of the ship unit is known.

To this resistance must be added the contribution of environmental conditions, the longitudinal trim of the ship, and finally the cleanliness of the hull due to the presence of fouling.

3.2.2 Increased Resistance due to Weather Condition

To calculate the required brake power, it is necessary to estimate the additional resistance acting on the ship's hull.

Depending on the weather conditions, the power consumed can vary with the speed of the ship. To estimate the additional resistance, environmental data (weather data) of the ship's position is required. Indeed, meteorological data can be obtained from climate data centres and include the time, position, speed and direction of wind, waves and current in order to make simulation concerning the benefit from a chosen rout and optimize it. Moreover, the weather data can be matched with AIS data based on time and position information in on-line approach.

In particular, by means of methods for estimating the hull resistance increase described in ISO15016:2015 [14], is possible to assess additional resistance to measure the effects of the weather.

In the ISO15016:2015, additional resistance is divided into three main components; resistance due to wind, resistance due to waves, and resistance due to water temperature and density. The total increased amount of resistance ΔR is:

$$\Delta R = R_{AA} + R_{AW} + R_{AS}$$

where R_{AA}, is the resistance increase due to wind, R_{AW}, is the resistance increase due to wave and R_{AS} is the resistance increase due to density and water temperature. This last contribute can be omitted in due to its small magnitude.

The resistance increase due to wind is calculated by:

$$R_{AA} = \frac{1}{2}\,\rho_A\,C_{AA}(\psi_{WRref})\,A_{XV}\,V_{WRref}^2 - \frac{1}{2}\,\rho_A\,C_{AA}(0)\,A_{XV}\,V_G^2$$

where ρ_A is air density, $C_{AA}(\psi_{WRref})$is the wind resistance coefficient; $C_{AA}(0)$ means the wind resistance coefficient in head wind, A_{XV} the transverse projected area above the waterline including superstructures in square metres, V_{WRref} is the relative wind velocity at the reference height in metres per second; V_G is the measured ship's speed over ground and ψ_{WRref} is the relative wind direction at the reference height in degrees.

Concerning the wave, the head waves the encounter frequency of the waves is high. In these conditions the effect of wave induced motions can be neglected and the added resistance is dominated by the wave reflection of the hull on the waterline. The water line geometry is approximated based on the ship beam and the length of the bow section on the water line.

The following formula estimates the resistance increase in head waves provided that heave and pitch are small. The application is restricted to waves in the bow sector (less than ± 45 degrees off the bow). For wave directions outside this sector no wave correction is applied.

$$R_{AWL} = \frac{1}{16}\,\rho_S\,g\,H_{1/3}^2\,B\,\sqrt{\frac{B}{L_{BWL}}}$$

where R_{AWL} is the mean resistance increase in long crested irregular waves in newtons, as substitute for R_{AW}, ρ_S is the water density, g is the acceleration of gravity, B is the ship's breadth, $H_{1/3}$ is the significant wave height in meters and L_{BWL} is the distance of the bow to 95 % of maximum breadth on the waterline in metres.

3.2.3 Increased Resistance due to Ship's Trim

The ship's trim refers to its longitudinal balance or the distribution of weight along its length. It is a critical aspect of ship stability and performance. The trim of a ship is determined by the difference between the ship's draft forward and aft. The draft refers to the depth of the ship's hull below the waterline.

When a ship is perfectly trimmed, its draft is equal both forward and aft, meaning it floats level in the water. However, various factors can cause the ship's trim to deviate from this ideal condition. These factors include the distribution of cargo, fuel, ballast water, and the presence of passengers.

The trim of a ship affects its hydrodynamic properties, manoeuvrability, fuel efficiency, and overall safety. Improper trim can lead to decreased stability, increased resistance, reduced speed, and difficulties in steering the ship. Therefore, maintaining the correct trim is essential for optimal ship performance.

For such a reason, ship's trim optimization involves adjusting the distribution of weight along the ship's length to achieve the most efficient and favourable trim condition. By optimizing the trim, ships can reduce resistance, improve fuel efficiency, enhance stability, and ensure a smoother ride. Indeed, the mains key aspects of ship's trim optimization are:

The fuel efficiency: Proper trim optimization can impact a ship's fuel consumption. By achieving the optimal trim condition, the ship can reduce resistance and drag through the water, leading to lower fuel consumption. This is especially important for long voyages where even small improvements in fuel efficiency can result in substantial cost savings and environmental benefits.

Resistance reduction: A ship experiences hydrodynamic resistance as it moves through the water. Resistance increases with a poorly optimized trim, resulting in higher power requirements and reduced speed. By adjusting the trim to the optimal condition, the ship can minimize resistance, allowing it to sail more efficiently and at higher speeds.

The trim of a ship during its navigation can afflict its fuel consumption by going to change the hull resistance. For this reason, the ability to change hull resistance as the ship's trim changes has been built into the pipeline.

For this purpose, a generalized model was searched in the literature, as in the previous cases that was numerically implementable and emulated the physical behaviour of trim variation.

Unfortunately, no generalized formulas were found in this case that met the requirements. In fact, almost all of the scientific literature pertaining to the topic is based on studies using CFD (computational fluid dynamics) [15, 16, 17]. A CFD-based approach is certainly a very rigorous method of study that almost perfectly emulates the real physical phenomenon. Unfortunately, the concept of generalization is completely lost in this case. For these reasons, it was thought to leave available in the pipeline the possibility of including one's own hull-based study and not generalize to other ships. Indeed, in case studies on the variation of hull resistance as the trim changes are not available this increment is neglected.

Moreover, another method to perform the ship's trim optimization is based on a data-driven approach. This method involves utilizing advanced technologies, data analysis, and predictive modelling to achieve the most efficient trim condition. By leveraging real-time data and historical performance data, ship operators can make informed decisions to optimize trim and enhance ship performance. Here's an overview of the data-driven approach to ship's trim optimization:

- Data Collection: The first step is to collect relevant data from various sources onboard the ship, such as sensors, gauges, and monitoring systems. This data includes information on the ship's draft, trim, speed, fuel consumption, engine performance, weather conditions, and other operational parameters. Additionally, historical data from previous voyages is also valuable for analysis.
- Data Analysis and Modelling: The collected data is then processed and analysed using advanced data analytics techniques. Statistical methods and machine learning algorithms can be applied to identify patterns, correlations, and relationships between the variables affecting trim optimization. This analysis helps to gain insights into the ship's performance under different trim conditions and identify potential areas for improvement.
- Trim Optimization Algorithms: Based on the data analysis, algorithms and models are developed to optimize the ship's trim. These algorithms consider factors such as fuel consumption, resistance, stability, and seakeeping performance. They can be customized to suit specific ship types, sizes, and operational requirements.
- Real-Time Monitoring and Decision Support: Real-time data from onboard sensors and monitoring systems are continuously fed into the trim optimization algorithms. This allows for real-time monitoring of the ship's performance and the ability to make informed decisions regarding trim adjustments.
- Performance Prediction and Simulation: Data-driven trim optimization allows for predictive modelling and simulation of different trim scenarios. By using historical data and predictive algorithms, operators can simulate the effects of various trim adjustments on fuel consumption, speed, stability, and other performance parameters. This helps in making informed decisions before implementing trim changes.

This approach has been described in [18] by means of a mixed Gray and Black box approach.

Again, a generalized white-box approach is not feasible. In fact, a data-driven approach requires a large dataset useful for training the predictive model specific to the vessel under consideration and therefore not available to all a priori. The data-driven approach can be used in the case where the owner has available a data history and the necessary expertise to create a predictive model based on the history and its validation of the model on vessel's data.

Eventually, the studies show that a maximum to 1% to 4% reduction on fuel consumption can be reached. as has been stated in MariEMS European Project [19].

For such a reason this can be considered negligible, and this approximation is not a serious shortcoming.

3.2.4 Increased Resistance due to Fouling Presence

An almost equally important aspect is the cleaning and maintenance of the hull and propeller. Indeed, the ship's resistances due to wet surfaces are composed of frictional resistance and wave resistance. Friction resistance is caused by the flow of water along the hull, for such a reason, the hull should be as smooth as possible so that the water can flow quickly and smoothly. Each additional 10μm to 30μm of roughness causes a 1% increase in the total resistance of the hull, and as mentioned above, the increase in resistance also increases fuel consumption. Normally, a new ship is delivered with a hull roughness of 75μm and later, when the ship is taken to dry dock, the hull roughness may be 250μm. Even with good maintenance, hull roughness Even with good maintenance, hull roughness can increase from 10 to 25μm per year, depending on the hull coating system.

Hull surface roughness can be divided into two categories, physical and biological.

In particular, biological roughness (fouling) occurs when an organic growth attaches to the ship's hull. For example, light slime covering the entire wetted surface can increase total strength by 7-9%. Heavy slough increases resistance by 15-18%, while small barnacles and weeds can increase total resistance by up to 20-30% [18].

This will be explored further in Section 4 Hull and robotics inspection models, where the role of hull inspection and suitable mathematical models to model this phenomenon will be specifically discussed.

3.2.5 Propeller Characteristics Branch

This section describes how to determine the propeller characteristics in particular how to assess the thrust coefficient K_T, torque coefficient K_Q and open water efficiency η_O.

The first block encountered within the pipeline establishes which model to use for the open water diagram assessment. In cases where the shipowner does not know the own propeller data, it can be determined using the Wageningen B-Series [20].

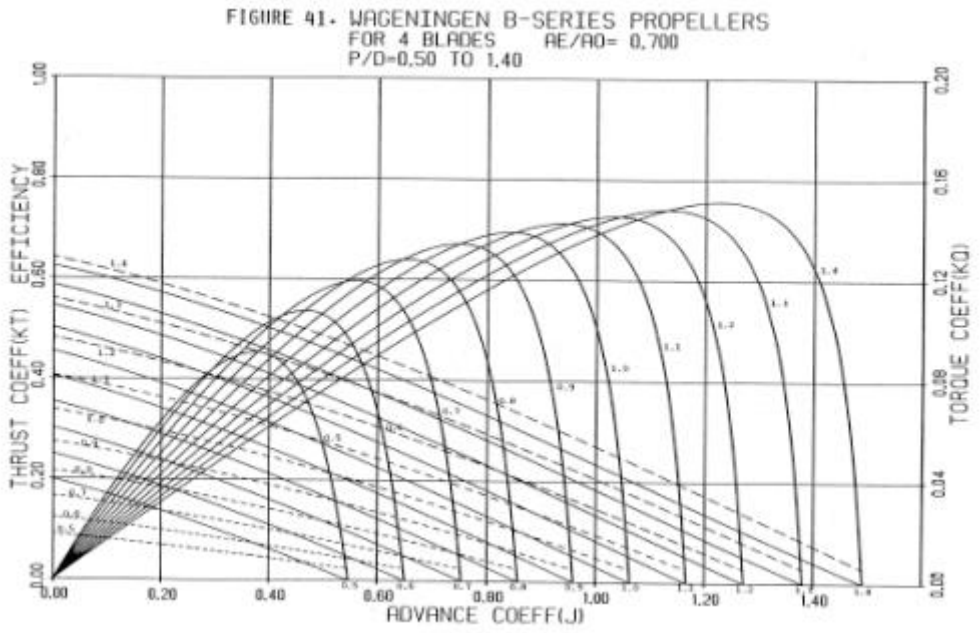

Figure 5. Example of B-series open water diagram with several P/D

The Wageningen Propeller B-Series are used by designers and engineers worldwide. These series comprise the open water characteristics of conventional fixed pitch propellers with various numbers of blades and blade area ratios for different pitch. For several of these propellers, also the characteristics in 4-quadrants (positive and negative rpm and positive and negative speed) were published by MARIN in the sixties and seventies. Today many ships are equipped with Controllable Pitch Propellers (CPP).

Both for ships and offshore structures, use is made of ducted CPPs. The thrust-torque performance of these units is not only of importance for ship designers but also for accurate analysis of speed trial results and manoeuvring simulators. Due to lack of this systematic information for CPPs in such cases, normally use is made of the B-series data. The characteristics of CPPs, however, differ substantially from those of fixed pitch propellers. For these reasons a Joint Industry Project called "Wageningen Propeller C- and D-Series" is initiated. For such a reason in the future development to obtain a better approximation of ducted and CPP the C and D series will be evaluated.

3.2.6 Matching Procedure

Given the propeller characteristic curves, the hull resistance and the engine diagram, matching could be performed. Matching is a procedure based on the balance of forces, resistance to motion and propeller thrust. To summarize, the two main inputs are the hull resistance and the open water diagram.

There are several procedures to perform matching, but as far as the case study is concerned, the most suitable one is the use of the auxiliary variable $\frac{K_T}{J^2}$, since the propeller diameter data is available, but the propeller working point per minute is not known. The mathematical procedure is reported hereinafter:

Begin from the hull resistance, the thrust has been evaluated as follow:

$$T_{shaft} = \frac{Rt}{(1-t)p} \; ; \forall \, V_{ship}$$

where: T_{shaft} is equal to the shaft thrust for every shaft line. This is a symmetry hypothesis between shaft line; p is the propulsor number; t is the thrust deduction factor.

Moreover, the formulae that define the thrust coefficient K_T, and the advance coefficient J, are the following:

$$K_T = \frac{T_{shaft}}{\rho\, {n_p}^2 D^4} \quad and \quad J = \frac{V(1-w)}{n_p\, D}$$

where: ρ is water density, n_p is the propeller revolution in RPS; D is the propeller diameter; w is the wave factor. Indeed, the K_T cannot be assess in by using this formula because that the propeller revolution (n_p) are unknown. For this reason, the variable $\left(\frac{K_T}{J^2}\right)_{hull}$ has been introduced.

$$\left(\frac{K_T}{J^2}\right)_{hull} = \frac{T_{shat}}{\rho\, D^2\, V^2\, (1-w)^2} = \frac{Rt}{\rho\, D^2\, p\, V^2\, (1-w)^2(1-t)} \;\forall\, V_{ship}$$

As previously stated, the matching is a procedure based on the balance between forces, in particular the hull resistance to motion and delivered thrust propeller. For this reason the balance is evaluate between $\left(\frac{K_T}{J^2}\right)_{hull}$ and $\left(\frac{K_T}{J^2}\right)_{prop}$ by means of interpolation or graphic method, in order to find the equilibrium advance coefficient, $J_{eq.}$.

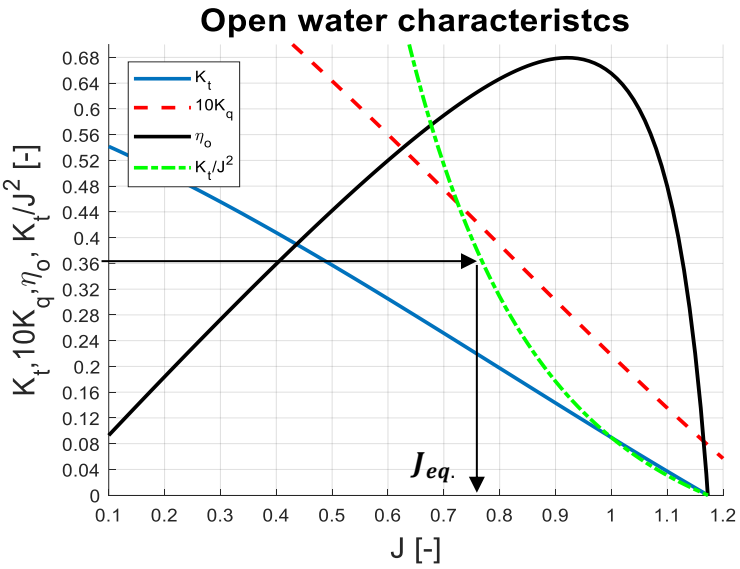

Figure 6. Matching procedure

Starting from the value of $J_{eq.}$ it is possible to obtain the values of K_T, K_Q & η_O.

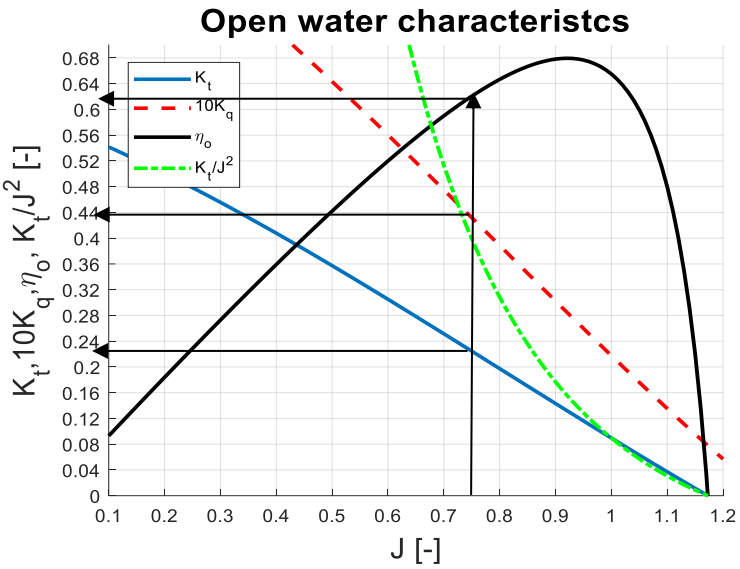

Starting from the values of K_T, K_Q & η_O it is possible to evaluate the required power curve.

$$K_Q = \frac{Q_o}{\rho\, {n_p}^2 D^5} \rightarrow Q_o = K_Q\, \rho\, {n_p}^2 D^5$$

$$Q_o = \frac{P_o}{2\,\pi\, n_p} \rightarrow P_o = 2\,\pi\, K_Q\, \rho\, {n_p}^3 D^5$$

$$P_B = \frac{P_o}{\eta_R\, \eta_S\, \eta_G}$$

$$n_p = \frac{V(1-w)}{J_{eq}\, D}$$

where: $Q_o$is the open water torque and P_o is the relative power; η_R is the rotative relative efficiency; η_S is the shaft line efficiency and η_G is the gear box efficiency (if gearbox is within the propulsive chain).

In case of a CPP propeller with several P/D the matching procedure is the same, the only exception is that it will have to be repeated as many times as the P/Ds considered. Indeed, the result will be as follows with a power requested curve for each P/D considered.

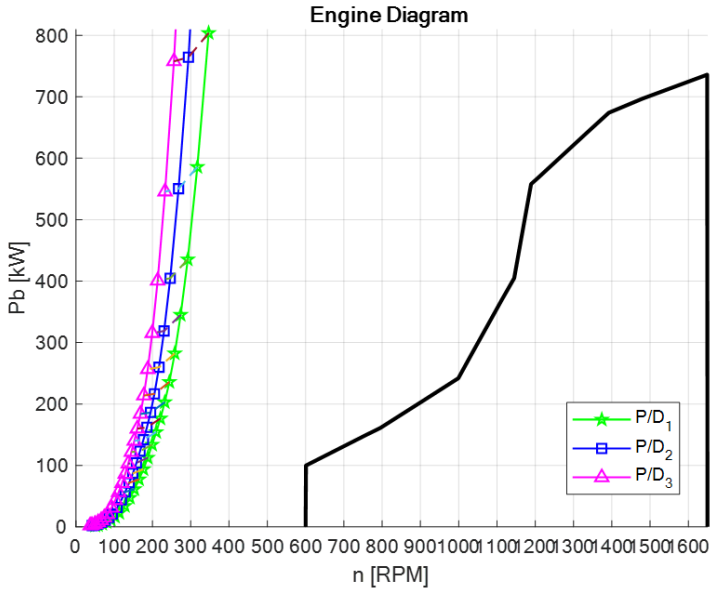

Figure 7. Matching procedure with CPP

After choosing the best gear ratio, the CPP matching procedure is concluded.

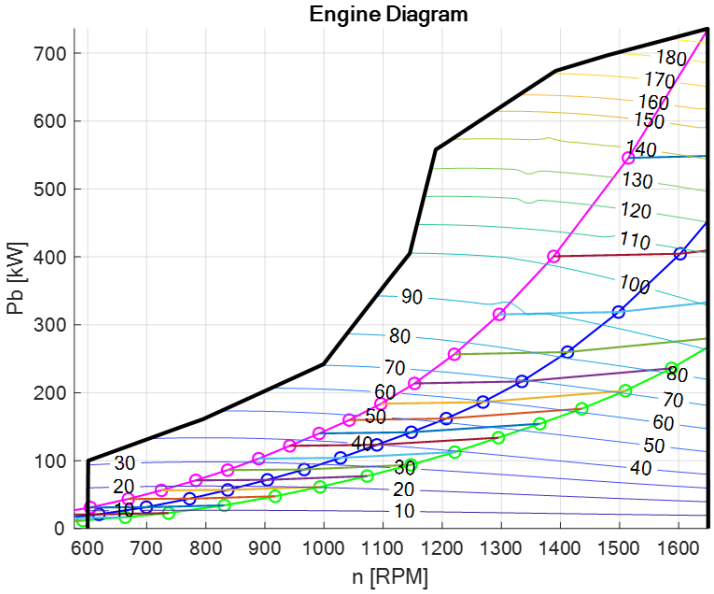

Figure 8. End of matching procedure

3.3 Data-driven Approach Pipeline

With an opposite philosophy, that of having strongly characterized data on the ship under analysis, a data-driven model fed by the high-frequency data collected from on-board sensors was evaluated. The disadvantages of this approach are the loss of generalization, the goodness of fit of the input data used to create the data-driven model strongly influences the result, and, finally, the fact that the data used to create the model must cover the entire operational range of the ship, as otherwise the risk is that an operational configuration other than the one used for training will be seen as an out-layer.

In the case of the model fed with data collected in the field using the gray box approach, it was decided to analyze the data knowing the assumptions that allow the operational curve to be evaluated using the perfect cubic approach. The perfect cubic method is often used when insufficient data are available, but at least one working point is known, and it is based on the following assumptions:

- $Rt = aV^2$ hull resistance with a quadratic relation with speed;
- $(1-t)\,,(1-w)$ & $\eta_R\ constant\ \forall\ V$;
- η_G & $\eta_S\ constant\ \forall\ V$;
-

These assumptions are easy to respect in a ship operating regime that is displacement. These are no longer respected in the case of a planning vessel. Nonnegligible errors are made in assessing resistivity for planning boats in which the classic humped pattern, in the hull resistance is present in the pre-planning phase. In such boats, resistivity remains valid only for the range of Froude numbers in which it is displaced (low speeds). Eventually, under these assumptions there is no longer any correlation with speed according to this demonstration.

$$\left(\frac{K_T}{J^2}\right) = \frac{Rt}{\rho\, D^2\, p\, V^2\, (1-w)^2(1-t)} = \frac{a\, V^2}{\rho\, D^2\, p\, V^2\, (1-w)^2(1-t)} = \frac{a}{\rho\, D^2\, p(1-w)^2(1-t)}$$

In fact, simplifying the velocity from the relationship, it is determined that all other quantities are constant K_T, K_Q & η_O, and this implies that the relationship linking revolutions to power is in cubic relation to each other.

$$P_B = \frac{2\,\pi\, K_Q\, \rho\ D^5}{\eta_R\, \eta_S\, \eta_G}\, {n_p}^3 \rightarrow \frac{2\,\pi\, K_Q\, \rho\ D^5}{\eta_R\, \eta_S\, \eta_G} = const \rightarrow P_B = \beta\, {n_p}^3$$

By knowing the theory that binds these quantities, it is possible to use it to obtain the operating curve comparable to the theoretical approach in the case of the data-driven approach. In fact, by plotting the operating points collected from the sensors, it is possible to perform a 3rd degree polynomial fit on the Pb vs. RPM working plane in order to find the relationship between the points.

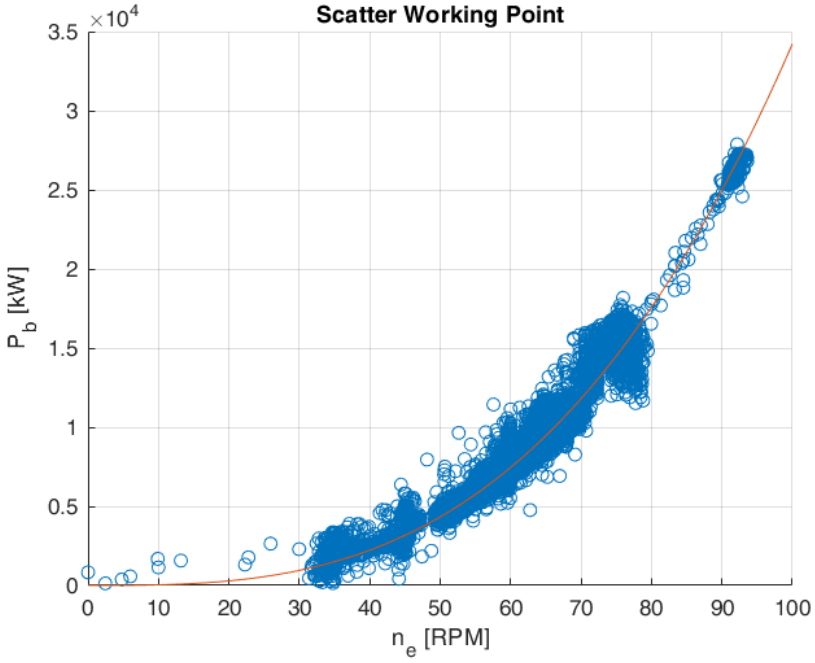

Figure 9. III grade polynomial fit based on HF data.

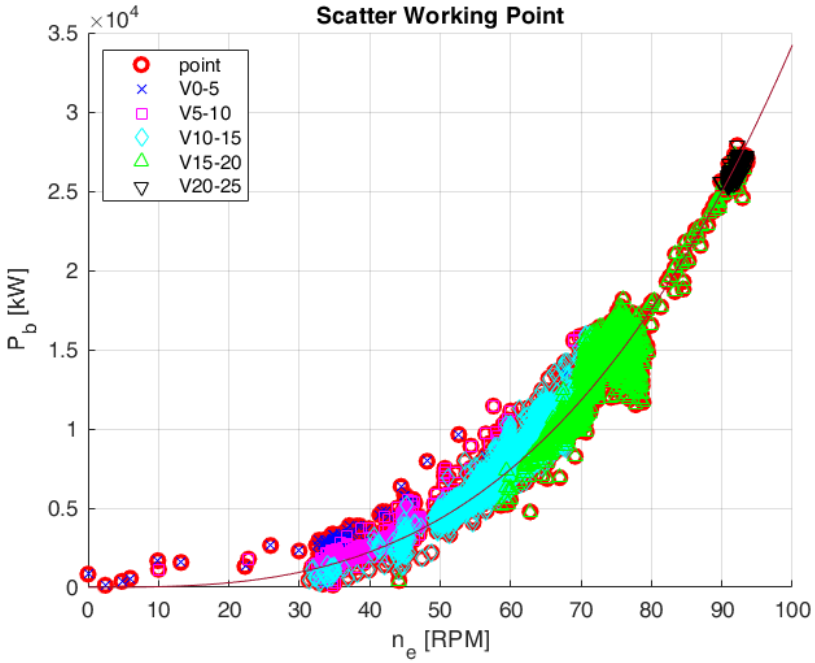

Figure 10. III grade polynomial fit based on HF data subdivided into group as a function of speed.

Third-degree fitting on the complete cloud of points acquired in high frequency is related to the points generated during the navigation of the ship belonging to DANAOS for a navigation period of about two months. In addition, clustering techniques were used to compare the original fitting curves with those obtained from down-sampling.

Two methods, k-medoids [21] and k-means [22] were used to make the comparison. Both are based on the a priori choice of the number of clusters into which to partition the point cloud, the value of k. For

this case study and knowing that the curve is generated by an adaptation of degree III points, it was chosen to divide it into 3^2 clusters.

The results, as can be seen from the images, are comparable, with differences of negligible magnitude.

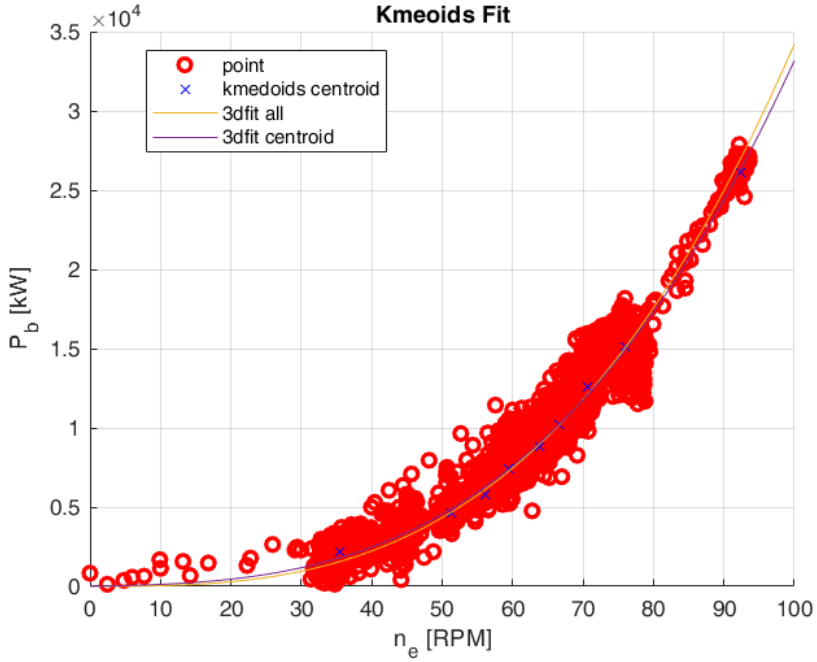

Figure 11. K-medoids clustering fitted.

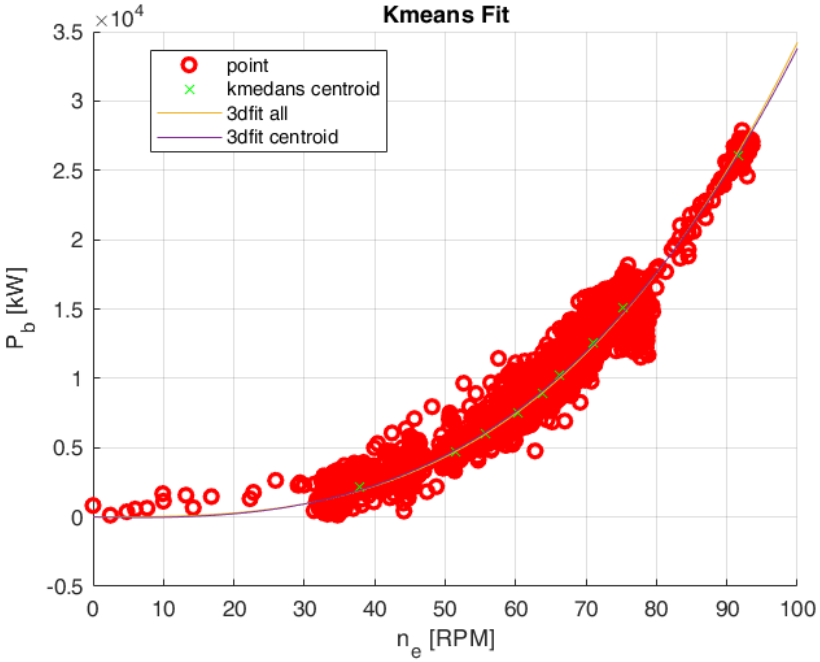

Figure 12. K-means clustering fitted.

A potential drawback with this approach is quantifying the effect that the individual elements, environmental conditions, and hull, have on the variation in power required by the ship. For example, clean hull, no change in trim, and change in weather conditions. It will only be possible to quantify this criticality after the initial analyses have been performed. Moreover, this is highly dependent on the size of the database, since it is a sufficiently large database with a lot of historical data.

3.4 FOC – CO2 Model Architecture

After showing how to evaluate the ship's demand curve in terms of power versus rpm, several approaches to evaluate ship consumption will be shown and discussed below.

3.4.1 Theoretical Models (White Box Modelling)

This section illustrates how a FOC estimate can be made on the basis of the High frequency data input (velocity measurements) and output (RPM) of the proposed method, in conjunction with basic vessel's particulars, and standard Marine-Engineering knowledge.

We will illustrate the accuracy of our FOC estimation via comparison with actual FOC data of a container ship for different voyages, demonstrate the potential of the proposed method.

In summary, the proposed FOC estimate can be written as:

$$FOC = \frac{2\pi\rho\ K_Q(J) {n_P}^3 D^5\ SFOC}{\eta_G\ \eta_S\ \eta_R}$$

where:

- ρ is the sea density [1026 kg/m^3],
- **SFOC** is the *Specific Fuel Oil Consumption* of the Main Engine per energy unit, which is available by the ship owner [g/kWh] provided by engine manufacturer,
- **D** is the diameter of the propeller [m],
- n_P is the propeller revolution in [rps],
- $\eta_G\ \eta_S\ \eta_R$ are the gear box (if present), shaft and relative rotative efficiencies, respectively,
- $\mathbf{K_Q(J)}$ is the torque coefficient, depending on the so-called *advance coefficient* **J**, further analysed in the sequel, both are dimensionless coefficient,

Q_o is the open water torque and it is delivered by the Main Engine. For the Wageningen B-series of propellers, which are widely used by the Marine-Engineering practitioners, regression analysis of a large-volume of experimental data produced by the Netherlands Ship Model Basin (NSMB) in Wageningen via open-water experiments with 120 propeller models, led to the following regression formula:

$$Q_o = \rho\ K_Q(J) {n_P}^2 D^5$$

Here $\mathbf{K_Q(J)}$ is a polynomial function of J provided some further propeller particulars are known, such as the pitch over diameter ratio P/D, the number z of propeller blades and the blade-area ratio A_E/A_o. As it is readily seen from Figure 13, the primary parameter for $K_Q(J)$ is the advance coefficient J

$$J = \frac{V_A}{nD},$$

where V_A is speed of advance of the propeller relative to the water in which it is working, which is lower than the speed of the vessel V. This is expressed by,

$$V_A = V(1 - w),$$

where w is referred to as the wake fraction coefficient. For ships with one propeller w is normally in the range of 0.20 to 0.45. Furthermore, since containerships do not have large block coefficient, we have used values w in [0.25, 030] reflecting the fact that the distribution of the water velocity around the propeller will not be strongly non-homogeneous.

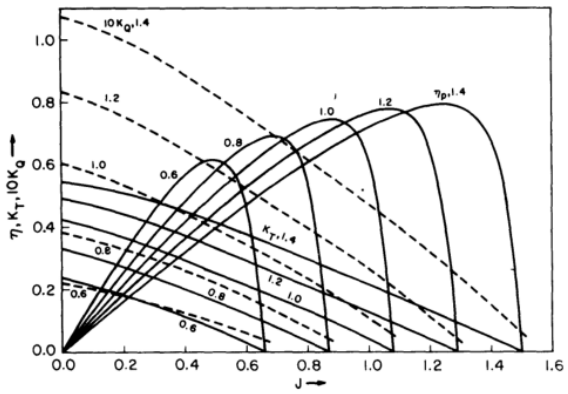

Figure 13. Thrust, Kt, torque, Kq and efficiency, η0, coefficients for Wageningen-series three-bladed (z = 3) propellers with pitch/diameter (P/D) ratios 0.6, 0.8, 1.0, 1.2 and 1.4

Based on the above, it is concluded that:

1. Monitoring the velocity V and acquiring or estimating RPM via data driven schemes, we can have a good overview of the fluctuation of the advance coefficient J, which constitutes a key indicator of the vessel's propulsion system performance.
2. Using basic propeller particulars and the polynomial regression results provided by [20], enables an easy and robust estimation of FOC.
3. To validate this assertion, we provide in Figure 14 and Table 3 at section 3.5 the actual and predicted average FOC of our vessel as calculated by our method, after adjusting transitional speeds (acceleration, deceleration) for four different voyages that were not included in the training set. Red circles indicate number of observations for a specific range of velocity (V_i +- 0.25) during a voyage.

3.4.2 Data Driven Models (Black Box Modelling)

Features related to the prediction task

The motion of a ship through water requires energy to overcome resistance, i.e., the force working against movement. Therefore, FOC is highly impacted by the total resistance of the vessel as it moves forward. Total resistance of the vessel incorporates three major components: frictional resistance, wave resistance and air resistance.

The **frictional resistance** depends on the size of the wetted area of the vessel. It represents often about 70-90% of the ship total resistance for low-speed ships (bulk carriers and tankers), and sometimes less than 40% for high-speed ships (containers and passenger ships).

Wave Resistance measures the effect of waves and may rise to 30% of the total resistance. The characteristics of waves like their amplitude and wave length are determined from the ocean-wave spectra along the voyage path.

Finally, **air resistance** normally represents about 2% of the total resistance, but for loaded container ships in head wind, it can be as much as 10%.

Based on the above standard marine engineering knowledge we aim to utilize meaningful features that have a prominent impact in the total resistance of the vessel like:

- Features that correspond to the frictional resistance and can be utilized in the context of a Routing Optimization algorithm, such as Speed Through Water (STW) and Draft.
- Features that describe the wave resistance component, such as Wave height/Direction, Wave Period, Swell Wave Height/Direction, and Swell Period.
- Features that model the air resistance component, such as Wind Speed/Direction, Combined Wind Wave Height/Direction, and Current Speed/Direction.

In Table 3 below we depict the experimental results from conducting regression analysis in order to rank the importance of the aforementioned features in estimating FOC, a process thoroughly described in [57].

Table 3. Feature Importance

Ranking	Feature	Importance
1	STW	0.94
2	WS	0.13
3	DRAFT	0.011
4	VSL_H	0.005
5	COMBH	0.0058
6	SWH	0.0054
7	CS	0.004
8	$WAVE_H$	0.0039
9	SWP	0.0036
10	COMBD	0.0032
11	SWD	0.0028

The exact process and workflow adopted to conclude to the exact feature set, depicted in Table 3 , is not in the scope of this deliverable and is rather part of the broader DT4GS data pre-processing unit described in detail in the context of deliverable D2.2 , concerning the **Dataspace**.

Model implementation

The dynamic estimation of FOC based on vessel state and environmental conditions can be examined as a multivariate time-series prediction problem that takes into account the actual values as well as their recent history, and captures the information hidden in the values' evolution over time.

Based on the superiority of Long Short-Term Memory Neural Network (LSTM) models over traditional time-series prediction methods (e.g., ARIMA) [58, 59], LTSMs are chosen as the basis of our solution.

The initial feature set, collected by AIS and sensor instalments comprises the vessel speed, draft and heading and some basic weather features such as wind speed and direction.

In order to take maximum advantage of this feature set, we employ a LSTM architecture, using a pre-training step that extracts information from the original features, using spline-based regression [60]. In what follows, we describe how LSTM is used for FOC estimation and detail the proposed LSTM model and its novel aspects.

Utilizing LSTM Neural Network for FOC estimation

LSTM is a variation of traditional Recurrent Neural Network (RNN) architecture [61], which has been extensively used for time-series prediction tasks [62, 64].

Unlike standard feed forward neural networks, LSTM also contains feedback connections and can process single data points (e.g., images) as well as entire sequences of data (e.g., speech, video or object trajectories). Compared to RNNs, Hidden Markov Models and other sequence learning methods, LSTMs are not so sensitive to the length of gaps between important events in a time series, which makes them preferable in numerous applications. To this end, we adopt an LSTM architecture for the prediction of FOC value from the consecutive observation, corresponding to the aforementioned features, in a time window, as described in the following paragraphs.

The input of the LSTM network at timestep t_u comprises N time-series, one for each feature of interest (speed through water, wind speed, wind angle etc) and in order to use the recent history of values in each feature, we employ a fixed-length time-window (time-lag of length m). As a consequence, the window contains the values for each time step $t_i \in [t_{k-m}, t_u]$ for the weather and vessel state features that are used for the estimation of FOC at time t_u, resulting in N time-series, of length m+1, of the form $F_{N(u-m)}, \ldots, F_{N(u-1)}, F_{N(u)}$, for each feature F_N. Given a sequence of consecutive time-steps, and a multivariate feature set, we get the following correspondence between the input and the output of the LSTM:

$$\begin{bmatrix} [F_{1(u-m)} \dots F_{j(u-m)} \dots F_{N(u-m)}] \\ \vdots \\ [F_{1(i)} \dots F_{j(i)} \dots F_{N(i)}] \\ \vdots \\ [F_{1(u)} \dots F_{j(u)} \dots F_{N(u)}] \end{bmatrix} \longrightarrow \begin{bmatrix} FOC_{u-m} \\ \vdots \\ FOC_i \\ \vdots \\ FOC_u \end{bmatrix},$$

where N is the number of monitored features (and respectively of the time-series fed to the LSTM), m is the window length, and $F_{j(i)}$ is the value of feature $j \in [1, N]$ at timestamp t_i. FOC_i is the FOC value that we want to predict.

3.5 FOC – CO2 Model Reporting – Visualization

In this section we will first demonstrate results corresponding to different voyages of a real container vessel utilizing the aforementioned FOC estimation models described in sections 3.4.1 and 3.4.2.

Dataset

All the experiments were conducted with real data, from a dataset of an existing container ship vessel with a carrying capacity of 3000 TEUs (Twenty-foot Equivalent Unit - unit of cargo capacity used for container ships and terminals). The values collected correspond to a vast majority of different round-trip voyages at different periods and geographical locations. As a whole, the dataset extracted for the purpose of this work, covers a time span of one year (December 2019 - December 2020) with approximately $4 * 10^5$ data points.

In order to examine the statistical significance of our results, we created 10 statistically independent subsets extracted from different time periods of approximately $5 * 10^3$ observations each that cover 84 hours or 3.5 days of the vessel's trip.

A timeframe large enough to represent all the different states (weather impact/engine state) of the vessel during a voyage. From these datasets, 80% was used for training and the rest for testing.

Statistical independence was preserved between different datasets with the use of the Kolmogorov-Smirnov test (KS-test). This is a two-sided test for the null hypothesis that 2 independent samples are drawn from the same continuous distribution. The dataset used in the context of this work is available, in sanitized form, upon request to the first of authors. It contains the values for the features described Table 3, and their corresponding timestamp.

Theoretical model Performance in different voyages

In section 3.4.1, we demonstrated a theoretical approach to construct a robust FOC predictive scheme by utilizing the speed of the vessel, basic propeller characteristics and polynomial regression formulas to extract thrust coefficient (K_T) and torque coefficient (K_Q) for a specific vessel.

To validate this assertion, we provide in Figure 14 and Table 4 the actual and predicted average FOC of our vessel as calculated by our method, after adjusting transitional speeds (acceleration, deceleration) for four different voyages that were not included in the training set. Red circles indicate number of observations for a specific range of velocity ($V_i \pm 0.25$) during a voyage.

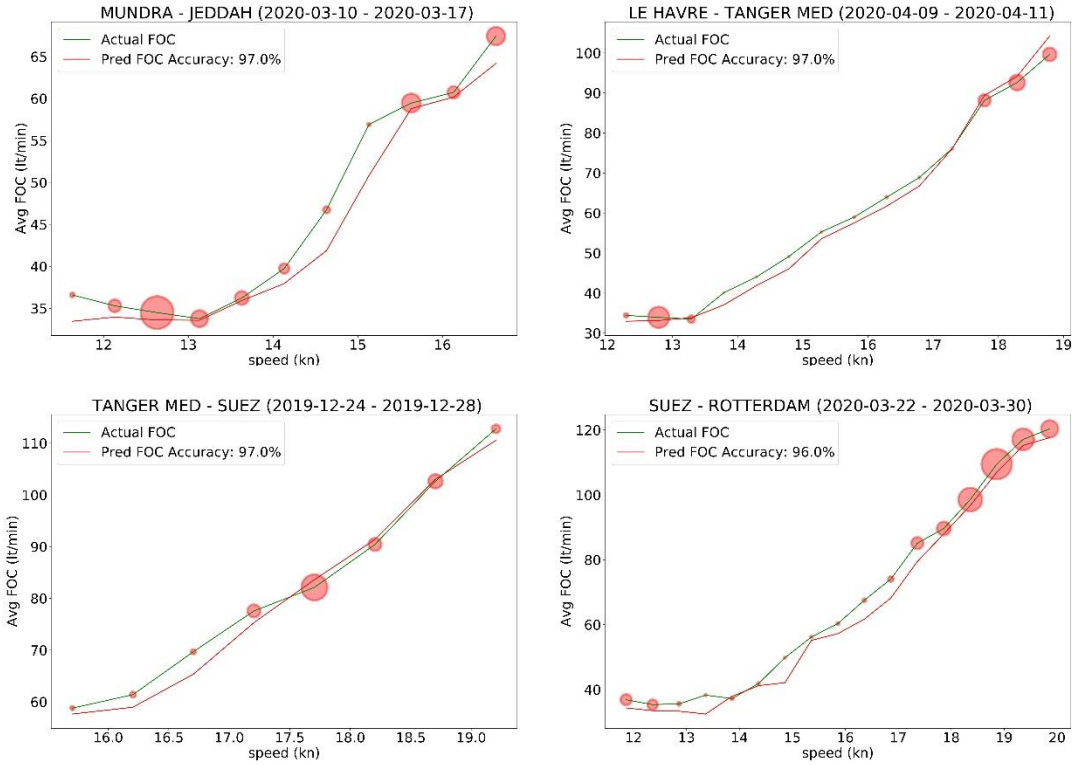

Figure 14. Actual/Predicted FOC (lt/min) comparison for different legs

Table 4. Computational performance of the FOC-estimate formula

	Total Act FOC(MT/d)	Total Pred FOC(MT/d)	FOC Abs Diff(MT/d)	FOC Perc Diff %	Mean STW(kt)
SUEZ - ROTTERDAM	1100.62	1104.59	3.97	0.35	18.15
TANGER MED - SUEZ	411.7	413.42	1.72	0.41	17.84
MUNDRA JEDDAH	437.04	439.38	2.33	0.53	13.97
LE HAVRE TANGER MED	284.26	288.81	4.55	1.57	15
Total	**2233.62**	**2246.2**	**12.58**	**2.86**	**16.24**

LSTM NN Performance in different voyages

In this section we evaluate the approximation capabilities of the proposed LSTM-based FOC predictive model. This is performed for four different voyages extracted from the initial test set. The voyages correspond to different locations, time periods and weather conditions for the same container ship.

To demonstrate the results, we depict, in Figure 15 and Table 5, the deviation between the actual and the predicted FOC measured in Metric Tonnes for one day (MT/day), per speed(V) range (+-0.5 V).

Bar size indicates the number of observations found for a particular speed range.

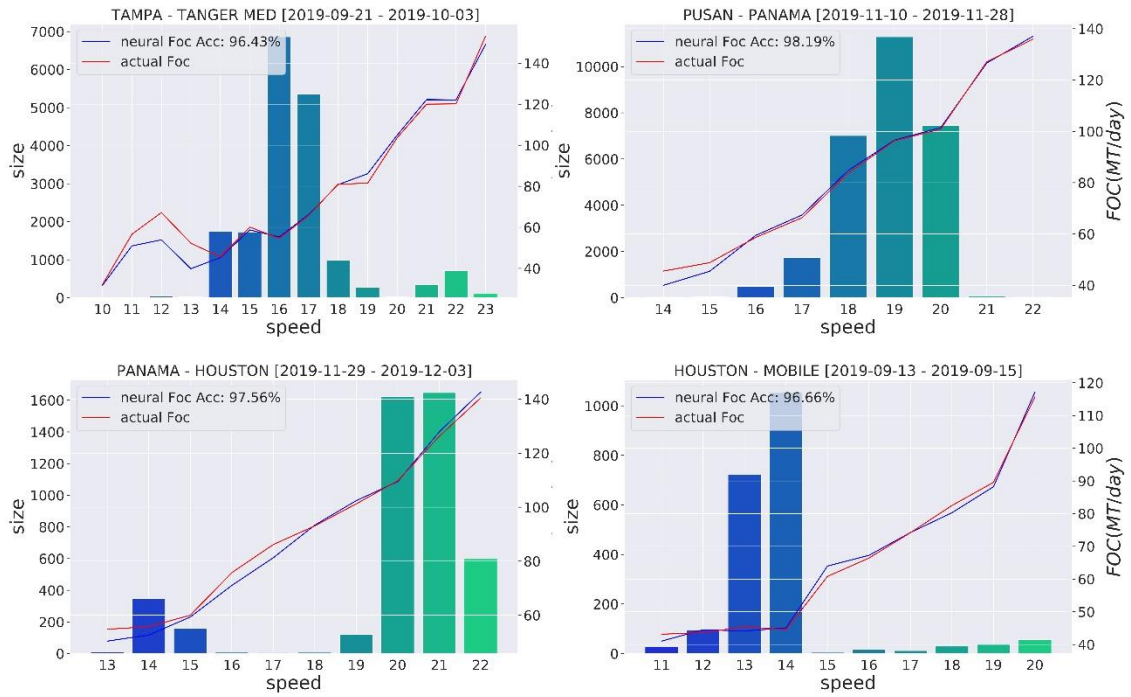

Figure 15. LSTM performance in 4 different voyages of the same container ship

Table 5. Computational performance of the FOC-model (LSTM)

	Act. FOC	Pred. FOC	Abs. Diff	Perc. Diff (%)
HOUSTON - MOBILE	71.84	72.68	0.84	1.16
PANAMA - HOUSTON	360.24	362.04	1.8	0.5
PUSAN - PANAMA	1725.14	1714.98	10.16	0.59
TAMPA - TANGER MED	774.53	771.45	3.08	0.4
Total	**2921.57**	**2931.94**	**10.56**	**0.36**

Computational performance superiority of the LSTM neural network model, as presented above, allows us to utilize it in the context of a weather routing optimization algorithm.

3.6 CO2 Emissions Model

After describing how the ship's demand curve (engine rpm vs engine power) can be evaluated under varying boundary conditions and showing different approaches for estimating consumption, it is possible to introduce the modelling that allows estimating the emission of greenhouse gases into the atmosphere, particularly CO2.

In detail, the International Maritime Organization (IMO) has established guidelines related to CO2 emissions under the MARPOL Annex VI [63]. These guidelines are aimed at reducing greenhouse gas

emissions from ships. However, it's important to note that the IMO guidelines do not provide a simple correlation factor for CO2 emissions but rather establish regulatory measures and standards to control and reduce emissions.

MARPOL Annex VI is an international convention that sets out regulations for the prevention of air pollution from ships. It includes provisions related to sulfur oxide (SOx) emissions, nitrogen oxide (NOx) emissions, and greenhouse gas emissions, including CO2.

The IMO has adopted specific Energy Efficiency Design Index (EEDI) and Ship Energy Efficiency Management Plan (SEEMP) requirements to address CO2 emissions from ships. The EEDI sets energy efficiency standards for new ships, considering their size and type, and aims to promote the use of more energy-efficient technologies. The SEEMP is a management plan that helps ship operators improve energy efficiency throughout the ship's operational life.

The guidelines also encourage the use of alternative fuels, such as liquefied natural gas (LNG), to reduce CO2 emissions. LNG has lower carbon content compared to traditional marine fuels like heavy fuel oil, which helps reduce greenhouse gas emissions.

While the IMO guidelines provide a framework to reduce CO2 emissions, the specific correlation factor for CO2 emissions would depend on various factors such as the ship's size, type, fuel consumption, and operational efficiency. It's important to note that the correlation between CO2 emissions and these factors is not a simple linear relationship but rather a complex interplay of multiple variables.

However, the CO2 emissions from ships are typically calculated based on fuel consumption and the carbon content of the fuel used. The formula used to estimate CO2 emissions can be expressed as follows:

$$CO2\ emissions\ =\ Fuel\ consumption\ x\ Carbon\ content\ of\ the\ fuel$$

The fuel consumption is usually measured in metric tons or metric tonnes (t), and the carbon content of the fuel is expressed in terms of the amount of carbon dioxide (CO2) produced per unit of fuel. This carbon content can vary depending on the type of fuel used, such as heavy fuel oil, marine diesel oil, liquefied natural gas (LNG), or other alternative fuels.

It's important to note that the actual calculation of CO2 emissions may involve additional considerations, such as the energy efficiency of the ship, operational factors, and specific measurement methodologies. These factors can vary depending on the specific guidelines and regulations in place.

In detail, the carbon content of different fuels used in the shipping industry can vary.

Hereinafter, are some general estimates of the carbon content for common marine fuels:

- Heavy Fuel Oil (HFO): Heavy fuel oil is a residual fuel derived from crude oil. Its carbon content is approximately 3.1 metric tons of CO2 per metric ton of fuel.
- Marine Diesel Oil (MDO) and Marine Gas Oil (MGO): These are lighter distillate fuels compared to heavy fuel oil. The carbon content of MDO and MGO is around 3.2 metric tons of CO2 per metric ton of fuel.
- Liquefied Natural Gas (LNG): LNG is a cleaner-burning fuel compared to conventional marine fuels. Its carbon content is significantly lower, approximately 2.75 metric tons of CO2 per metric ton of fuel. It should be noted that LNG emits fewer CO2 emissions during combustion, but there are other considerations regarding methane slip during storage and handling.
- Methanol: Methanol is an alternative marine fuel that can be produced from natural gas or renewable sources. Its carbon content is approximately 1.5 metric tons of CO2 per metric ton of fuel.

- Ethanol: Ethanol is another renewable fuel option. Its carbon content is approximately 2.2 metric tons of CO_2 per metric ton of fuel.

It's important to note that the carbon content values provided are estimates and can vary depending on the specific composition and production methods of the fuel. Additionally, the carbon content of alternative fuels can differ significantly from conventional fossil fuels, contributing to lower carbon emissions.

4 Navigation Management Models

4.1 Literature Overview

Navigation optimization algorithms are a class of algorithms that are used to optimize the performance of navigation systems. These algorithms can be applied to a wide range of navigation systems, including land, sea, and air navigation systems. Navigation optimization algorithms can be used to improve the efficiency and safety of navigation systems by reducing the risk of collisions, reducing fuel consumption, and improving the overall performance of the navigation system.

In recent years, there has been a significant amount of research on navigation optimization algorithms, with many different algorithms proposed in the literature. Some of the most popular navigation optimization algorithms include:

Genetic Algorithms (GA) are optimization algorithms that are based on the principles of natural selection and genetics. They are particularly well-suited for solving problems that are difficult to solve using traditional optimization algorithms [23].

A* algorithm is a popular algorithm for pathfinding and graph traversal. It uses a heuristic function to estimate the cost of reaching the goal and to guide the search process [24].

Dijkstra's algorithm is algorithm is similar to A*, but it does not use a heuristic function. Instead, it explores all possible paths from the start to the goal and selects the path with the lowest cost [25].

Rapidly exploring Random Tree (RRT), is an algorithm used for motion planning in high-dimensional configuration spaces. It creates a tree-like structure of possible paths and uses random sampling to explore the space and find the optimal path [26].

Particle Swarm Optimization (PSO) is an optimization algorithm that is inspired by the behavior of swarms of birds or fish. It is a population-based algorithm that can be used to find the global minimum of a function [27].

Ant Colony Optimization (ACO) is an optimization algorithm that is inspired by the behavior of ant colonies. It is a population-based algorithm that can be used to find the global minimum of a function [28].

These are just a few examples of navigation optimization algorithms that have been proposed in the literature. Each of these algorithms has its own strengths and weaknesses and is suitable for different types of navigation systems and different types of optimization problems.

Eventually, a navigation algorithm has not been chosen at this time, and further analysis needs to be conducted to assess which is the best option for the case study. Eventually, the most promising approaches seem to be the first ones listed, namely, A* & RRT.

4.2 Promising Navigation Optimization Algorithms

As already mentioned earlier the most promising and suitable algorithms for the case study under consideration are certainly A* and RRT.

A* (pronounced "A-star") is a popular pathfinding algorithm used to find the shortest path between two points on a graph or map. It is an informed search algorithm, meaning that it uses heuristics to guide its search towards the goal.

The A* algorithm maintains two lists: the "open list" and the "closed list". The open list contains nodes that have been visited but have not yet been fully explored, while the closed list contains nodes that have been fully explored. The algorithm starts by adding the starting node to the open list.

At each iteration, the algorithm selects the node on the open list with the lowest cost (the sum of the cost to reach that node and the estimated cost to reach the goal from that node), removes it from the open list, and adds it to the closed list. It then expands the node by generating its neighbouring nodes and adding them to the open list if they have not already been visited. The cost of each neighbouring node is calculated as the sum of the cost to reach the current node and the cost to move from the current node to the neighbouring node.

A* uses a heuristic function to estimate the cost from the current node to the goal. The heuristic function must be admissible, meaning that it never overestimates the actual cost to reach the goal, and consistent, meaning that the estimated cost from a node to its neighbour plus the cost from the neighbour to the goal is never less than the estimated cost from the node to the goal.

The algorithm continues to iterate until either the goal node is found, or the open list is empty. If the goal node is found, the algorithm reconstructs the path from the starting node to the goal node using the parent pointers stored in each node. If the open list is empty and the goal node has not been found, then there is no path from the starting node to the goal node.

In the marine sector, A* path planning is commonly used in autonomous underwater vehicles (AUVs) and unmanned surface vehicles (USVs) to navigate through underwater or surface environments. AUVs and USVs are used for various applications, such as oceanographic research, marine surveying, environmental monitoring, and offshore oil and gas exploration.

A* path planning can be used to help AUVs and USVs avoid obstacles, plan efficient routes, and navigate through complex underwater or surface environments. The algorithm can take into account factors such as current, water depth, and the presence of other vehicles or obstacles.

One application of A* path planning in the marine sector is in the field of oceanographic research. AUVs can be used to collect data on ocean currents, temperature, and salinity, which can be used to study ocean circulation and climate change. A* path planning can help the AUVs navigate through the ocean efficiently and avoid obstacles such as undersea mountains and canyons.

In the shipping industry, A* path planning can be used to optimize ship routes and avoid collisions. Ships can use real-time data such as weather conditions, ocean currents, and traffic density to calculate the most efficient route to their destination. A* path planning can also help ships avoid collisions with other vessels or obstacles in the water.

In particular, the A* algorithm uses two main equations to determine which node to visit next:

$$f(n) = g(n) + h(n)$$

where: $f(n)$ represents the total cost of node n; $g(n)$ is the cost to travel from the starting node to node n and $h(n)$ is the estimated cost to travel from node n to the goal node. This equation is known as the "f-cost" equation and is used to prioritize which node to visit next.

$$g(n') = g(n) + c(n, n')$$

$g(n')$ represents the cost to travel from the starting node to the neighbouring node n', where $c(n, n')$ is the cost to move from node n to n'. This equation is used to calculate the cost of each neighboring node and is used to update the parent pointer of each neighbouring node to point to the current node.

The A* algorithm also uses a heuristic function, which is used to estimate the cost from a given node to the goal node. The heuristic function is denoted as $h(n)$ and must be admissible (i.e., it never overestimates the actual cost to reach the goal) and consistent (i.e., the estimated cost from a node to its neighbour plus the cost from the neighbour to the goal is never less than the estimated cost from the node to the goal). The choice of heuristic function can greatly affect the efficiency and accuracy of the A* algorithm.

The other interesting method is the RRT a popular path planning algorithm used in robotics and motion planning. RRT* (RRT-star) is an improved version of the RRT algorithm that uses a more optimal tree structure and a better cost function to find a higher-quality path.

In RRT*, the algorithm maintains a tree structure that grows iteratively from the starting point towards the goal. The algorithm generates random nodes in the search space and extends the tree towards the new node. The tree is built incrementally by selecting the node in the tree that is closest to the new node and adding a new node in the direction of the new node. The algorithm continues to extend the tree until the goal is reached or a maximum number of nodes have been added to the tree.

In RRT*, the cost of each node is calculated using the "backtracking" technique. This technique involves calculating the cost of a node by considering its parent node and the cost of moving from the parent node to the current node. The cost of a node is the sum of the cost of its parent and the cost of the transition to the current node.

The RRT* algorithm improves upon the RRT algorithm by introducing a better cost function and a more optimal tree structure. RRT* uses a cost function that takes into account the cost of the path to the node, as well as the distance from the node to the goal. This cost function encourages the algorithm to explore the search space more efficiently and find higher-quality paths.

RRT* also uses a more optimal tree structure that balances the trade-off between exploration and exploitation. The algorithm uses a "rewiring" step that connects nearby nodes to the tree and updates the parent-child relationships of nodes to improve the overall cost of the tree.

Moreover, RRT* is an "anytime" algorithm, which means that it can return a solution at any time during the search. This can be useful in applications where it is important to quickly find a feasible path, even if it is not optimal. The algorithm can then continue searching to improve the quality of the path.

Another crucial characteristic of RRT* method is that can also be extended to handle multiple objectives, such as minimizing travel time, energy consumption, or risk of collision. This is done by using a multi-objective cost function and finding the Pareto-optimal solutions, which are the paths that cannot be improved in one objective without sacrificing the other objectives.

Overall, RRT* is a versatile algorithm that can be applied to a wide range of path planning problems. Its ability to handle high-dimensional search spaces and complex environments makes it a popular choice in robotics and motion planning research.

4.3 COLREG Rules

Speaking of navigation algorithms, i.e., path planning, it is necessary to introduce the concept of COLREG rules if route re-planning is to perform a dynamic function, operating in real time during navigation, i.e., suggesting a route that ensures collision between two vessels.

In detail, The COLREG rules, short for "International Regulations for Preventing Collisions at Sea," is a set of rules established by the International Maritime Organization (IMO) to prevent collisions between vessels at sea. The COLREG rule applies to all vessels, regardless of size, type, or nationality, when they are in international waters or in the waters of a country that has adopted the rule.

The COLREG rule is designed to ensure that all vessels navigate safely and avoid collisions, regardless of their size or type. The rule emphasizes the importance of maintaining a proper lookout, taking action to avoid collisions, and using lights, sounds, and signals to communicate with other vessels. It also establishes a hierarchy of vessels, with larger vessels having the right of way over smaller vessels.

Violating the COLREG rule can result in serious consequences, such as fines, imprisonment, or even loss of life. Therefore, it is important for all mariners to be familiar with the rule and to follow its provisions in all circumstances.

The main types of approach between ships in the COLREG rules are defined as follows:

- Head-on approach: This is when two vessels are approaching each other in such a manner that there is a risk of collision if both vessels maintain their course and speed. In this situation, both vessels must alter their course to starboard (right) so as to pass port-to-port.
- Crossing situation: This is when two vessels are crossing each other's course in such a manner that there is a risk of collision if both vessels maintain their course and speed. In this situation, the vessel which has the other vessel on its starboard side must give way and take early and substantial action to avoid collision.
- Overtaking situation: This is when one vessel is overtaking another vessel in such a manner that there is a risk of collision if both vessels maintain their course and speed. In this situation, the vessel that is being overtaken has the right of way and should maintain its course and speed while the overtaking vessel should keep out of the way of the vessel being overtaken.

Eventually, the COLREG rule provides specific guidance on the actions that vessels should take in each of these situations in order to ensure the safety of all vessels involved. For such a reason it is mandatory develop a navigation algorithm COLREG complied if route re-planning is to perform a dynamic function, operating in real time during navigation.

An example of this approach was achieved using RRT*. Dynamically for each instant the ship recalculated the path so as to circumvent fixed and moving obstacles (other ships). The information used to determine the speed and position of other ships was obtained from the AIS device readings [29,30,31].

4.4 Navigation Management Models Repository

In the following sections we describe briefly the project on-going repository on Path Planning/ Weather Routing optimization models that aims to act as the cornerstone to transcend beyond SOTA Voyage Planning solutions and offer a versatile platform towards a zero-emission operational blueprint.

4.4.1 Shortest Path Extraction

Project partner DANAOS has developed a baseline approach in order to derive shortest path routes based on user-defined origin/ destination waypoints via an API call. The methodology adopted is based on AtoBviaC [1]library which provides offline access to distances and routes from the AtoBviaC route network. More specifically the algorithm transcends beyond the "trivial" shortest path finding problem by incorporating a variety of constraints concerning sensitive aquaculture, piracy zones and ECA/SECA areas. These constraints are included in the algorithm by applying appropriate weighting on the graph provided by AtoBviaC library. The dedicated API call with a detailed list of parameters to generate a candidate shortest path between two waypoints is presented in Figure 16 in the swagger UI.

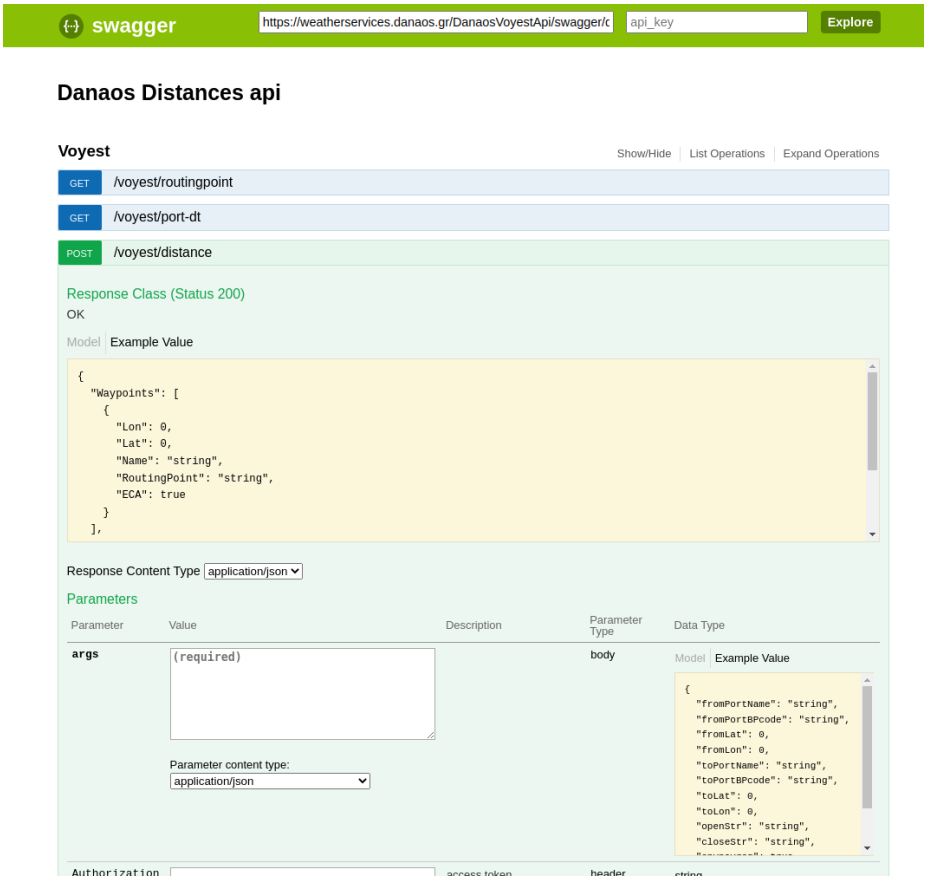

Figure 16. Swagger UI for the dedicated shortest path API call

Once the origin and destination waypoints have been defined, the AtoBviaC library can be used to calculate the shortest path route between them. This is achieved using a variant of the Dijkstra algorithm, which is a graph search algorithm that is used to find the shortest path between two nodes in a graph.

In addition to finding the shortest path, the algorithm incorporates the aforementioned constraints by modifying the weights of the edges in the graph. For example, edges that pass through sensitive aquaculture areas can be given a higher weight, making them less likely to be included in the shortest path. Similarly, edges that pass-through piracy zones or ECA/SECA areas can be given a higher weight to avoid them whenever possible.

[1] https://autobviac.com

Once the weights of the edges have been determined, the algorithm can be run to find the shortest path route between the user's origin and destination waypoints while taking into account the constraints imposed by sensitive aquaculture, piracy zones, and ECA/SECA areas.

Eventually, the results can be presented to the user in a user-friendly format, such as a map or a list of waypoints along the route. The user can then modify the route as necessary, for example, by adding or removing waypoints, to optimize the route further.

In the following figure we demonstrate the result of the API call utilizing the dedicated DT4GS GUI for an example route between port Tamp (FL) and port Tange Med (MR).

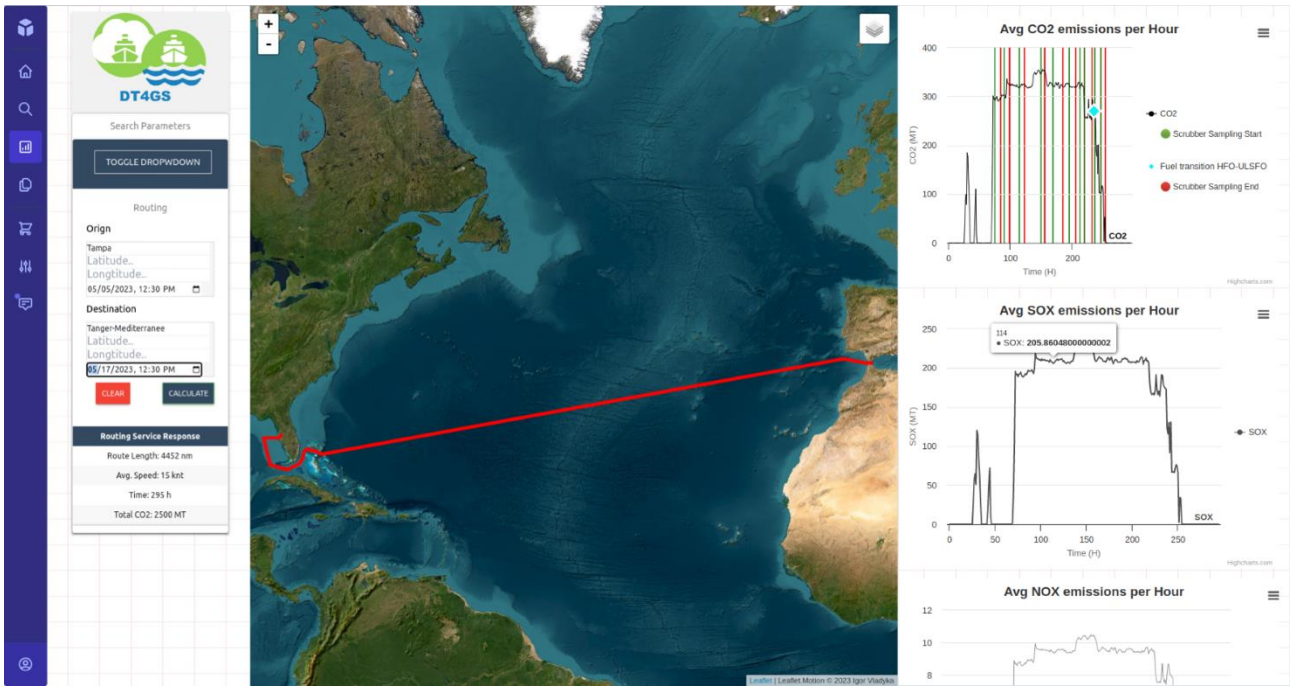

Figure 17. Shortes path between TAMPA – TANGER MED

5 Integrated Modelling Framework for Ship Performance improvement

In the Voyage optimization pipeline the main inputs are the mission to be accomplished by the ship, in terms of time and place of port departure and arrival, and the weather conditions that will be encountered along the route.

The route can be divided into several legs to estimate the speed it will need to maintain along the route of a single leg.

In the context of voyage optimization, the weather routing module and the Just in time (JIT) model can be observed.

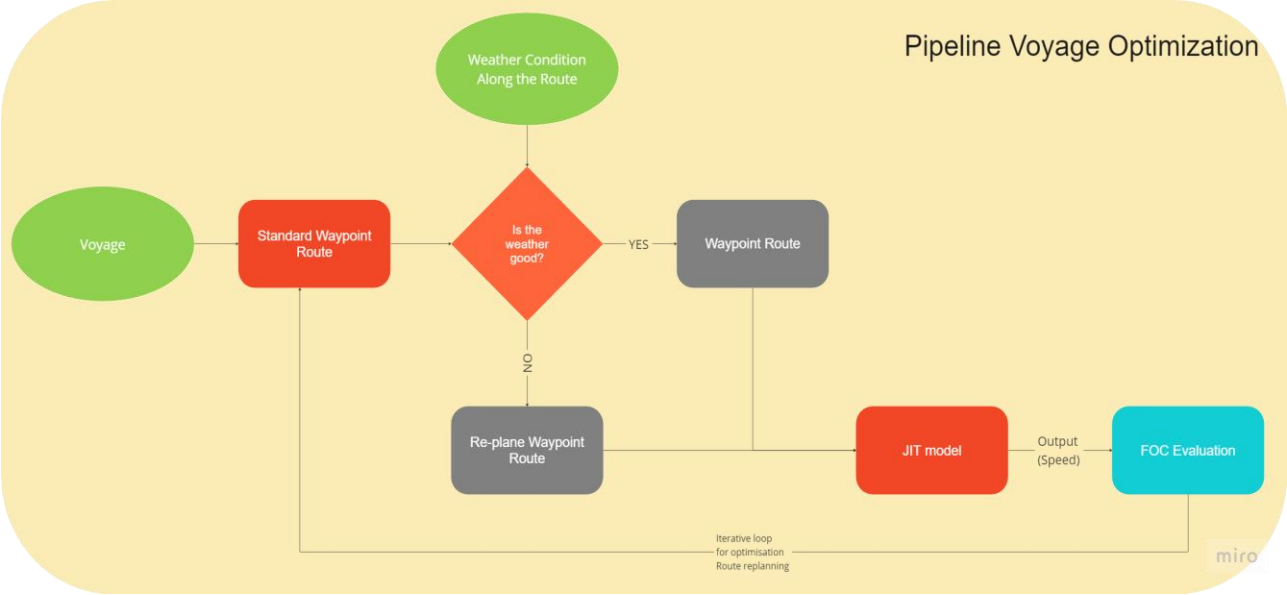

Figure 18. pipeline voyage optimization

5.1 Weather Routing Model

In detail, the weather routing model is the process of optimizing a vessel's route and speed to avoid hazardous weather conditions while minimizing fuel consumption and maximizing the safety of the crew and cargo. Weather routing involves analyzing weather data, including wind, wave height, current, and other factors, to determine the most efficient and safe route for a vessel to take.

The primary goal of weather routing is to minimize the time and distance required for a vessel to reach its destination, while also ensuring the safety of the crew and cargo. This involves taking into account factors such as the vessel's size, speed, and maneuverability, as well as the weather conditions it may encounter along its route.

Modern weather routing technology uses advanced computer models and algorithms to analyze weather data in real-time, allowing vessel operators to make informed decisions about their route and speed. This technology can also provide alerts and recommendations based on changing weather conditions, helping operators to avoid dangerous weather and adjust their route as needed.

There are different approaches to implementing weather routing on-board a vessel, depending on the vessel type and available technology. However, the main approach typically involves the following steps:

1. Gathering weather data: Real-time weather data is collected from various sources, such as weather satellites, buoys, and weather models. This data is used to create a weather forecast for the vessel's intended route.
2. Analyzing weather data: The weather data is analyzed using advanced algorithms to predict how weather conditions will affect the vessel's speed, fuel consumption, and safety. This analysis takes into account the vessel's characteristics, such as its size, speed, and maneuverability.
3. Generating a route plan: Based on the weather analysis, a route plan is generated that optimizes the vessel's route and speed to minimize fuel consumption, reduce voyage time, and avoid hazardous weather conditions. The plan takes into account factors such as wind, waves, currents, and other hazards.
4. Monitoring weather conditions: Throughout the voyage, the crew monitors weather conditions and adjusts the vessel's route and speed as needed to avoid dangerous conditions and optimize fuel consumption.

A potential mathematical approach, using optimization techniques, to optimize a ship's route with weather routing has been reported hereinafter:

Define Variables:

Let R be the set of possible route segments, each representing a potential path between two waypoints.

Let x_r be a binary variable indicating whether route segment r is included in the optimized route.

Let d_r be the distance of route segment r.

Let F_r be the fuel consumption associated with route segment r.

Let W_r be a weather factor associated with route segment r, representing the adverse effects of weather conditions.

Set Objective Function:

Define the objective function to be minimized, considering fuel consumption and weather effects:

Minimize: $\sum(x_r * F_r * W_r)$

Subject to Constraints:

Connectivity Constraint: Ensure that the optimized route is a connected sequence of route segments.

$\sum(x_r) = 1$ for each waypoint except the initial and final waypoints.

Time Constraint: Set a maximum time constraint for the voyage, if applicable.

$\sum(x_r * d_r) \leq T_{max}$

Weather Avoidance Constraint: Avoid route segments with adverse weather conditions, if possible.

$x_r = 0 \; for \; segments \; with \; W_r > W\_threshold$

Vessel Performance Constraints: Consider the vessel's performance limitations, such as maximum speed or stability requirements.

Additional constraints can be added based on vessel-specific considerations.

Solve the Optimization Problem:

Formulate the optimization problem as a mixed-integer linear program (MILP) or nonlinear program (NLP), depending on the complexity of the problem and the desired level of accuracy.

Utilize optimization solvers or software packages to solve the formulated problem and obtain the optimal route solution.

Analyze and Validate Results:

Analyze the obtained optimized route and assess its feasibility and practicality.

Consider any additional factors or constraints not included in the optimization model that may affect the route selection.

Validate the results by comparing them with expert knowledge or previous successful routes.

Continuous Monitoring and Updates:

Weather conditions may change during the voyage, requiring route adjustments.

Continuously monitor weather forecasts and update the route plan accordingly using the same optimization approach.

This mathematical approach provides a framework for systematically optimizing the ship's route considering fuel consumption, weather conditions, and other constraints. However, the implementation may require customization and fine-tuning based on the specific needs and available data for the weather routing problem at hand.

An example, to benchmark further the approach shown in 4.4.1, we demonstrate in this section a novel weather routing algorithm to support vessel routing decisions towards the reduction of FOC. The WR algorithm that has been utilized is based on the isochrone principle. It builds upon a predetermined basic route; this route can be the original route planned by the vessel's master or provided by a basic routing algorithm (like the method proposed in the previous section). In the context of this work an initial route was employed on the basis of shortest path principles. The original (initial) route is then broken into segments, with respect to a given time step (indicating the master's routing decision horizon, e.g., every 6 hours), and a graph is built around it that enables course and speed deviations, while ``following'' the direction of the vessel's original course. To this end, for each node of the original route, a set of nodes is added in a ''parallel'' fashion on both sides of the route (i.e., parallel to the direction of the original route). Edges are added between all nodes of subsequent sets. Note that nodes that are identified to be on land as well as edges that go above land segments are naturally excluded from the graph.

Once the graph is created (Figure 19), a data driven FOC model that is demonstrated in section 7, is used to obtain the FOC of each edge of the graph, i.e., of each corresponding sea route, given the vessel's STW, draft and corresponding weather conditions along that sea route. After scoring each sea route (i.e., graph edge), a variation of Dijkstra's algorithm for the shortest path problem is utilized to obtain the route that minimizes the total route FOC (i.e., considering the calculated FOC of each edge as its corresponding ``edge weight'' or ``distance'').

Note that since the algorithm is isochrone, the produced route also satisfies any constraints concerning the time of arrival (if any).

Note also that the decision variables for the WR algorithm are only the STW and the vessel's direction, since these are the aspects that the vessel's master can control. Obviously, any change in the vessel's speed affects directly FOC (since STW is a basic feature of the corresponding model). However, changes in speed and direction also affect FOC indirectly since they alter the spatio-temporal state of the vessel and hence the corresponding weather conditions.

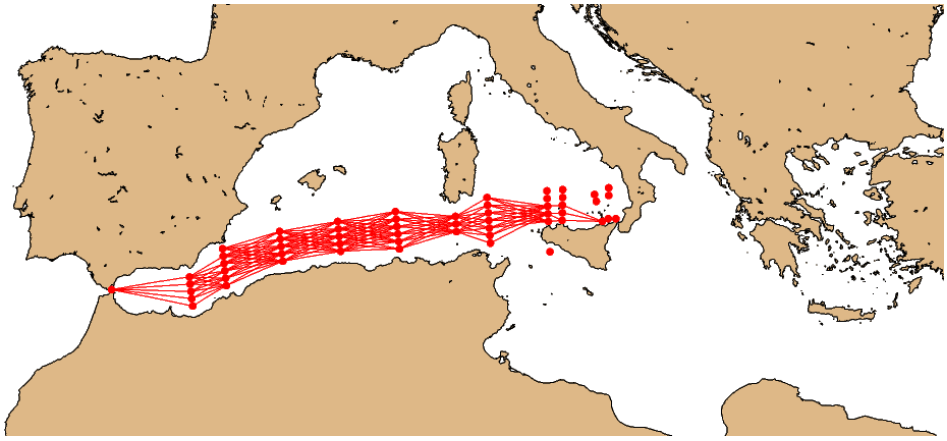

Figure 19. Graph construction comprised of alternative waypoints (red circles) for an example route.

We continue by demonstrating the results of the WR optimization algorithm explained briefly above. We compare the total FOC of an initial transatlantic voyage conducted by the vessel's master, with the suggested optimized route produced from the WR algorithm by utilizing the aforementioned LSTM FOC model. Furthermore, we calculate the total distance travelled, the estimated time of arrival, the average speed and the emissions emitted for the two alternative routes by incorporating Figure 20, and we exhibit the results in Table 6.

Consecutively we demonstrate the weather [wind speed (m/s)] of the initial and the optimized route per hour, in Figure 20.

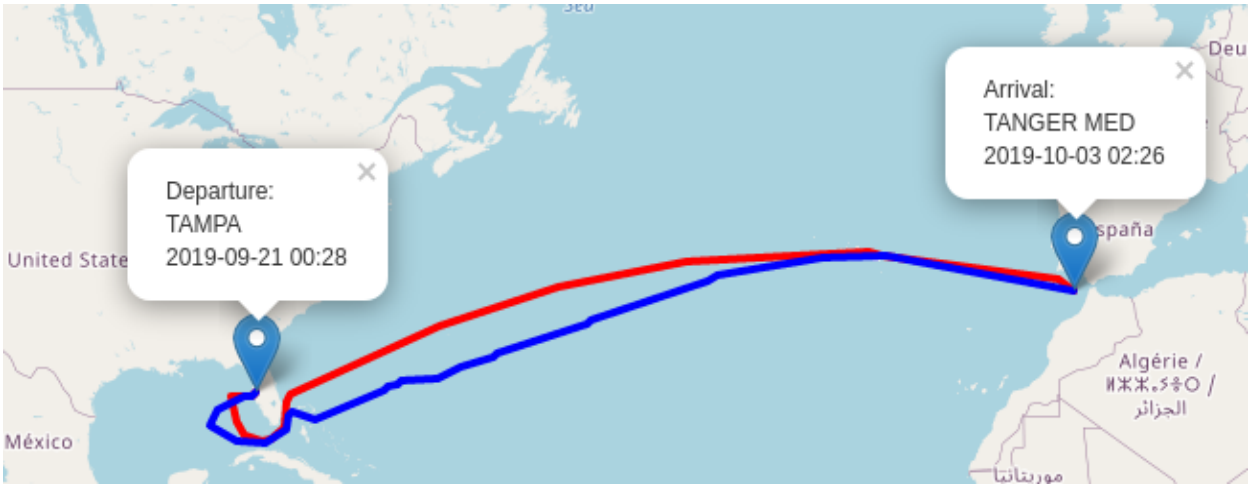

Figure 20. Initial (blue) and Optimized (red) route for one leg: TAMPA (FLORIDA U.S) - TANGER MED (MOROCCO)

Table 6. Estimation based on Weather Service (NOAA)

Voyage	Date	Latitude	Longitude
Departure	2019-09-21	27.7° N	82.5° W
Arrival	2019-10-03	35.8° N	6° W
BASIC COMPARISON	**Actual route estimation**	**Optimized route estimation**	
Distance (nm)	4787.4	4369.36	
Time (hours)	289.97	264.63	
Avg Speed (kt)	16.52	16.51	
Total FOC (MT)	774.53	759.97	
CO_2 (MT)	2411.88	2366.54	

It is evident from Table 6 above that by utilizing an advanced WR algorithm we are able to further optimize the shortest path route explained in 4.4.1 and provide a fine-grained optimal, route in terms of speed, ETA and overall environmental footprint (overall CO2 emitted).

Eventually, weather routing is particularly important in the shipping industry, where large vessels must navigate through often unpredictable weather conditions to transport goods across the world's oceans.

Several approaches are available in the literature, some of which perform route optimization not only in terms of waypoint displacement, but also in terms of route speed [32, 33]. Indeed, by optimizing routes and speeds, weather routing technology can help shipping companies reduce fuel consumption and emissions, lower operating costs, and improve the overall efficiency and safety of their operations. In the approach shown, ship speed was not taken into account because this aspect was evaluated in the just-in-time module.

5.2 Just in Time (JIT) Model

In the marine sector, the "just-in-time" model refers to an approach that aims to optimize navigation time and vessel arrival schedules. It involves coordinating the movement of vessels to minimize waiting times at ports and maximize efficiency in the maritime supply chain.

Traditionally, vessels arriving at ports have been subject to fixed schedules and must adhere to predetermined arrival times. However, the just-in-time model recognizes that these fixed schedules often lead to inefficient operations, with vessels spending significant time waiting at ports before they can unload or load cargo.

To overcome these inefficiencies, the just-in-time model leverages advanced technologies and data sharing between various stakeholders, such as port authorities, shipping companies, and terminal operators. This allows for improved coordination and real-time information exchange, enabling vessels to arrive at ports at the most optimal time.

For example, by using an advanced planning and scheduling is possible to perform an accurate estimation of vessel arrival times. Indeed, by considering factors such as weather conditions, sea currents, traffic congestion, and berth availability the most favourable time for a vessel to arrive at the port can be assess.

It is crucial that stakeholders share relevant data in real-time, including vessel positions, port conditions, and cargo availability. This information exchange facilitates efficient planning and decision-making, allowing vessels to adjust their speed and course to maintain the scheduled arrival time.

Indeed, the just-in-time model requires collaboration among different parties involved in the maritime supply chain. This includes vessel operators, port authorities, pilots, tug operators, and terminal operators. By working together, they can optimize operations, reduce congestion, and minimize waiting times for vessels.

The main advantage by using this approach is the optimization of vessel speed, indeed, the just-in-time model considers the optimal speed for vessels to maintain throughout their journey. By adjusting the speed based on factors like traffic congestion, weather conditions, and port schedules, vessels can arrive at their destination at the most appropriate time. This optimization helps minimize waiting times and improve overall efficiency.

The optimization of the speed archives three importance aims:

- Improved Operational Efficiency: The just-in-time model optimizes vessel schedules and arrival times, reducing waiting times at ports and improving overall operational efficiency. It helps vessels minimize idle time and ensures that necessary resources are available when needed, leading to streamlined processes and reduced costs.
- Cost Savings: By minimizing waiting times and optimizing navigation, the just-in-time model can result in significant cost savings for shipping companies and port operators. Reduced fuel consumption, improved berth utilization, and efficient cargo handling contribute to lower operational costs.
- Environmental Benefits: The model supports sustainability goals by reducing fuel consumption and greenhouse gas emissions. Optimized navigation and reduced waiting times lead to lower carbon footprints, aligning with global efforts to mitigate climate change and improve environmental performance in the maritime sector.

Nowadays, the used methodology is called "hurry up and wait". It is a scheduling and operational approach that involves assigning fixed arrival times for vessels at ports or other facilities. In this method, vessels are required to hurry or expedite their journey to reach the designated location by the specified time. However, despite the urgency and the need to hurry, vessels often experience delays and periods of waiting once they arrive at the intended destination. These waiting periods can vary in length and occur due to various reasons, such as limited berth availability, congestion at the port, customs clearance processes, or other operational constraints.

The "hurry up and wait" method has been criticized for its inefficiencies and potential negative impacts on operational performance. Some drawback of this approach is, for example, that vessels may arrive at the port before their scheduled berthing time, leading to idle periods where resources, such as berths, cranes, and labour, are underutilized. This can result in wasted time and increased costs.

Moreover, fixed arrival times can lead to congestion at ports when multiple vessels arrive simultaneously or when there is a delay in berthing. This congestion can cause further delays and disruptions in the overall supply chain.

It is worth noting that the "hurry up and wait" approach may have been more prevalent in the past when technology and real-time information sharing were not as advanced. In recent years, there has been a shift towards adopting more dynamic and flexible scheduling models, such as the just-in-time model, to optimize vessel arrival times and minimize waiting periods.

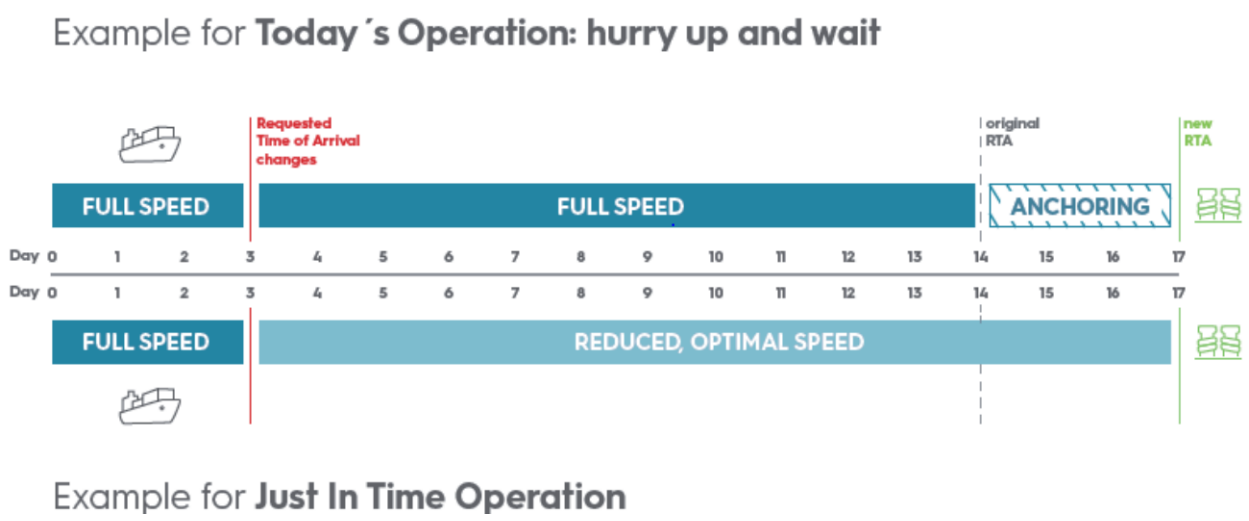

Figure 21. Comparison between Just in Time and Hurry up & Wait methods [34]

The benefits of implementing the just-in-time model in the marine sector are numerous. It can help reduce fuel consumption and greenhouse gas emissions by minimizing unnecessary vessel idling time. It also enhances operational efficiency by reducing congestion at ports, improving berth utilization, and optimizing cargo handling processes. Moreover, the model can enhance reliability and predictability in the maritime supply chain, leading to better planning and cost savings for shipping companies and port operators.

By knowing the legs, by the several waypoints (x_n) of the route and the scheduled time it is possible to evaluate the distance by means of the Haversine Formula and evaluate the ship's speed mean (V_{mean}) for the route. The optimization consists of to change the value of the speed in single leg, decreasing it, to achieve the request time of arrival by this it is possible to reduce the fuel oil consumption.

$$x_{n-1}\begin{cases} lat_{ini}\ [rad] \\ lon_{ini}\ [rad] \end{cases} \quad ; \quad x_n\begin{cases} lat_{fin}\ [rad] \\ lon_{fin}\ [rad] \end{cases}$$

$$a = \sin\left(\frac{lat_{fin} - lat_{ini}}{2}\right)^2 + \cos(lat_{ini})\cos(lat_{fin})\sin\left(\frac{lon_{fin} - lon_{ini}}{2}\right)^2$$

$$c = 2\,\mathrm{atan}\left(\frac{\sqrt{a}}{\sqrt{1-a}}\right)$$

$$dist_{leg\ n} = (x_n - x_{n-1}) = c\ R_{earth}$$

where, R_{earth} is the mean radium of the Earth equal to 6371 km.

$$V_{mean} = \frac{1}{N}\sum_{i=1}^{N}\frac{(x_n - x_{n-1})}{(t_n - t_{n-1})}$$

Eventually, the implementation of the just-in-time model requires close collaboration and coordination among various stakeholders. It may involve overcoming challenges related to data privacy, standardization, and ensuring the compatibility of systems and processes across different entities. However, with the advancements in technology and increased emphasis on sustainable and efficient operations, the just-in-time model holds significant potential for optimizing navigation time in the marine sector.

5.3 Trade-off Between JIT and Weather Routing

The trade-off between weather routing and just in time (JIT) method is an important consideration for companies involved in marine transportation. While weather routing can help vessels avoid hazardous weather conditions and optimize their routes to save time and fuel, JIT emphasizes the importance of delivering goods to their destination precisely on time, without unnecessary delays or inventory build-up.

There are several factors to consider when balancing these two approaches, including:

- Cost: JIT can be more costly due to the need for faster and more frequent deliveries, while weather routing can help reduce fuel consumption and lower transportation costs.
- Safety: Weather routing prioritizes safety by avoiding hazardous weather conditions, while JIT may require vessels to take risks to meet tight delivery schedules.
- Reliability: JIT requires precise timing and coordination between suppliers, shippers, and receivers, while weather routing may involve delays due to weather conditions, which could affect the reliability of delivery schedules.
- Flexibility: Weather routing allows for more flexibility in terms of adjusting delivery schedules to avoid dangerous weather, while JIT relies on strict schedules and may not allow for much flexibility.
- Ultimately, the choice between weather routing and JIT depends on the specific needs and goals of the company. Some companies may prioritize speed and reliability and opt for JIT, while others may prioritize safety and efficiency and choose weather routing. In some cases, companies may use a combination of both approaches to balance the benefits and trade-offs of each method.

In addition to the factors mentioned earlier, there are other important considerations when balancing weather routing and JIT, including:

Customer expectations: The expectations of customers for timely delivery can also influence the decision between weather routing and JIT. If customers place a high priority on fast and reliable delivery, JIT may be the preferred approach, even if it comes with higher costs and risks.

Risk tolerance: Companies with a low risk tolerance may prefer weather routing to minimize the risks associated with hazardous weather conditions, while companies with a higher risk tolerance may be willing to take more risks to meet delivery schedules.

Market competition: The level of competition in the market can also influence the choice between weather routing and JIT. If competitors are offering fast and reliable delivery, companies may need to implement JIT to remain competitive, even if it comes with higher costs and risks.

In general, the voyage optimization involves integrating various factors, this approach can help vessels to minimize fuel consumption, reduce voyage time, and ensure timely delivery of goods to their destination.

In the context of JIT delivery and weather routing, voyage optimization involves balancing the competing demands of timely delivery and safe, efficient navigation. For example, if weather conditions are hazardous, the vessel may need to adjust its route to avoid these conditions, even if it means delaying delivery. On the other hand, if delivery is time-sensitive, the vessel may need to take more risks and navigate through hazardous weather conditions to meet the delivery schedule.

Voyage optimization can help companies to achieve a balance between JIT delivery and weather routing by providing a data-driven approach to voyage planning and execution. By integrating various factors and optimizing the voyage plan accordingly, companies can reduce transportation costs, improve reliability and efficiency, and enhance customer satisfaction.

For a commercial ship, voyage optimization considering JIT and weather routing involves integrating various factors to optimize the voyage plan and ensure efficient, safe, and timely delivery of goods to their destination.

The trade-off between weather routing and JIT is a complex and multifaceted decision that requires careful consideration of a variety of factors. Companies should evaluate the benefits and risks of each approach, as well as the specific needs and expectations of their customers and stakeholders, to make an informed decision that aligns with their overall business goals and values.

Moreover, considering fuel consumption and greenhouse gas emissions, the trade-off between the just-in-time model and weather routing lies in finding the right balance between operational efficiency and weather-related considerations. While the just-in-time model primarily focuses on optimizing schedules and reducing waiting times, weather routing prioritizes safety and minimizing fuel consumption in relation to weather conditions.

Finding the optimal trade-off involves evaluating the potential fuel savings and emissions reduction from operational efficiency improvements achieved through the just-in-time model against the benefits of weather routing in terms of minimizing fuel usage and emissions by avoiding adverse weather conditions. It is essential to consider factors such as the frequency and severity of adverse weather, vessel characteristics, and the availability of accurate weather forecasts and routing advice.

Integrating elements of both models, where feasible, can lead to synergistic benefits. For example, the just-in-time model can consider weather information to adjust vessel schedules and routes, accordingly, optimizing both operational efficiency and fuel consumption. This integrated approach allows for better fuel management, reduced emissions, and improved sustainability in the maritime sector.

Overall, the trade-off between the just-in-time model and weather routing regarding fuel consumption and greenhouse gas emissions involves balancing operational efficiency, safety, and weather-related considerations to achieve the most sustainable and environmentally friendly outcomes.

6 Hull and robotics inspection models

6.1 System Overview

Inspecting the condition of a ship's hull is of utmost importance due to the potential problems associated with biofouling and the significance of maintaining clean cargo holds. These factors have a profound impact on a ship's performance, efficiency, and overall safety. To address these challenges effectively, advanced inspection techniques, including the utilization of robotic platforms, can play a pivotal role in ensuring thorough assessment and maintenance processes.

Biofouling, the accumulation of marine organisms on the hull's surface, presents considerable risks. Algae, barnacles, and other organisms can increase drag and resistance, adversely affecting the hydrodynamics of a ship. This leads to decreased speed, heightened fuel consumption, increased operating expenses, and elevated carbon emissions. By meticulously inspecting the hull for biofouling, shipowners can promptly identify and address this issue, ensuring optimal vessel performance while minimizing the environmental consequences associated with the introduction of invasive species to new marine environments.

Equally important is the need to maintain clean cargo holds. Lingering remnants from previous cargoes can contaminate subsequent loads, resulting in cargo damage and potential claims from cargo receivers. Certain cargoes, such as sulphur or coal, may contain corrosive elements that can pose a threat to the hull and steel structures if not adequately removed. Moreover, inadequately cleaned cargo holds can lead to wastage, off-hire disputes, and delays in the transportation process. Ensuring the cleanliness of cargo holds is critical to upholding the integrity of the vessel, adhering to regulations, and safeguarding the quality of the transported goods.

To enhance the inspection processes, advanced techniques such as robotics can be employed to conduct thorough assessments of the hull's condition. These inspections utilize sophisticated sensors and cameras to accurately detect signs of biofouling and potential areas of concern. Integrating advanced inspection techniques, including robotics, into the evaluation of a ship's hull condition, addressing biofouling concerns, and maintaining clean cargo holds significantly enhances overall efficiency and safety. By embracing these technologies, shipowners can proactively preserve vessel performance, mitigate costly damages, and ensure compliance with environmental regulations. The implementation of advanced inspection methods promotes safer operations, more effective resource management, and the advancement of sustainable practices within the maritime industry.

In the following paragraphs, these two concerns will be presented separately, and inspection models with robotic platforms will be proposed. These advanced inspection models, incorporating AI algorithms, sensors, and recognition techniques, will offer innovative solutions for the assessment of the ship's hull condition, the detection of biofouling, and the assurance of thorough cleanliness in cargo holds. By employing robotic platforms in these inspection processes, the efficiency, accuracy, and safety of evaluations can be enhanced, allowing for proactive maintenance and timely intervention to mitigate potential risks.

6.2 Biofouling: A literature Review

The escalating menace of climate change and global warming has emerged as a major subject of apprehension due to the widespread discharge of pollutants into the environment owing to human activities. These alterations in the environment have resulted in catastrophic outcomes such as melting of glaciers, escalation of sea levels, exacerbation of droughts, and an amplification in occurrences of severe weather phenomena [35]. In response to this burgeoning crisis, the Paris Agreement has been ratified by 196 nations, which have jointly pledged to reduce greenhouse gas emissions to limit global warming below the 2℃ threshold relative to pre-industrial levels, with the objective of averting any further deterioration of the environment [36].

The International Maritime Organization, IMO, has, also, responded decisively to the challenge of escalating emissions focusing in shipping sector, which accounted for a staggering 1,076 million tons of air pollutants in 2018, contributing to 2.9% of global human-generated emissions. IMO is committed to decarbonizing international shipping and has adopted various strategies to achieve this objective. These include decreasing carbon emissions from new vessels through the Energy Efficiency Design Index (EEDI), minimizing carbon emissions in shipping by a minimum of 40% by 2030 and 70% by 2050 (compared to 2008 levels), and enhancing the energy efficiency of existing vessels [37].

Multiple approaches are being explored to reduce the energy footprint of shipping, such as transitioning to cleaner fuels like liquefied natural gas, hydrogen, and ammonia, implementing energy-saving devices on ships, and optimizing ship routes to improve efficiency. The accumulation of marine organisms on the submerged surface of ship hulls, called biofouling, has a significant impact on a vessel's hydrodynamic performance [38, 39]. When a ship is submerged in seawater, a biofouling attachment begins to form on the structure. Before bacteria and single-celled organisms settle and aggregate into layers of a film known as slime, organic molecules begin to adhere as shown in the figure.

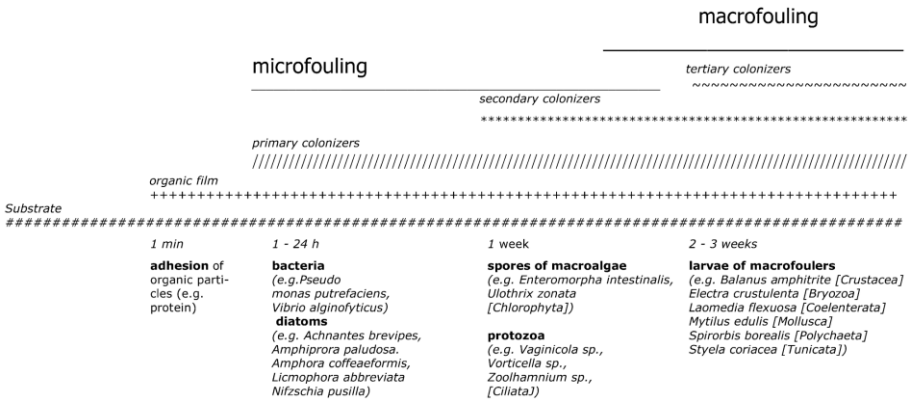

Figure 22. Temporal structure of settlement [40]

After this, the sludge secretes a number of chemicals that cause the concentration of multicellular and macrofouling species as a result of the amount of food available to them, and calcareous fouling develops [35].

The roughness of the hull surface due to bio-fouling results in increased friction and, consequently, greater power requirements and fuel consumption [35,38], leading to an increase in vessel fuel consumption, emissions, and cleaning expenses.

6.2.1 Biofouling Treatment Methods

Marine organisms adhering to a ship's hull cause major issues for both the environment and maritime transportation performance. Biofouling increases ship resistance, which leads to higher power requirements and greater fuel consumption. Research examining commercial ships has revealed that a thin layer of sludge, up to 50% on the hull's surface, can result in a 20 to 25% rise in fuel consumption, thereby increasing the emission of gaseous pollutants [41]. It is, therefore, essential to implement strategies for cleaning the hull and using antifouling systems to prevent organism attachment.

An anti-fouling system refers to any coating, surface treatment, or equipment used on a ship to control or prevent the attachment of unwanted marine organisms. Antifouling coatings are currently the most popular system used by ships, but there are other options available that can be used in conjunction with or without the existing coating. These include ultrasound, ultraviolet radiation, marine growth prevention systems, and robotic biofouling clean-up systems.

Biocidal antifouling systems

Biocidal antifouling systems involve using paints that gradually release biocides from the paint film on the hull surface, preventing marine organisms from adhering. These paints typically contain copper biocides, with or without organic co-biocides or organic biocides. It's important to note that different types of biofoulings develop at varying rates in different environments. Therefore, the appropriate paint for preventing microorganism growth on a ship's hull must be chosen accordingly. For example, in freshwater environments, biofouling has a slower growth rate than in saltwater environments. As such, the paints used in freshwater contain biocides with a lower concentration and release rate.

Using biocidal paints has several advantages, such as providing protection year-round, being easy to apply, and being readily available on the market. However, there are concerns about the potential effects on marine life due to the release of biocides and metals into the marine environment. Additionally, the application and removal of these paints may pose an increased hazard to human health.

There are several types of biocidal antifouling paints available on the market, each with their own unique advantages and disadvantages. Soft biocidal antifouling paints are designed to slowly release biocides as the paint film erodes and can be used on most ships except those with high performance hulls that are regularly treated for optimal performance. However, the use of soft biocidal antifouling paints raises concerns due to the release of biocides and metals into the sea, as well as the release of microplastics. Hard biocidal antifouling paints, on the other hand, release biocides from an insoluble paint film that doesn't wear off, making them more suitable for use on ships operating at high speeds. These paints release fewer toxic substances compared to soft antifouling paints, but regular cleaning is still required to ensure their effectiveness. Lastly, hard epoxy resin with copper is highly efficient at preventing fouling, but its application requires precision and can be costly. Furthermore, it's not effective against copper-resistant fouling species.

Non biocidal anti-fouling systems

Another type is non biocidal antifouling systems that include different approaches for prevention and treatment. Indicatively include:

Biocide-free antifouling paints are hard tape films that can be applied to both the hull and propellers. However, their effectiveness, especially in waters with a high degree of pollution, has not been verified. Ultrasonic equipment includes transducers that emit ultrasonic waves of multiple frequencies, resulting

in a pattern of positive and negative pressure. Negative pressure creates tiny bubbles while positive pressure causes them to burst due to the cavitation effect. Thus, single-celled organisms are killed, and further growth of biofouling organisms is prevented. The advantages include the lack of use of chemical substances and therefore the protection of marine life, which is not a goal, the possibility of their use with other antifouling systems and their application in specialized areas of the ship with great efficiency. Ultrasonics require a large initial outlay, a suitable power source, possibly lifting the ship and larger vessels many ultrasonic transducers. Reactive cleaning and preventive cleaning are two methods used for hull maintenance while the ship is in the water. Reactive in-water cleaning involves cleaning the hull with equipment such as water jets or robotic cleaning systems and can only be applied with hard antifouling film paints. This method is fast and can be done before the ship sails to improve its hull performance. On the other hand, preventive in-water cleaning, also known as hull grooming, involves brushing the hull by a diver or autonomous robot to remove surface biofilms and prevent further pollution. This method can be done alongside antifouling paint films and is effective when the biofouling thickness is small. Regular implementation of preventive cleaning is necessary to ensure its effectiveness.

Biofouling clean-up methods within water can be further categorized into manual cleaning, Powered rotary brush cleaning systems, and non-contact cleaning technology. Manual cleaning involves using brushes or scrapers to remove organisms, but it can be difficult to remove all biofouling. Song & Cui report that in a survey conducted to determine the degree of residual biofouling after manual cleaning, specifically by a diver using a hand brush, approximately 60% of the organisms were removed from the area. Powered cleaning systems use large rotary brushes for fast cleaning, while non-contact cleaning methods such as high-pressure water jet, cavitation water jet, ultrasonic cleaning, and laser cleaning are less damaging to the hull. Non-contact methods are especially useful for avoiding damage to welds and protrusions on the hull. However, there is no autonomous robotic system available that has nozzles for cavitation water jets [42].

6.2.2 Mathematical Model for Ship Resistance Prediction due to Biofouling

Biofouling, which affects the performance of ships and biodiversity in ecosystems, necessitates the development of a mathematical model for predicting the increase in resistance based on factors such as cleaning frequency. To this end, an in-depth literature review has been conducted to identify the variables required for the development of the proposed model.

The overall resistance of the ship in calm water has been studied by many researchers. A well-known method is the Holtrop-Mennen method, which has been shown to be adequate due to its simplicity and accuracy [43, 44]. Ship resistance is composed of frictional, residual, and air drag resistance, as expressed hereinafter.

$$R_T = R_F + R_R + R_{AA}$$

Residual resistance includes wave making and viscous pressure resistance, which can be combined using the form factor $(1 + k)$. Increased biofouling results in higher frictional resistance. Thus, the equation can be written as follows [38, 45]:

$$R_T = (1 + \gamma * k)R_F + R_R + R_{AA} + \Delta R_F$$
$$C_T = (1 + \gamma * k)C_F + C_R + C_A + \Delta C_F$$

The equation for calculating the total resistance coefficient (C_T) includes several factors: the hull form factor (k) and γ is the form factor correction determined by the Holtrop-Mennen method outlined in ITTC-57, the residuary resistance coefficient (C_R), the correlation allowance (C_A), and the increase in frictional resistance due to biofouling (ΔC_F).

According to literature review, two different methods have been studied and evaluated to determine the added frictional coefficient due to biofouling (ΔC_F), using the resulting equivalent sand roughness height from the marine biofouling growth model:

Method 1: Experiments involve converting the equivalent sand roughness height (ks) into roughness function (ΔU^+) using Granville's similarity law. This method is used to calculate the added friction resistance coefficient due to biofouling (ΔC_F). To take into account, the effect of the biofilm on the hydrodynamic behaviour of the ship, modified the above method. Specifically, similarity law scaling method of Granville and roughness functions (ΔU^+) is used, which are directly related to the percentage of biofilm surface coverage (%SC), namely:

$For\ \%SC > 25\%$: $$\Delta U^+ = \begin{cases} \frac{1}{\kappa}\ln(0.27767k^+), & for\ k^+ \geq 3.61 \\ 0, & for\ k^+ \geq 3.61 \end{cases}$$

$For\ 10\% < \%SC < 25\%$: $$\Delta U^+ = \begin{cases} \frac{1}{\kappa}\ln(1.14492 + 0.0988k^+), & for\ k^+ \geq 4.5 \\ 0, & for\ k^+ \geq 4.5 \end{cases}$$

$For\ \%SC < 10\%$: $$\Delta U^+ = \begin{cases} \frac{1}{\kappa}\ln(1.06492 + 0.05332k^+), & for\ k^+ \geq 4 \\ 0, & for\ k^+ \geq 4 \end{cases}$$

It should be noted that κ = 0.42 is von Karman constant, and k^+ is the roughness Reynolds number, which is calculated as the quotient $\frac{k\,u_\tau}{v}$, with u_τ is the friction velocity, ν = 1.1882·10^{-6} m^2/s is the kinematic viscosity and k is the roughness length scale estimated by the following equation

$$k = 0.055h\sqrt{\%SC}$$

h is the average biofilm height.

Granville's method states that the roughness function can be obtained as follows:

$$\Delta U^+ = \overline{U}_S^+ - \overline{U}_R^+ = \sqrt{\frac{2}{C_{FS}}} - \sqrt{\frac{2}{C_{FR}}}$$

The subscripts "S" and "R" refer to smooth and rough surfaces, respectively, at the same friction Reynolds number value (Re_τ). Inner normalization is indicated by the "+" sign, which means that velocities are normalized by the friction velocity (Uτ), while lengths are normalized by the viscous length scale (m=Us). The friction Reynolds number is calculated as $Re_\tau = \frac{U_\tau * h_\tau}{v}$, where the channel half-height is used as a value for " h_τ," and "ν" is the fluid kinematic viscosity [46].

Method 2: The other model directly computes the added frictional resistance coefficient due to biofouling (ΔC_F) based on the equivalent sand roughness height (k_s), ship length (L_{WL}), and Reynolds number (Re). ΔC_F is the roughness allowance calculated using the following expression:

$$\Delta C_F = 0.044\left[\left(\frac{k_s}{L_{WL}}\right)^{\frac{1}{3}} - 10Re^{-\frac{1}{3}}\right] + 0.000125$$

Where, L_{WL} is ship waterline length, Re is Reynolds number and k_s is the equivalent sand roughness height. The Reynolds number is calculated as $Re = \frac{u*L_{wl}}{v}$, where u is the flow speed and v is the kinematic viscosity. So, the added resistance due to biofilm on the hull is determined with the following equation:

$$\Delta R_F = \frac{1}{2} * \rho * V_s^2 * S * \Delta C_F$$

where ρ = 1026 kg/m^3 is the sea density, v is the ship speed, and S is the wetted surface area.

It should be noted that high flow regions with higher Reynolds numbers are known to be more affected by added roughness.

In addition, to account for this, the previous equation of ΔR_F can be split into different regions of the vessel with varying flow speeds and wetted surface areas, each having different equivalent sand roughness heights. This approach provides insight into the effect of different antifouling coatings on total ship resistance, considering the varying Reynolds numbers in different regions.

$$\Delta R_F = \frac{1}{2} * \rho * V_s^2 * \left(\sum_{i=1}^{n}\left[S_i * \Delta C_{F(i)}\right]_i + \left[S_{i+1} * \Delta C_{F(i+1)}\right]_{i+1} + \left[S_n * \Delta C_{F(n)}\right]_n\right)$$

$$\Delta C_{F(m)} = 0.044\left[\left(k_{s(m)}\right)^{\frac{1}{3}} * \left(\frac{1}{\frac{L_{WL_m}}{L_{WL}} * L_{WL}^{\frac{1}{3}}}\right) - 10 * Re_m^{-\frac{1}{3}}\right] + 0.000125$$

Taking the above into consideration, the first method is not preferred as it combines multiple steps and is limited to certain surface coverage conditions. Also, the modified version of this method, based on diatoms surface coverage, is not suitable as it does not accurately predict calcareous surface coverage fouling. Therefore, this method may underestimate the roughness and resulting resistance due to biofouling. On the other hand, the most optimal method (method 2), is to use a direct function to calculate the added frictional hull resistance due to biofouling roughness (ΔC_F).

6.2.3 Calculation of Propeller Drag and Lift Coefficient Changes for Rough and Smooth Conditions

The fouling issue is not relevant only for the hull indeed, also for the evaluation of the performance of the propeller. Indeed, the presence of fouling on the propeller results in a decrease in its performance. This phenomenon is less significant than increased hull friction, but in some cases, where possible, it is important to take it into account.

In propeller analysis, it is important to account for the effects of roughness on the performance of the propeller. This is typically done by calculating the changes in drag and lift coefficients for rough and smooth conditions, which are denoted by K_{TR} and K_{QR}, respectively. These coefficients are used to

characterize the dynamic performance of the propeller in different operating conditions. The subscripts "S" and "R" refer to smooth and rough surfaces, respectively.

$$K_{TR} = K_{TS} - \Delta K_{TD} - \Delta K_{TL}$$
$$K_{QR} = K_{QS} - \Delta K_{QD} - \Delta K_{QL}$$

The calculation of K_{TR} and K_{QR} involves several intermediate steps. First, the changes in drag coefficient (ΔC_D) between rough and smooth conditions must be computed. This is done by subtracting the drag coefficient in rough condition (C_{DR}) from the drag coefficient in smooth condition (C_{DS}).

$$\Delta C_D = C_{DS} - C_{DR}$$

The drag coefficient in smooth condition (C_{DS}) is determined by the equation hereinafter, which takes into account the frictional resistance coefficient for smooth condition (C_{FS}), as well as the maximum thickness (t) and chord length (c) of the propeller blade.

$$C_{DS} = 2\left(1 + \frac{t}{c}\right) * C_{FS}$$

Accurate estimation of C_{FS} is essential for precise prediction of the frictional resistance of the propeller blade and overall propeller performance in such conditions.

The frictional resistance coefficient (C_{FS}) for smooth conditions is given as:

$$C_{FS} = \frac{0.075}{[\log(Re) - 2]^2}$$

The drag coefficient in rough condition (C_{DR}), on the other hand, which incorporates the frictional resistance coefficient for rough condition (C_{FR}), as well as the maximum thickness (t) and chord length (c) of the propeller blade.

$$C_{DR} = 2\left(1 + \frac{2t}{c}\right) * C_{FR}$$

Once ΔC_D is determined, it is used in the following formulae to calculate the changes in drag coefficient (ΔK_{TD} and ΔKQD) for rough and smooth conditions, respectively

$$\Delta K_{TD} = -\Delta C_D * 0.3 * \frac{P * c * Z}{D^2}$$
$$\Delta K_{QD} = \Delta C_D * 0.25 * \frac{c * Z}{D}$$

ΔK_{TD} is given by multiplying ΔC_D with coefficients based on the propeller characteristics including pitch (P), diameter (D), number of blades (Z), and chord length (c) of the propeller blade. Similarly, ΔK_{QD} is given by multiplying ΔC_D with coefficients based on the propeller characteristics. The resulting values of ΔK_{TD} and ΔK_{QD} provide insights into the changes in drag coefficients for rough and smooth conditions

and are used in further propeller analysis to evaluate the performance of the propeller in different operating conditions. Properly accounting for the effects of roughness on the drag and lift coefficients is critical in accurately predicting the performance of propellers in real-world scenarios and can help optimize the design and operation of propeller systems for various applications.

The changes in drag coefficient (ΔC_D) allow for the determination of changes in lift coefficient (ΔC_L) for both thrust and torque coefficients using the equations provided.

$$\Delta C_L = -1.1 * \Delta C_D \ (28)$$

$$\Delta K_{TL} = \Delta C_L * \frac{c * Z}{D} * \frac{0.733 + 0.132 * J^2}{\sqrt{1 + 0.18 * \left(\frac{P}{D}\right)^2}}$$

$$\Delta K_{QL} = \Delta C_L * \frac{c * Z}{D} * \frac{0.117 + 0.021 * J^2}{\sqrt{1 + 0.18 * \left(\frac{P}{D}\right)^2}}$$

Where, J is the advance coefficient, $J = \frac{v_\alpha}{n*D}$, v_a is the advance velocity, n is the propeller speed.

Finally, the new propeller open water efficiency for rough conditions (η_{OR}) can be determined.

$$\eta_{OR} = \frac{J}{2\pi} * \frac{K_{TR}}{K_{QR}}$$

6.2.4 Predictive Models for Biofouling Growth

The correlation between environmental conditions and the growth of biofouling was explored using laboratory or field experiments. By analysing ample experimental data, the relationship between the parameters and the growth of marine biofouling (BG) on a specific surface can be accurately formulated.

Equation 1: Growth of marine biofouling according to different parameters

$$BG = f_1(SST, psu, pH, v, I, S, t, m_t, \sigma, \theta_c, R_t, \eta_c)$$

These factors include seawater surface temperature (SST), salinity (psu), acidity (pH), water flow speed (v), light intensity (I), nutrient concentration (S), exposure time (t), micro-texture of the surface (m_t), surface potential (σ), contact angle (θ_c) as a measure of wettability, roughness parameter (R_t), and the performance parameter (η_c) of an antifouling coating (representing the efficiency and chemical contents, including leaching rate). In addition, surface color and contour are believed to have various effects on biofouling growth, although their influence is not yet well-established.

While numerous experimental and modeling studies have been conducted on biofouling growth, they often focus on a single type of biofouling or only a few parameters, resulting in the absence of a comprehensive model that accurately predicts biofouling growth rates under varying environmental conditions. Developing such a comprehensive model poses significant challenges. Considering the effects of multiple parameters, as indicated in Equation 1, complicates the validation process. Validating a model with numerous parameters necessitates extensive data collection, which is time-consuming and resource

intensive. In addition, outdoor experimental studies often encounter variations in environmental conditions even within the same day. These regularly fluctuating parameters pose challenges for short-term prediction models. However, if the model is intended for long-term predictions, these complexities can be simplified. For example, the impact of seasonal changes on biofouling growth at a specific location can be assessed by averaging data collected over 2-3 years of field tests.

Uzun et. al [47] proposed a series of simplifications to create a simplified biofouling growth model for ships. The authors presented a list of these simplifications and the subsequent development of the simplified equation. The explanations provided were supported by existing research in literature.

- The surface properties of a ship, such as micro-texture (m_t), surface potential (σ), contact angle (θ_c), and roughness (R_t), profoundly influence biofouling growth. These properties impact the settlement and attachment of organisms like hydroids, bryozoans, and ascidians. Micro-texture, with its grooves, pits, cracks, and crevices, provides protective habitats against strong water flow, attracting these organisms. Surface roughness (R_t) is crucial for bio-adhesion, as it creates crevices where extracellular polymeric substances (EPS) can flow, leading to strong attachment. Conversely, smooth surfaces only offer adhesive contact on asperity peaks, resulting in weaker bio-adhesion. Researchers confirm the impact of surface roughness on attachment strength. Surface potential (σ), representing surface charge, affects micro-organism attachment. Kerr et al. [48] demonstrate the influence of negative surface potential on the attachment process. Surface properties, such as mt, Rt, and σ, directly influence the colonization and adhesion of biofouling organisms on ship surfaces. Newbuilding applications typically have peak-to-trough roughness heights ranging from 30 to 150 µm, depending on coating quality and type. For instance, SPC coatings may range from 30 to 129, while FR coatings fall between 7 and 85 [49, 50]. The simplification proposed here combines these surface properties into a simplified equation to account for their collective impact on biofouling growth, offering a practical and manageable modeling approach.
- Light intensity (I) is a significant factor influencing the biofouling community, specifically plant-based fouling from microalgae to weeds. It is associated with water depth in existing models. Photosynthetic macrofouling, primarily algae, thrives in nutrient-rich areas with high light levels within the 0–40-meter range. However, other organisms like mussels, barnacles, and tubeworms, which obtain energy from sources within the sea, can grow at greater depths unaffected by light intensity [51]. For large merchant vessels with draft ranges of 5-20 meters, light intensity variations are assumed to be minimal, with locations considered to have similar light intensity and spectrum.
- The availability of nutrients (S) and the velocity (v) of water flow significantly influence marine fouling. Nutrient abundance is closely tied to water flow rates and proximity to coastal areas, which tend to have higher nutrient levels due to human-related discharges. As ships approach shorelines, biofouling growth intensifies. When modeling biofouling growth during port stays, a stable water velocity is assumed, and the concentration of nutrients is considered uniform across all ports.
- Although the overall impact of pH on biofouling growth remains insufficiently studied, research suggests that pH levels ranging from 6.5 to 10 are conducive to a broad spectrum of biofouling organisms. Global seawater pH values typically fall between 7.74 and 8.4. Given the relatively limited variations in pH across the world's seas, the effects of pH on biofouling growth were simplified in the model.
- Salinity (psu) plays a decisive role in the growth of biofouling organisms, with different types of fouling organisms exhibiting diverse responses to changes in salinity. Despite its importance, no mathematical model specifically addresses the effect of salinity on biofouling growth rates. Existing studies on salinity primarily focus on examining the salinity tolerances of biofouling organisms rather than modeling the precise influence of salinity on growth rates. Additionally, the salinity values of

world seas typically range from 30 to 36 psu, which falls within the salinity tolerance range of biofouling organisms.

Based on these simplifications, the researchers focused on two key factors that have the greatest impact on biofouling growth: the performance of the antifouling coating and the exposure time to seawater. Their goal was to create a simplified model for predicting ship biofouling during idle periods, focusing on exposure time and antifouling coating performance. The simplified model expresses the biofouling growth (BG) as a function of the exposure time (t) and the antifouling coating performance parameter (ηc).

Equation 2: Growth of marine biofouling after simplifications

$$BG = f_2(\, t, \eta_c)$$

The antifouling coating performance parameter is determined by a function (g) that considers the change in sea surface temperature (ΔSST), as shown in Equation 3.

Equation 3: Antifouling coating performance in relation to changes in sea surface.

$$\eta_c = f_3(\, \Delta SST)$$

It is important to note that the performance of antifouling coatings can vary depending on the geographical region, mainly due to the significant influence of temperature on biofouling growth. Therefore, the model incorporates the change in sea surface temperature (ΔSST) as a parameter to predict the effects on the antifouling coating performance. Also, the model focused on the variations in sea surface temperature (SST) primarily based on latitude, while neglecting the relatively minor effects of changes in longitude. The authors recognized that the impact of longitude on SST is relatively small in comparison to the significant variations observed with latitude. Therefore, the model emphasized the more influential relationship between SST and latitude in predicting biofouling growth (Equation 4)

Equation 4: SST and latitude in predicting biofouling growth.

$$SSTa = 12.5 + 15\left(\cos\left(\frac{latitude\ degree}{28.64}\right)\right)$$

And

Equation 5: Linear extrapolation or interpolation process for antifouling coating performance parameters

$$\eta_{ca} = \frac{\eta_{cy}(SST_a - SST_x) + \eta_{cx}(SST_y - SST_a)}{SST_y - SST_x}$$

The coating performance parameter at an arbitrary location is denoted as η_{ca}, while η_{cy} and η_{cx} represent the coating performance parameters at field test locations y and x, respectively. SSTa represents the sea surface temperature at the arbitrary location, while SSTy and SSTx indicate the sea surface temperatures

at locations y and x. It's important to consider that the model takes into account the variations in coating performance and sea surface temperatures across different locations during the field tests.

6.3 Challenges for Inner Hull Inspections and Cleaning

Another challenge is to solve the main problems faced on the cargo hold cleaning procedure – as applied on merchant bulk carrier vessels. Cargo cleaning is very important especially for bulk carriers. In 2022, the combined capacity of bulk carriers amounted to about 44% of the total capacity of the global merchant fleet.[2] Cargoes transported via maritime routes exhibit significant variations from port to port, necessitating thorough cargo hold cleaning following unloading and prior to loading. The process of cargo hold cleaning plays a pivotal role in ensuring the purity and quality of transferred goods, particularly when food-grade specifications are involved. Moreover, it serves to safeguard the vessel itself from corrosive or aggressive cargo. Neglecting to remove loose scale and remnants from prior cargoes can have detrimental effects. It can lead to concealed cargo hold wastages and continuous exposure of steel structures to corrosive traces of cargoes like sulfur, which can be found directly or in other cargoes such as coal and certain fertilizers[3]. Given that the risks associated with cargo contamination are directly proportional to the cargo's value, typically ranging in the tens of millions of euros per cargo, the industry is diligent in closely monitoring this matter through accredited surveyors. Inadequate cleaning procedures can result in delays, port charges, charterer claims, and potential off-hire situations, all of which significantly impact the vessel's overall asset value [52]. However, current methods for cargo hold cleaning by specialized personnel carries significant health, safety, and environmental risks, in addition to being a costly and time-consuming process.

The current process involves manually jetting the hold surfaces with water or chemical additives and water – depending on the surface contamination [53]. Jetting is carried out by man-entry into the holds, always classed as closed-space entry, possibly a hazardous area due to toxic gases or lack of oxygen. Human operatives then utilize a single water nozzle – possibly with the use of chemicals / detergents – attempting to hose down the cargo hold surface – jetting from the tank-top deck. Holds are quite large; thus, hosing down a wall of steel, with apertures, at a distance of several meters can only achieve very average results, while being time-consuming and cumbersome. Not only time and effort are wasted, but also chemicals and water, which then need to be safely disposed of. Thus, the inefficiency of the process, combined by the sheer size and volumes involved, and the risks and costs of failure truly require an improvement.

Failure to properly clean cargo holds prior to loading can result in a range of negative consequences. Delays, off-hire, and disputes in charter parties can arise, causing costly interruptions in the transportation process. Furthermore, the presence of remnants from previous cargoes can lead to cargo contamination and infestation, resulting in expensive damage claims from cargo receivers. These challenges highlight the utmost importance of implementing effective and efficient cleaning procedures to ensure the safe and successful transportation of bulk cargoes. Taking proactive measures in cleaning not only mitigates risks but also helps maintain the integrity of cargo, protecting both the shipping company's reputation and financial interests.

[2] https://www.statista.com/statistics/264023/capacity-of-the-global-merchant-fleet-by-ship-type/
[3] https://bulkcarrierguide.com/carriage-of-sulphur.html

6.4 Underwater Inspection Model

The proposed underwater robotic inspection model aimed at developing and demonstrating a rapid, automated system dedicated to assessing hull biofouling. The objective of this cutting-edge system is to utilize underwater robotics equipped with advanced image analysis and AI algorithms, allowing for the evaluation of sea growth on the ship's hull. Notably, machine learning techniques will be employed to assess the levels of biofouling by analyzing previous data and using it to inform the evaluation process.

The primary aim of this innovative system is twofold: first, to establish a more efficient and optimized schedule for hull cleaning, and second, to enhance the performance of hull coatings. To achieve these goals, the robotic platform will be deployed to conduct inspections and monitor the extent of sea growth on the hull's surface. Using sophisticated mapping and pattern recognition techniques, the robot will follow pre-defined paths, systematically identifying and evaluating all affected areas.

To further enhance the capabilities of the inspection system, additional advanced sensors and equipment will be incorporated. Integrating a range of advanced sensors such as accelerometers, gyroscopes, LVDTs, pressure sensors, LIDAR, and cameras, this state-of-the-art inspection system also leverages machine learning techniques to enhance its capabilities. Accelerometers and gyroscopes provide valuable information on motion and orientation, while LVDTs and pressure sensors assess the structural integrity of the hull. The inclusion of LIDAR allows for the generation of three-dimensional models, facilitating accurate mapping and identification of biofouling areas. Additionally, cameras with high-resolution imaging capabilities capture visual data that aids in the assessment and documentation of the hull's condition.

The system will encompass a comprehensive reporting capability, providing detailed and accurate data on the hull's condition. By utilizing machine learning algorithms, the system will analyze previous paradigms of biofouling to aid in the assessment process. This integration of machine learning with real-time image analysis will enable the system to make informed decisions about the extent of biofouling and determine the appropriate course of action.

This approach has the potential to revolutionize the monitoring and maintenance practices of marine vessels. By effectively measuring and tracking biofouling levels, this automated inspection system promises to optimize maintenance operations, improve the efficiency of cleaning processes, and significantly enhance the overall performance and longevity of the vessel's hull. The incorporation of advanced machine learning techniques, together with the integration of additional sensors and equipment, highlights the progressive nature of this technological advancement, emphasizing the value of a comprehensive and data-driven approach to hull assessment and maintenance.

6.5 Inner Inspection with Cable Robots

To address the above shortcomings, a novel, autonomous cable robot for cleaning and inspection could be designed, aiming to settle the issues of quality of operation, safety, and environmental protection. Cable robots form a new generation of robots based on a novel architecture called cable-driven parallel robots (CDPR), where a set of cables whose lengths can be modified by the use of winches, connect the mobile platform to fixed points. A typical cable robot system consists of a fixed base and a movable platform connected by multiple cables. The cables are attached to both the base and the platform, forming a network of interconnected wires. By adjusting the cable lengths and tensions, the robot can achieve various poses and orientations, enabling it to reach confined spaces and navigate complex environments in conjunction with a digital twin of the workspace. In short, cable robots offer innovative,

modular, and large-scale manipulation systems for industrial applications as well as in situations where human intervention is infeasible or undesirable [54].

They are unique in their dexterity and flexibility, their adaptive nature and speed of installation, as well as their low cost. Moreover, they have been very well studied including kinematics, control, and calibration [55], therefore they are today technologically ready for industrial-strength applications and commercial use. It is possible to use the revolutionary modularity of cable robots to solve complex and heavy-duty tasks, which are too dangerous and costly for human agents in the merchant marine.

The use of cable robots can lead to a system that is simple, transportable, easy to maintain and able to be packed in a standard sea-worthy container. When deployed, it can be suspended from 4 winches mounted on the hatch cover guide rails, possibly with another 4 at the hold's bottom. Motion planning may rely on 3D scanning by a camera [56] (and possibly floodlight) or on using a digital twin of the hold's. On the platform, a jetting nozzle with 2 Degrees of Freedom (DoFs) undertakes cleaning at relative proximity, while a camera undertakes inspection. An important feature of this solution is the proximity of the jetting nozzle to the surface.

The user will need to enter the hold geometry, selecting from pre-defined shapes/volumes – using purpose-built software. The unit could then self-calibrate for position in Euclidean 3d space (xyz coordinates). The cleaning of each surface would be automated and adapted to the plane of the steel surface to be cleaned. Auto-mode should allow unmanned washing of the hold, including control of all DoFs, on/off nozzle operation & safety interlocks, "fast-clean" and "detailed-clean" algorithms. Manual override would allow the operator to take process in full manual mode, reverting to auto-mode in a simple fashion. On the platform, equipment is required so as to undertake (i) cleaning using jetting nozzle, and (ii) inspecting the hold walls by camera, and possibly floodlight. For (i), the platform holds a rotating mechanism to allow 360-yaw, and 360-pitch. Single or multiple nozzle configurations can be used.

Overall, the advantages of the cable robot in such an application are listed below:

- Ability to vary the angle of attack of the nozzle (yaw and pitch) to maintain best angle for steel plates of various angles.
- Safety enhancement – as human operatives will not work in the cargo holds.
- Green shipping – as improved efficiency will require much less water, and much less chemical volume.
- Automation of the process, by mapping the cargo hold volume either by 3D scanning or by employing a digital twin of the cargo hold's.
- Simplicity- The equipment needed is very simple and easy to maintain.
- Allows both important tasks of cleaning and inspection to be carried out at the same time.
- Allows for possible extensions: to tanker vessels – for tank cleaning operations, for spot repairs, and for probe / thickness measurement.

6.6 Vessel Structure and Condition Assessment: Model's Framework

Marine biofouling on the hull and cargo holds cleanliness are major concerns, that pose a variety of risks. Some of them are related to the financial burden on the shipping companies, due to the reduced performance of the ships, and the environmental damage mainly due to the increased emissions of gaseous pollutants, as well as the transfer of Invasive organism to other ecosystems. And others are about delays, port charges, charterer claims, and potential off-hire situations, all of which significantly

impact the vessel's overall asset value. Assessment of the inner and outer hull condition can be supported by the rapid technological development of time, with the use of fast and automated inspection systems. These advanced systems will enable precise evaluations of biofouling on the ship's hull, and they can contribute to ensuring the cleanliness of cargo holds, effectively addressing the challenges associated with cargo transportation. Therefore, the contribution of this new technological system lies in improving the efficiency of maritime operations and in reducing the environmental and economic impact of maritime industry.

Underwater robotics outfitted with image analysis, sensors, machine learning and artificial intelligence (AI) algorithms can be used to accomplish this as a solution to biofouling issue. These robots would be developed specially to assess sea growth and evaluate the degree of biofouling on a ship's hull. The robot would be able to navigate along a pre-defined path and identify areas of the hull that are impacted by biofouling by utilizing cutting-edge mapping and pattern recognition techniques. The use of underwater robotics for hull biofouling assessment offers several advantages over traditional inspection methods. Firstly, it is much faster and more efficient than manual inspection methods, allowing for a more frequent assessment of hull condition. Additionally, it is also more accurate, as the robots can identify areas of biofouling that may be missed by human inspectors. Accurately assessing the level of biofouling on a ship's hull is a crucial step in optimizing the maintenance schedule and ensuring that the vessel operates efficiently. The results of these assessments can inform the cleaning schedule and contribute to improved coating performance, which ultimately reduces fuel consumption and emissions. The inspection system mentioned above would include a reporting capability, providing accurate and thorough information on the condition of the hull, in order to accomplish this goal. Real-time monitoring of biofouling levels and the ability to make maintenance decisions informed by this reporting capability would help to lower costs and lengthen the useful lives of marine vessels. This creative inspection system promises to revolutionize the way marine vessels are monitored and kept in good health by measuring and tracking biofouling levels. For maintaining effective and environmentally friendly marine transportation, it offers an objective and precise assessment of the hull's condition. The environmental impact of marine transportation could be significantly reduced with the help of this innovative method for assessing biofouling, which also promises to increase safety and cut costs. In addition to the benefits for marine transportation, this new system could also have broader implications for the marine ecosystem. By reducing the spread of invasive species through biofouling, this technology has the potential to improve the health of the marine environment and protect biodiversity. In this way, the use of underwater robotics equipped with image analysis and AI algorithms has the potential to make a significant contribution to environmental sustainability. Another advantage of using robotics for biofouling assessment is that it reduces the need for divers to perform dangerous and time-consuming underwater inspections. This not only reduces the risk of injury or death to divers but also saves time and resources by eliminating the need for specialized equipment and personnel.

On the other hand, the effective assessment and cleanliness of cargo holds have emerged as significant challenges in the maritime industry, particularly for merchant bulk carrier vessels. To address these issues, a new solution is being explored: the utilization of autonomous cable robots for inspection and cleaning tasks. This innovative approach aims to enhance the quality of operations, prioritize safety, and protect the environment. Autonomous cable robots represent a new generation of robotic systems, characterized by their unique architecture known as cable-driven parallel robots (CDPR). These robots consist of a fixed base and a movable platform interconnected by multiple cables. By adjusting the lengths and tensions of these cables, the robots can achieve versatile poses and orientations, enabling

them to navigate complex spaces and reach confined areas within cargo holds. In the context of cargo hold inspections and cleaning, autonomous cable robots offer numerous advantages. Their flexibility and dexterity empower them to tackle challenging environments and access areas that may be difficult for human operators to reach. With the support of digital twin technology, these robots can efficiently maneuver and perform tasks with exceptional precision. One of the key benefits of autonomous cable robots is their modularity and scalability, making them well-suited for heavy-duty tasks in the merchant marine industry. Their adaptive nature and rapid installation process contribute to cost-effective operations. Moreover, extensive research and development efforts have focused on cable robot kinematics, control, and calibration, ensuring their readiness for industrial-strength applications and commercial use. By incorporating autonomous cable robots into cargo hold cleaning procedures, significant improvements can be achieved in terms of operational quality, safety, and environmental protection. These robots eliminate the need for manual jetting and human entry into the cargo holds, thereby mitigating the risks associated with toxic gases, oxygen deprivation, and confined spaces. Instead, the robots utilize their cable-driven mechanisms to efficiently clean the surfaces of cargo holds, delivering consistent and thorough results. This approach not only saves time and effort but also optimizes the use of chemicals and water, reducing waste and facilitating proper disposal practices. Ensuring the cleanliness of cargo holds prior to loading is paramount for preventing delays, disputes, and cargo contamination. By implementing autonomous cable robots for inspection and cleaning purposes, cargo hold operations can be conducted with heightened efficiency and effectiveness. This transformative approach enhances the overall safety and success of transporting bulk cargoes, safeguarding the reputation and financial interests of shipping companies.

The picture shows the entire architecture of the system.

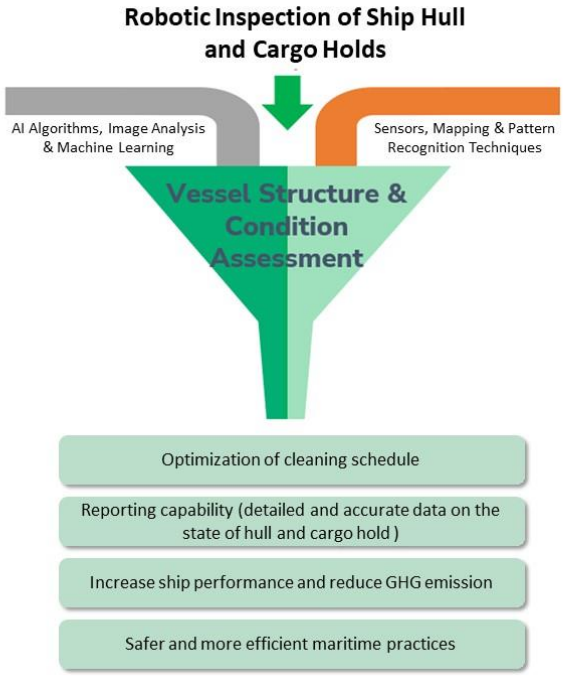

Figure 23. Hull inspection and condition assessment model

7 Integrated Machinery Performance Management and Remote Control

Predictive maintenance is a proactive approach to maintenance that uses data analysis and machine learning algorithms to predict when maintenance should be performed on a machine or equipment, in order to prevent unexpected downtime and reduce maintenance costs.

The idea behind predictive maintenance is that by analyzing data from sensors and other sources, such as historical maintenance records, an algorithm can identify patterns and anomalies that are indicative of potential equipment failures. Based on these predictions, maintenance teams can plan and schedule maintenance activities before equipment failure occurs, reducing downtime and increasing equipment reliability.

Predictive maintenance typically involves the use of sensors, machine learning algorithms, and data analytics tools to collect and analyze data on equipment performance, such as temperature, vibration, and other operational parameters. This data is used to build a model that can predict when maintenance is needed, based on the current state of the equipment.

By using predictive maintenance techniques, organizations can avoid unscheduled downtime, improve safety, and reduce maintenance costs. This approach can also help organizations optimize maintenance schedules and minimize the need for emergency repairs, ultimately improving the overall performance and reliability of their equipment.

In the marine sector, predictive maintenance is used to improve the performance and reliability of ships, offshore platforms, and other marine equipment. Marine equipment is subjected to harsh environments and operating conditions, which can result in unexpected failures, downtime, and costly repairs.

Predictive maintenance in the marine sector involves the use of sensors and data analytics tools to monitor the performance of critical equipment, such as engines, turbines, and propellers. By analyzing data on factors such as temperature, vibration, and oil quality, machine learning algorithms can predict when maintenance is required and recommend the appropriate action to be taken.

For example, a ship's engine may be monitored using sensors that collect data on oil quality, temperature, and other operational parameters. This data is then fed into a machine learning algorithm that analyzes the data and generates a maintenance plan that includes tasks such as oil changes and component replacements.

By using predictive maintenance techniques in the marine sector, organizations can reduce downtime and maintenance costs, while also improving the safety and reliability of their equipment. This can be especially important in the case of offshore platforms, where equipment failures can pose a significant risk to human life and the environment.

The approach to implementing predictive maintenance in the marine sector typically involves the following steps:

- Identify critical equipment: The first step is to identify the equipment that is critical to the operation of the vessel or offshore platform. This includes equipment such as engines, turbines, and propellers, as well as equipment that is essential to the safety of the crew and the environment, such as fire suppression systems.
- Install sensors: Once critical equipment has been identified, sensors can be installed to monitor the performance of the equipment. These sensors may include vibration sensors, temperature sensors,

and oil quality sensors.

- Collect data: The sensors will generate data on the performance of the equipment. This data can be collected and analyzed to identify patterns and anomalies that may be indicative of potential failures.
- Analyze data: The data can be analyzed using machine learning algorithms to identify patterns and anomalies. These algorithms can be trained using historical data to improve their accuracy in predicting potential failures.
- Predict maintenance needs: Based on the data analysis, the algorithms can generate predictions about when maintenance will be required. This information can be used to schedule maintenance activities and minimize downtime.
- Take action: Finally, maintenance teams can use the predicted maintenance needs to take action, such as performing preventive maintenance, ordering replacement parts, or scheduling repairs.

The approach used is based on baseline maintenance that involves comparing the current performance of a piece of equipment to a known baseline performance. The baseline is established by measuring the performance of the equipment when it is in good condition and using this as a reference point for future performance analysis.

The goal of maintenance analysis based on baseline is to identify changes in equipment performance that may be indicative of potential failures or maintenance needs. By monitoring the performance of equipment over time and comparing it to the baseline, maintenance teams can identify deviations from normal performance and take action before equipment failure occurs.

Maintenance analysis based on baseline involves the following steps:

- Establish a baseline: The first step is to establish a baseline performance for the equipment. This may involve conducting tests or measurements when the equipment is new or in good condition and using this data to establish a reference point for future analysis.
- Monitor performance: Once a baseline has been established, the performance of the equipment can be monitored over time. This may involve measuring factors such as temperature, pressure, vibration, or other operational parameters.
- Compare to baseline: The performance data is then compared to the baseline to identify any deviations from normal performance. This may involve statistical analysis or visual inspections of charts or graphs.
- Identify potential issues: Deviations from normal performance may be indicative of potential issues or maintenance needs. Maintenance teams can use this information to identify potential issues and take action, such as scheduling preventive maintenance or repairs.

Detecting anomaly signals is an essential part of any maintenance predictive system. An anomaly signal is an indication that the performance of a piece of equipment is deviating from its expected or normal behavior.

It is important to note that anomaly detection is not a one-time activity, but rather an ongoing process. Maintenance predictive systems should be continually monitored and adjusted based on new data and changing conditions to ensure that anomaly signals are detected in a timely and effective manner.

7.1 System Overview

The data monitored by the system are raw and from other systems that usually record at very high frequencies. Such data are subject to large local fluctuations that are not representative of the signal itself, as they result from changes in machine regimes. In order to make the data from the sensors useful and usable for diagnostic purposes, they are analysed and characterized statistically. The extrapolated statistical parameters with which the software will work are as follows:

- Mean Value;
- Standard Deviation;
- Skewness (coefficient of skewed distribution);
- Kurtosis (coefficient of statistical repeatability);
- Crest Factor (waveform coefficient);
-

The generation of these statistical parameters must be based on a sufficiently large sample (about 300 measurements). Considering that the system can receive data at a frequency of 1Hz, it is necessary to perform the calculation of the above parameters at set time intervals of not less than 5 minutes in order to comply with the sampling of 300 measurements.

The first two parameters (mean value and standard deviation) are used to assess the diagnostic performance of the component, i.e., to evaluate its performance relative to normal operation in order to produce the baseline that establishes its standard operation. The other three parameters, on the other hand, are useful for assessing the "stationarity" of the analysed data, i.e., whether it is sufficiently variable to be considered a real data, but not exaggeratedly variable to make it unusable. Generally, signals that are too steady are the result of sensor or acquisition panel malfunctions, while signals that are too variable are related to simple changes in machine speed.

Descriptive signals of the same object are grouped into "Diagnostic groups". Diagnostic groups referring to the physical structure of the same machinery are grouped under the same "Equipment." In turn, the equipment that go to make up the same piece of equipment are grouped into "Main Components."

An example of the component hierarchy will be as follows:

Diesel Generators -> DG1 (comp. princ.) -> DG1Motor (equip.) -> Cooling (diagn. group) -> Temperature_Water_Motor_Input_Exchanger_B (signal).

A "Primary parameter" (primary control parameter) is selected for each equipment, representative of the behaviour of all data contained in the group. In the example given, the primary parameter for the equipment "DG1Motor" is the "percent electrical load" (a quantity between 0 and 100). Although the analysis theories are totally identical for each component, it is possible to intuitively distinguish equipment into two broad categories:

1. Continuous equipment, whose primary variable can take any value within the established range (e.g., percent electrical load);
2. Boolean equipment, whose primary variable can take on only discrete values (e.g., running status i.e., on and off or on, half power and full power).

The proper generation of these baselines is crucial. In fact, CBM systems base all their diagnostic analysis on the standard running condition. In fact, if the baselines are not properly processed or if they do not

represent the correct operation of the device, the system will not be able to perform a reliable evaluation of the component.

7.2 Statistics Background

A continuous variable is a type of variable that can take on an infinite number of values in a given interval. All signals that are part of the data sets of the frigate's sensor systems can be treated as variables of a continuous type, to which all the theoretical tools presented later in this appendix are applicable.

In probability theory, a probability density function, or probability density function (PDF), is a function whose value at a given point (sample) in the sample space, that is, in the set of possible values taken by the random variable, can be interpreted as the relative probability that the value of the random variable is equal to that sample. The normal distribution is a particular continuous probability distribution.

The normal has a bell shape, is also called Gaussian, and is symmetrical with respect to its mean, denoted by η. It extends indefinitely in either direction along the x-axis, but most of the area subtended by the curve gathers around the mean. The curve has two points, called inflection points, which coincide with a distance of one standard deviation more or less from the mean and at which the curve itself changes convexity. The reference quantities for characterizing a particular Gaussian are:

- η i.e. the mean, coincident with fashion and median;
- σ i.e., the standard deviation;
- Skewness (equal to 0 in the case of Gaussian);
- Kurtosis (equal to 3 in the case of Gaussian).

The main characteristics of the Gaussian can be summarized as follows:

- It is symmetric with respect to η;
- The value x = μ defines the fashion, mean and median;
- It is increasing for x < η and decreasing for x > η;
- It is asymptotic to the x-axis on both sides;
- It possesses two inflection points for x = η ± σ;
- Skewness value equal to 0 and Kurtosis value equal to 3;
- Assumes maximum value equal to 1/(σ√2π) at x = η.

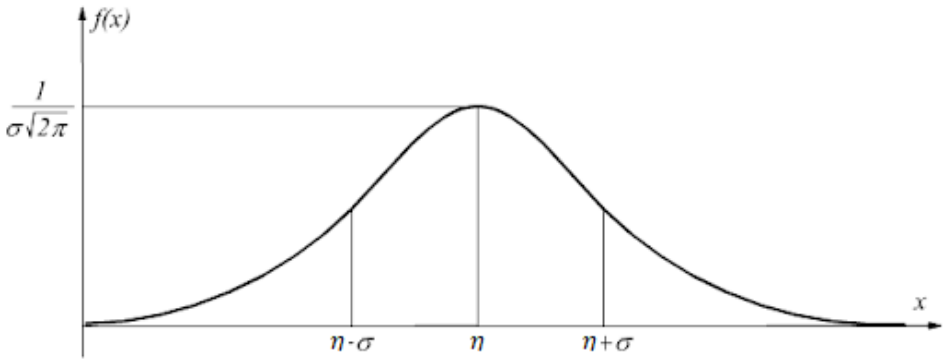

Figure 24. Gaussian Distribution

7.2.1 Mean

Denoted by the symbol η, the mean value, or simply mean, is also referred to as the centre of the distribution. Its value characterizes the position of the Gaussian curve along the x-axis. Its value is expressed by the following formula:

$$\eta = \int_{-\infty}^{+\infty} x f_x(x) dx \cong \sum_{i=1}^{N_{bin}} x_i f_X(x_i) \Delta x$$

As η changes, the curve shifts along the x-axis, but its shape remains unchanged. A value of η_1<η results in a shift to the left while, conversely, in the case of η_1>η, the curve is shifted to the right.

7.2.2 Standard Deviation

The mean, as a positional index, while very important for summarizing a statistical distribution, provides only a partial view of the distribution of the variable being analysed. It is useful to evaluate an index of variability, or dispersion index, such as variance or standard deviation to better characterize the signal under investigation.

The standard deviation of a variable corresponds to the second order of the expected value (m2), or the second power of the differences of the values of each observation from the mean of the variable. In fact, the deviation (or deviation, or deviation) from the mean can be defined for each observation; this is 0 if the observation has exactly the same value as the mean. On the other hand, the deviation will be negative if the observation has a value less than the mean. Conversely, the deviation will be positive if the observation has a value greater than the mean.

We mentioned that the squares of the deviations are used to calculate the standard deviation. This gives a positive number, whether the deviation is higher or lower, and negative deviations can be added to positive ones without the opposite signs affecting the result, making it zero. The sum of all deviations of the mean squared is called the deviance, while the mean of the squared deviations is called the variance.

As constructed, variance (σ_x^2) is expressed as the square of the unit used for the variable. Its formula is as follows:

$$m_2 = \sigma_x^2 = \frac{\sum_{i=1}^{N}(x_i - \eta)^2}{N-1}$$

With: η mean of values, x_i value of the i-th observation, N number of observations available.

Note that in this type of representation we have used the value N-1 in the denominator instead of just N in order to correct for the value of the variance, which will tend to be underestimated if calculated on a small sample compared to the entire population of values that can be assumed by the variable under consideration.

The unit of variance is the square of the unit of the measured quantity. Consequently, it is often preferred to use the square root of variance, which has the same unit of measurement as the variable and the mean. The square root with positive sign of the variance is called the standard deviation or mean square deviation:

$$\sigma_x = \sqrt{\frac{\sum_{i=1}^{N}(x_i - \eta)^2}{N-1}}$$

As the variability among observations increases, the deviations from the mean increase, the greater the sum of squares and, therefore, the greater the value of the variance and, consequently, the mean square deviation as well.

The standard deviation is 0 only when there is no dispersion. This situation occurs when all observations considered coincide with the same value. In all other cases, the further the values deviate from the mean, the larger the standard deviation will be.

7.2.3 Skewness (Static Momentum of the 3rd Order)

The third-order moment is related to the concept of symmetry/asymmetry, or ''Skewness", of the distribution. A distribution of data is said to be symmetrical if there is a value that divides the distribution itself into two parts, with the elements of each part symmetrical with respect to the corresponding elements of the other part. This is, for example, the case of the Gaussian. The formula for Skewness is as follows.

$$m_3 = \frac{\sum_{i=1}^{N}(x_i - \eta)^3}{N}$$

Using the third power of the differences between expected value and observations here, it is often preferred to normalize this factor by the variance in order to have an index that is easier to understand:

$$\gamma_3 = \frac{m_3}{{\sigma_x}^3}$$

The skewness index provides an indication of how much the distribution under consideration concentrates around its mean or disperses to the left or right of it. Specifically, when the skewness index is < 0, the phenomenon tends to form a hump to the right of the mean, consequently forming an elongated tail to the left; conversely, when it is > 0, the tail tends to elongate to the right, forming a hump to the left of the mean.

7.2.4 Kurtosis

Going up another order, we can still find information about the convexity of the probabilistic distribution of a population. The statistical moment of the 4th order has the following formula:

$$m_4 = \frac{\sum_{i=1}^{N}(x_i - \eta)^4}{N}$$

Again, having a fourth power, the kurtosis index is often normalized always through the second-order moment:

$$\gamma_4 = \frac{m_4}{m_2^2}$$

The Kurtosis index, from the Greek "kurtosis" or "convex," measures the greater or lesser pointedness of a distribution of data, relative to the normal distribution. Accordingly, it indicates the greater or lesser weight of values at the extremes of the distribution, compared to those in the middle.

A curve that is sharper than that of the normal distribution is called leptokurtic and corresponds to a kurtosis index γ_4>3. A form of distribution that is less sharp than that of the normal distribution is called platykurtic. In this case, the value of Kurtosis is γ_4<3.

7.2.5 Crest Factor

Finally, the crest factor is an indicative measure of the presence and sharpness of peaks in a wave function. In the context of a distribution of signals, it indicates the presence of peaks in the distribution and how pronounced they are, so it can be a useful indicator of the width of the distribution of values. A value of 1 indicates the absence of peaks, while a higher value is indicative of the presence of peaks in the signal, as in the case of a sinusoidal function.

The crest factor is calculated as the peak amplitude value (x_{peak}) divided by the mean square (x_{rms}):

$$CF = \frac{|x_{peak}|}{x_{rms}}$$

$$x_{rms} = \sqrt{\frac{1}{N}\sum_{i=1}^{N} x_i^2}$$

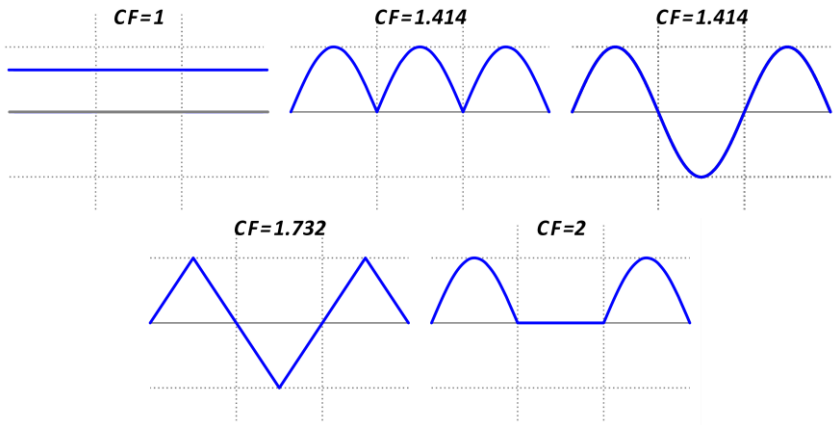

Figure 25. Examples of CF.

7.2.6 Stability Condition Values

In general, the points considered stationary and used to calculate the reference condition (baseline) for the signal of interest must meet the following characteristics:

- Crest Factor $\geq$ 0.16;
- Skewness $\leq$ 0.3;
- Kurtosis (for continue signal) $1 \leq |\gamma_4| \leq 3.5$
- Kurtosis (for discrete signal) $0 \leq |\gamma_4| \leq 3.5$

7.2.7 Pearson Index

In statistics, a correlation is a relationship between two variables such that each value of the former corresponds to a value of the latter, according to a certain regularity. The type of relationship between two quantities can be evaluated either qualitatively, using graphs, or quantitatively, by taking advantage of one or more usable indices. By arranging the two quantities under consideration on a scatter plot (also called a scatter plot), it is possible to assess whether a correlation between them can be detected and, if so, what kind. To express quantitatively the strength of the link between two variables, as already stated, indices called correlation indices are used. The choice of an index in particular generally depends on various factors, and in particular the nature of the distribution of the variables under consideration (continuous or discrete) and the characteristics of the distribution of the points in the scatter plot (linear or nonlinear). In this type of application, the most commonly used index is the Pearson correlation index (or coefficient). Given two statistical variables (or quantities) X and Y, the Pearson correlation index is defined as:

$$\rho_{XY} = \frac{\sigma_{XY}}{\sigma_X \sigma_Y}$$

Where ρ_{XY} represents the covariance between variables X and Y, σ_X and σ_Y represent the standard deviation of X and Y respectively.

Pearson's coefficient takes values between -1 and +1.

Specifically:

$\rho_{XY} > 0$ X and Y are said to be directly correlated or positively correlated -> positive correlation;

$\rho_{XY} = 0$ X and Y are said to be uncorrelated, that is, independent variables;

$\rho_{XY} > 0$ X and Y are said to be inversely correlated or negatively correlated -> negative correlation.

In more detail, narrowing down to the case of positive correlation:

$0 < |\rho_{XY}| < 0.3$ weak correlation;

$0 < |\rho_{XY}| < 0.7$ moderate correlation;

$|\rho_{XY}| > 0.7$ strong correlation.

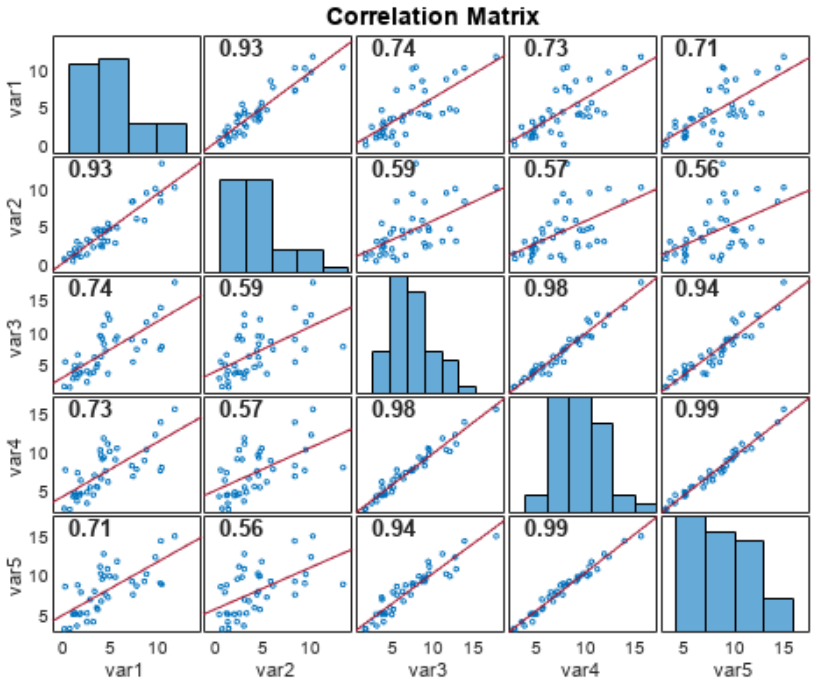

Figure 26. Example of correlation matrix composed by Pearson's coeff.

7.3 Baselines

The processed stationary points were sorted by each bin. The bin is a slice of x values.

For each bin there is a group of points where the mean along x and y and the standard deviation were evaluated. The values for each bin are stored in a table. The table represents the standard behaviour of a single device. According to this approach, there will be a table describing the standard behaviour of a given device quantity, temperature, pressure, or vibration. In this way, it is possible to determine whether a signal is representative of abnormal behaviour or aligned with normal operation.

In general, if an operating point classified as stationary falls within the standard deviation, the point is to be considered non-alarming. Conversely, if an operating point falls outside the baseline limit, either as a positive or negative limit, this point is to be considered alarming as far from standard operation.

The severity with which to report alarms and the nature of the alarm itself should be related to the length of time the operating points are outside the standard deviation and how far they deviate in magnitude. Potentially, a signal that deviates stationary for multiple time intervals from 3 σ_x should be considered an anomaly. Moreover, it is possible to determine whether there has been any degradation of the device, since most points would start working in a different regime from the original one.

In the following figure has been reported an example of base line table, the baseline figure, the scatter plot used to generate the baseline and the idea of two potential events, with star marker, represented the anomaly and normal behaviour.

id	Primary tag	Value[mean]	StD
0	17.917	37.728	4
1	25.284	34.502	3
2	34.994	10.999	7
3	44.484	8.987	2
4	52.995	11.741	1.5
5	61.553	15.141	3.523
6	75	20	3.523
7	85	23	3.523
8	95	26	3.523

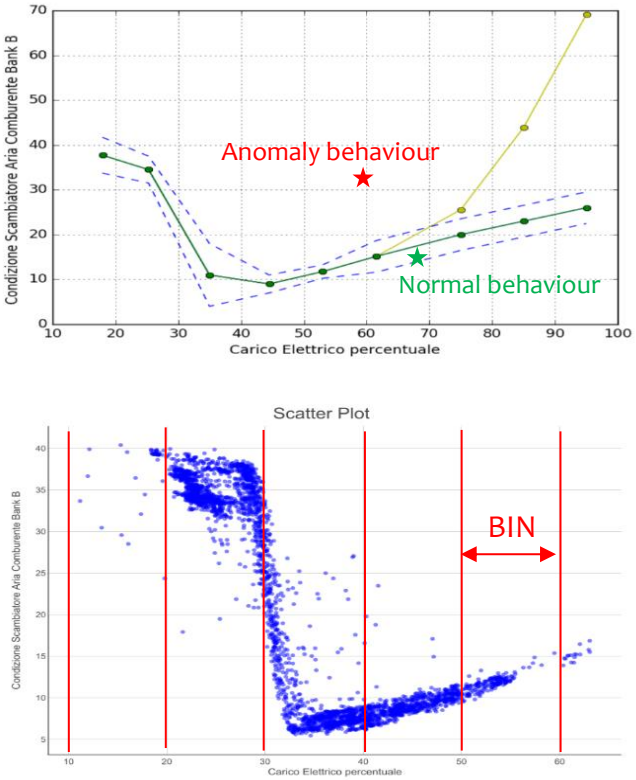

Figure 27. Example of baseline creation.

7.4 Analysed Devices

The devices that can be monitored are numerous, and the system has no limitations.

The only limitation is the necessary instrumentation that must be present, since the system is completely data-driven. Indeed, the baselines are created from the data collected by the sensors, and the controls for signal deviation from its standard operation always come from the sensors.

Baselines can consist of data of different natures from each other, such as pressures, temperatures, and vibrations. An example of monitoring a diesel generator might be as follows: Primary variable equal to the electrical load; Secondary variables to be monitored:

- Cylinder exhaust gas temperature;
- Vibration;
- Oil temperature;
- Temperature delta between engine and heat exchanger heat flows;
- Fuel pressure;

The system thus structured is very flexible and allows for easy expansion of the devices involved, with the only constraint being the sensors that must be present.

8 Integrated Ship Energy Production, Distribution, Recovery and Management

Approach based on evaluation of thermal fluxes of on-board installed devices. In this context it will be possible to include Waste Heat Recovery (WHR) system to optimize energy dissipation. With this approach it will be possible to perform an energy assessment according to potential refitting of the system.

The idea is that, knowing all the devices installed on board the ship, it is possible to calculate the heat flux exchanged between them. In general, it is possible to divide all the components installed aboard the ship into three macro categories of energy users. The devices used for power generation, the devices that power the propulsive load, and the other shipboard loads that may be of a different nature, such as hotel or cargo handling. By knowing the relationship between these, it is possible to make predictions as operating conditions change and as installed components change, simulating the addition of useful devices to recover lost energy in the form of heat as exhaust fumes.

The main step in conducting the above discussion is to know the plant schematics of the devices installed on board.

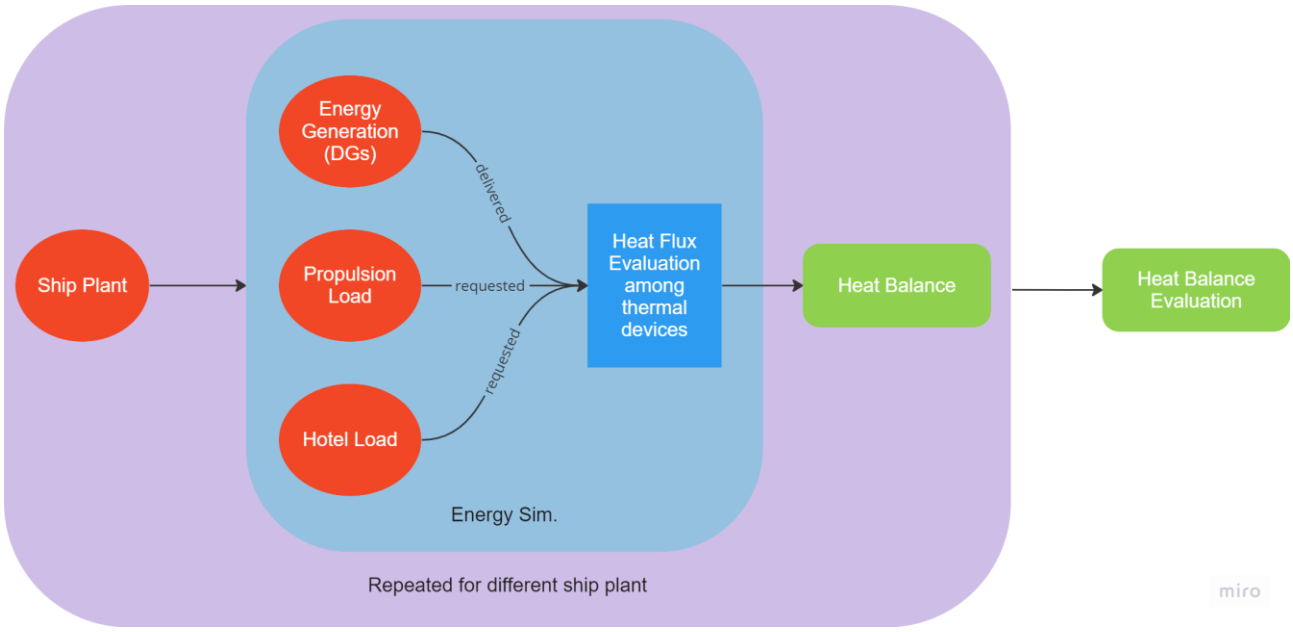

Figure 28. pipeline of heat flux evaluation

8.1 Model's Performance Analysis

In general, the heat flux equation for a heat exchanger involving water with specific heat capacity (cp) can be expressed as:

$$q = m\ cp\ (T2 - T1)$$

where: q is the heat flux (in Watts); m is the mass flow rate of water (in kg/s); cp is the specific heat capacity of water (in J/kg*K); $T1$ is the inlet temperature of water (in degrees Celsius or Kelvin); $T2$ is the outlet temperature of water (in degrees Celsius or Kelvin).

This equation represents the amount of heat transferred per unit time between the water and the heating medium through the heat exchanger. The specific heat capacity of water is an important parameter in this equation, as it represents the amount of energy required to raise the temperature of water by 1 degree Celsius or Kelvin.

There are usually plate exchangers installed on board in which circuits exchange heat; these can be of different nature, air-water, water-oil, water-water. In general, ships use seawater as the main flow for open circuits. This is superheated to give up excess heat and release it to the outside.

A plate heat exchanger is a type of heat exchanger that uses a series of thin plates, typically made of stainless steel, to transfer heat between two fluids. The fluids flow in separate channels, and heat is transferred between them through the plates, which have a large surface area relative to their volume.

The basic design of a plate heat exchanger consists of a series of plates that are clamped together with gaskets between each plate to form two separate channels. The hot fluid and the cold fluid flow through each of the channels, and heat is transferred through the plates from the hot fluid to the cold fluid. Plate heat exchangers offer a number of advantages over other types of heat exchangers. They have a compact design, which allows for high heat transfer rates in a relatively small space. They are also highly efficient, with heat transfer coefficients that can be several times higher than those of other types of heat exchangers. In addition, plate heat exchangers are easy to maintain and clean, as the plates can be easily removed and cleaned individually.

The heat transfer rate in a plate heat exchanger can be calculated using the heat flux equation described earlier, but the specific geometry of the plates can affect the heat transfer coefficient. In general, the heat transfer coefficient is proportional to the plate surface area and the velocity of the fluids, and inversely proportional to the plate thickness and the distance between the plates. The flow rate, temperature difference, and physical properties of the fluids also play a role in determining the heat transfer rate.

Indeed, the heat flux equation for a plate heat exchanger can be expressed as:

$$q = UA\Delta Tm$$

where: U is the overall heat transfer coefficient (in W/m2*K); A is the heat transfer surface area (in m^2); ΔTm is the logarithmic mean temperature difference (in degrees Celsius or Kelvin).

The overall heat transfer coefficient, U, takes into account the thermal resistance of the plates, the fluid properties, and the flow rates. The heat transfer surface area, A, is determined by the number and size of the plates, and the logarithmic mean temperature difference, ΔTm, is a measure of the average temperature difference between the two fluids as they flow through the heat exchanger.

The logarithmic mean temperature difference can be calculated using the following equation:

$$\Delta Tm = (\Delta T1 - \Delta T2) / ln(\Delta T1 / \Delta T2)$$

where:

$\Delta T1$ is the temperature difference between the hot fluid inlet and the cold fluid outlet (in degrees Celsius or Kelvin); $\Delta T2$ is the temperature difference between the hot fluid outlet and the cold fluid inlet (in degrees Celsius or Kelvin).

The heat flux equation for a plate heat exchanger can be used to calculate the heat transfer rate between the two fluids, which can be useful for designing and optimizing the performance of the heat exchanger.

As mentioned earlier, knowing the flows exchanged between the different circuits makes it possible to hypothesize and simulate the addition of devices useful for recovering the energy lost to the environment. In particular, the waste heat recovery (WHR) is becoming an increasingly important area of focus in the marine sector, as it offers a way to improve energy efficiency and reduce greenhouse gas emissions. Waste heat is generated by various systems and processes onboard a ship, such as the main engine, auxiliary engines, and exhaust gas boilers, and can be recovered and reused to provide power and heat for other systems.

One of the most common methods of waste heat recovery in the marine sector is through the use of exhaust gas boilers. These boilers use the waste heat from the ship's engines to generate steam, which can then be used to drive turbines and generate electricity or to provide heat for other systems onboard the ship. By recovering this waste heat, the ship can reduce its fuel consumption and emissions, as less fuel is needed to generate the same amount of power and heat.

Another method of waste heat recovery in the marine sector is through the use of Organic Rankine Cycle (ORC) systems. ORC systems use a working fluid, such as a refrigerant or hydrocarbon, to generate power from low-temperature waste heat sources. In the marine sector, ORC systems can be used to recover waste heat from the engine's cooling water and exhaust gas and can provide additional power and heat for the ship's systems.

Other waste heat recovery technologies that are being explored in the marine sector include thermoelectric generators, which can generate power directly from temperature differences, and heat pumps, which can provide heating and cooling for the ship's systems using waste heat as a source.

Eventually, the waste heat recovery in the marine sector is a crucial area of focus for improving energy efficiency and reducing emissions, and a variety of technologies are being developed and deployed to make use of this valuable resource.

8.2 Energy Production, Distribution, Management & Recovery Onboard Process Simulator

The DT4GS Simulation, Prediction, Optimisation, and Management Apps will include a simulator of the Energy Production, Distribution, Management & Recovery onboard processes.

This simulator will have a modular object-oriented open architecture in order to be applicable to most of the present / future ship propulsion-power plant configurations.

The most typical propulsion-power configurations for merchant ships are Diesel (adopted for instance by the majority of recent large container vessels), where the propulsion power is provided by one (or two) slow-speed Diesel Engines and the electric power for shipboard services is provided by a set of Diesel Generators, and Diesel-Electric (adopted for instance by the majority of recent large cruise ships), where the propulsion shaft is driven by two Electric Motors and the electric power for both propulsion and shipboard services is provided by a set of Diesel Generators.

Anyway, in both cases the main power source is a large slow-speed Diesel Engine with a thermal efficiency of about 50%, meaning that for each kW of utilizable shaft power about the same is dispersed as heat. Therefore, especially for vessels with high installed power (such as large container vessels and cruise ships), there is a large potential margin of fuel consumption reduction (and consequently of emissions reduction) from the recovery of this waste heat either directly in the form of thermal power or indirectly in the form of electric power: it is estimated that an optimized high-efficiency Waste Heat Recovery (WHR) Plant may enable up to 10% of the main Diesel Engine / Generator shaft power to be recovered.

Cruise ships, being characterized by a Hotel Load for the Electric Users almost as large as the Propulsion Load as well as by an important direct heat request from the Heat Users, may benefit the most from WHR strategies and as a matter of fact WHR plants are already installed on many of these vessels albeit mostly to recover heat for the onboard Heat Users (such as production of Potable Water by the Evaporators, heating of Potable Water for Galley and Accommodation, AC Cooling Water preheating). For merchant ships, which are usually characterized by a relatively low (with respect to propulsion shaft power) request of electric power and an even lower request of heat for shipboard services, the appeal of WHR strategies (with associated costs) is in general rather scarce in presence of a traditional Diesel-Engine Propulsion Plant whilst it is higher in presence of a Diesel-Electric Propulsion Plant where the recovery of electric power may significantly decrease the Propulsion Load.

It can then be concluded that the recovery of waste heat for use as additional electric power for ship propulsion and as additional electric power or heat for shipboard services may cut exhaust gas emissions and deliver fuel savings of ship transport up to 10%.

By neglecting the heat dispersed in the air of the Engine Room through direct convection / radiation from the engine surfaces, the Waste Heat from a thermal ship engine is dispersed in the outside environment through the following three media:

- LT Cooling Water from the LT cooling circuit of the engine jacket (about 60°C, low thermal value)
- HT Cooling Water from the HT cooling circuit of the engine jacket (about 90°C, medium thermal value)
- Exhaust Gas from the combustion within the engine cylinders (about 300°C, high thermal value)

As a reference, the thermal balance of a typical Diesel-Engine is provided in the figure below:

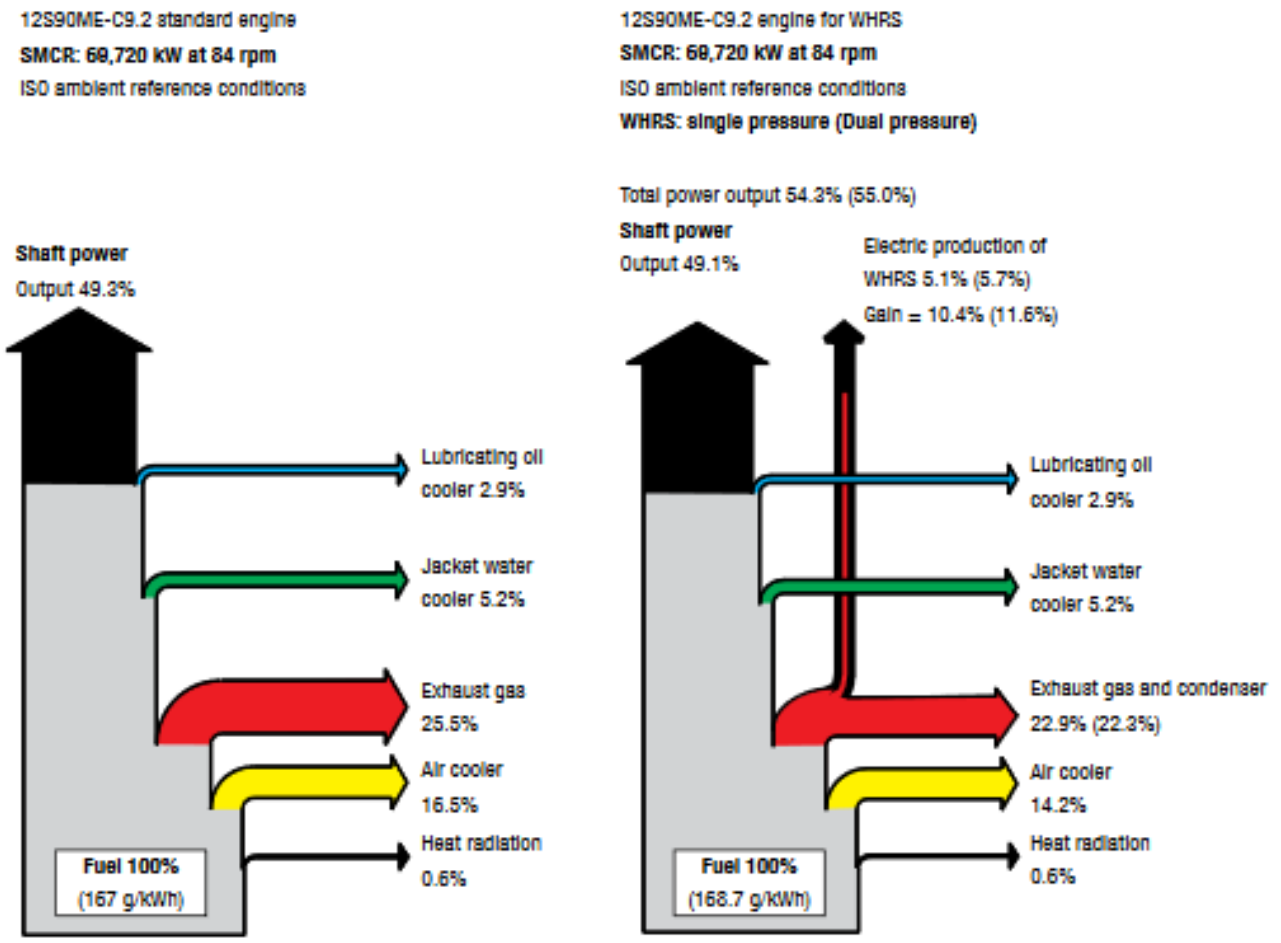

Figure 29. Comparison between standard (left) and WHR (right) solutions.

As for waste heat recovery from three waste heat sources, the following consideration hold:

Due to its low thermal value, WHR from the LT water-cooling circuit is both technologically complex and economically inconvenient.

- WHR from the HT water-cooling circuit can be used (and it is already implemented aboard many cruise ships) to distribute thermal power to the Heat Users (typically Hot Water Exhaust Gas Economizer for Fresh Water production or Potable Water / AC pre-heaters) through suitable Heat Exchangers.
- WHR from the HT water-cooling circuit may be also used to supply electric power to the Electric Users through suitable ORC (Organic Rankine Cycle) or OKC (Organic Kalina Cycle, to increase efficiency if the input temperature is too low) systems, provided this ground-plant technology is adapted to the constraints posed by ship installation in terms of power / dimension ratio).
- WHR from the HT water-cooling circuit may be also used to supply Cooling Water to the AC plant through suitable ACU (Absorption Chiller Unit) systems, thus reducing the electric power requested by the HVAC Chillers.
- WHR from the EG can be used (and it is already implemented aboard many cruise ships) to generate saturated steam through suitable EGB (Exhaust Gas Boiler) or Steam EGE (Exhaust Gas Economizer) directly fitted to the Diesel Engines exhaust outlet supplying directly the produced steam to the Steam Users (typically in the Laundry and the Galley) and / or distributing its high-value (i.e. 180°C) thermal power to the Heat Users through suitable Heat Exchangers.

- The thermal power of the saturated steam produced by the WHR from the EG may be also used to supply electric power to the Electric Users through suitable ORC (Organic Rankine Cycle) systems, again provided this ground-plant technology is adapted to the constraints posed by ship installation in terms of power / dimension ratio).
- The saturated steam produced by the WHR from the EG may be also used to supply electric power to the Electric Users through suitable Steam Power Turbine, provided this ground-plant technology is adapted to the constraints posed by the sub-optimal thermal value (too low) of the steam and by ship installation in terms of power / dimension ratio.
- As an alternative or an addition to the previous WHR strategy, the EG can be fed (either in parallel or downstream the turbocharger from the engine) to a Gas Power Turbine thus directly supplying electric power to the Electric Users, provided this technology is adapted to the constraints posed by ship installation especially when used in conjunction with Steam ORC / EGE.

The primary scope of the DT4GS baseline simulator should be the benchmarking of the energy efficiency of different WHR configurations, modelled through a limited set of design parameters, over a large set of service conditions representative of the whole operational profile of the ship.

Therefore, it should be intended as a support to End Users at the very beginning of a new ship design, when a fast screening of possible alternative solutions is most needed but can be as well helpful to the End Users when considering the retrofit of an existing ship in order to improve its WHR performance.

The WHR simulation will aim to evaluate the overall electric / heat energy balance of the ship and as such it will be able to manage the following processes:

- FW production / distribution / consumption
- Steam production / distribution / consumption
- Electric power production / distribution / consumption

From a steady-state point of view, thereby not modelling in real-time the internal processes occurring in each involved system and the regulation feed-back loop of the relevant mass flows and associated temperatures implemented to achieve the dynamic equilibrium.

The WHR simulation will therefore not be a time-domain simulation solving a system of differential equations driven by initial conditions to analyse the dynamic evolution of the energy processes but rather a logical state-machine solving a system of algebraic equations with given known terms to determine the resulting balance state.

Each simulation will thus correspond to a static set of operational conditions denoted as a "voyage condition", which could either represent a stay in port or a navigation leg. A chain of sequential voyage conditions will therefore represent a typical "voyage" of the ship whereas a chain of voyages will represent the "operational profile" of the ship that is the set of operational / environmental conditions which the ship will likely encounter during a year of standard service.

The WHR simulator should be therefore a part of a larger DT4GS baseline simulator, which will include a "voyage" simulator built-up according to the same organization principles as the former.

Indeed, the voyage simulator will have in input an operation profile, consisting of a set of voyage conditions, each comprising:

- a navigation leg to be crossed within an expected time.
- a set of environmental conditions (i.e. sea / wind / current) likely to be encountered on the leg.
- the service load expected on the leg.

The service load will have in general the following breakdown:

- propulsion power (in case of Diesel-Engine propulsion)
- electric power request
    - propulsion load (in case of Diesel-Electric propulsion)
    - hull & engine services load
- hotel load
- FW request
- CW request
- Steam request

In particular, the voyage simulator will provide the WHR simulator, for each voyage condition, the Propulsion Power requested to the Main Propulsion Plant and the Electric Power requested to the Power Generation Plant.

Based on this, the WHR simulator will estimate the Waste Heat produced by the Power Generation Plant and by the Main Propulsion Plant (in case of Diesel-Engine propulsion), which will be used as an input to the WHR Plant model.

Based on this input (and the prevalent internal / external environmental conditions), the WHR Plant model will provide an estimate of the electric power and thermal power recovery: it must be considered that, when electric energy recovery from the waste heat of Diesel Generators is implemented, the recovery process should be analyzed iteratively as the resulting reduction in the electric load will in turn reduce the waste heat and thus the recovery.

In short, the main features of the DT4GS baseline simulator will be:

a. Recommend an optimal configuration for the WHR Plant.
b. Estimate the effects and associated fuel savings of implementing one or more Energy Recovery Units.
c. Estimate the Energy Efficiency of a given WHR Plant.

As there is a diversity of possible WHR Plant configurations, depending on ship types and operational profile, it is of primary importance for the simulation tool to be easily configurable.

According to these agreed objectives, the simulation tool will be developed within a high-level systems theory framework using input/output functional blocks which can be easily added / removed / inter-linked to represent any viable WHR Plant.

The typical high-level functional architecture of the WHR process onboard of a cruise ship was used as a reference block-diagram for the Research Project as per the figure below:

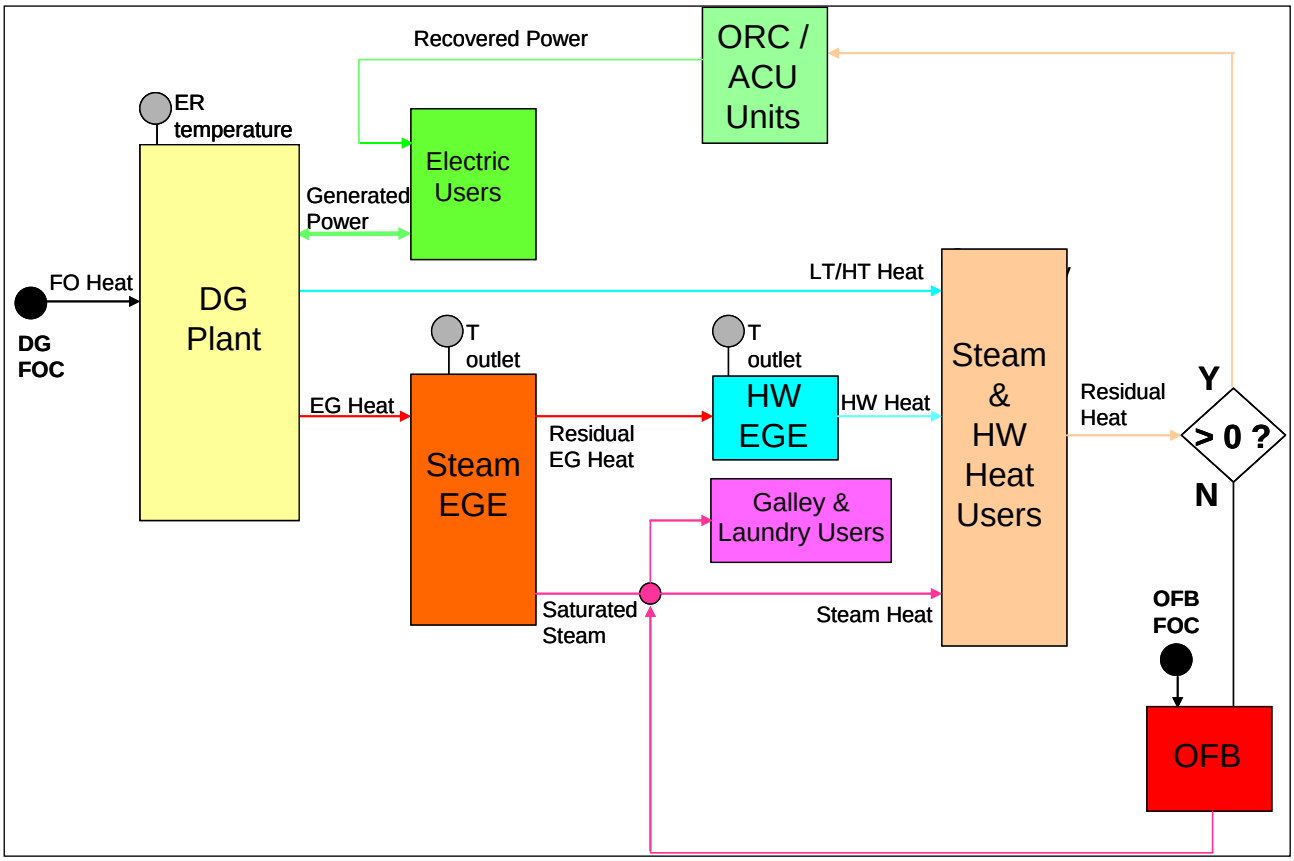

Figure 30. Example of high-level functional architecture of the WHR process in cruise ship.

Specifically, the model illustrated in the block-diagram is the following:

- the DG Plant is modelled in the simulator as a system which receives in input a given heat in the form of gross calorific power of fuel and provides in output, based on assumed electrical efficiency, a certain amount of waste heat dissipated through EG / HT / LT plus a certain amount of electric power.
- any recovery unit is modelled in the simulator as a system which receives in input a certain amount of waste heat conveyed by hot water / steam / exhaust flow and recovers its either directly as a water / steam flow (direct heat recovery) or indirectly as electric power (direct electric power recovery by ORC or indirect electric power recovery by ACU). The performance of the WHR Plant shall be ultimately measured in terms of equivalent FOC saving by OFB (in case of heat recovery) or DG (in case of power recovery).
- the waste heat recovery from the exhaust gas is performed by the EGE Units, which shall make available this recovered heat as saturated steam (through a Steam EGE) and *optionally* as hot water (if a centralised HW Recovery system is implemented with a HW EGE in sequence to a Steam EGE).

The total heat conveyed by hot water / steam shall be recovered by any of the following users:

- Steam / Water Heaters
- Evaporators
- ORC units or ACU

The efficiency of any thermal exchanges shall be ideally considered equal to one whereas the efficiency of any power recovery by ORC/ACU shall be taken according to their stated nominal performance.

A more detailed overall schematic overview of the Tri-Generation or CHCP (i.e., Combined Heat, Cooling & Power) Plant of a diesel-electric cruise ship, is illustrated in the block-diagram below.

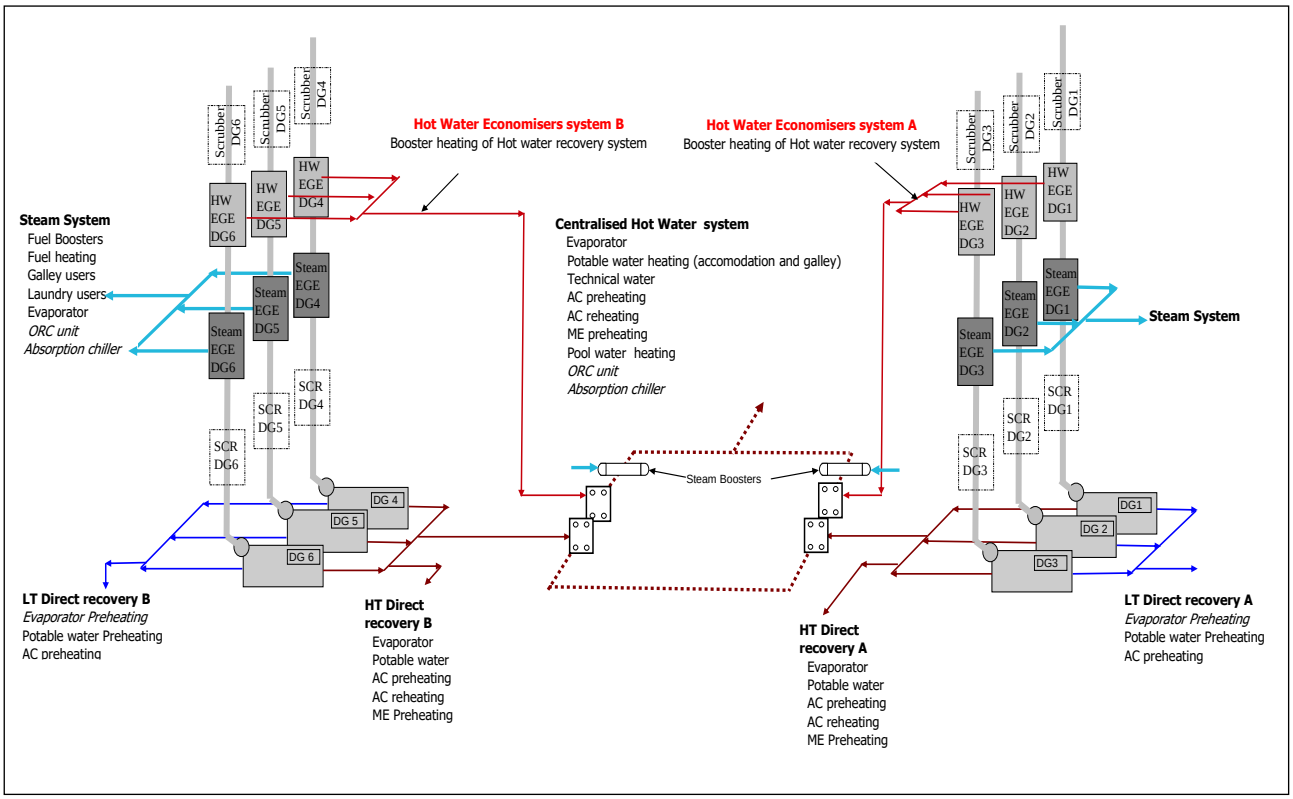

Figure 31. overall schematic overview of the Tri-Generation.

With reference to this figure please consider the following remarks.

- Steam system, HT Direct Recovery and Centralized Hot Water system are well known solutions which have been already installed on board of various cruise ships.
- Feasibility of a Hot Water Economizer system and of LT Direct Recovery is still to be ascertained.
- The heat dissipated by the LT circuit is assumed to result from engine Charge Air LT cooler and LO cooler, therefore only indirect heat recovery from the LO circuit through the LT circuit shall be considered.
- Evaporator pre-heating can be selected by the User as a possible LT Direct Recovery user.
- ORC Recovery Units and Absorption/Adsorption Chillers units can be selected by the User as possible users of recovered heat from hot water / steam. Considering the assumed temperature working ranges, ORC shall be preferably fed by Steam whilst ACU shall be preferably fed by Hot Water.
- SCR / Scrubbers (despite their being included in this overall view for sake of completeness) and counter-pressure type Steam Generators shall not be modelled in the simulation framework, as neither shall be the possibility to recover heat from incinerator exhaust gases.

Previous general remarks require some more detailed explanation.

It shall be possible for the User to define a better performing Steam EGE i.e. one with a lowest outlet temperature than that listed in the look-up tables of the devices available in the equipment library.

Whenever doing this the User should be aware that the main limitation on the maximum amount of recoverable heat from DG exhausts depends on two main factors:

- The maximum allowed counter-pressure recommended by the DG supplier.
- The minimum allowed temperature at the outlet of the EGE according to the EGE supplier.

The latter statement can be further elaborated.

A Steam EGE should always come along with an assumed operating steam pressure which in its turn fixes the temperature of the saturated steam. Existing Steam EGE typically have operating steam pressures of about 9 bar, so to ensure a safe circulation of the saturated steam through the steam system: this corresponds to a saturated steam temperature of about 180°C.The operating steam pressure could be somewhat lowered thus decreasing the temperature of the saturated steam, even if it is not recommended to go below a value of about 6 bar. As the latter pressure value corresponds to a saturate steam temperature of about 160°C, it would be ideally possible to lower the outlet temperature at the Steam EGE up to about 160°C. From a practical standpoint, however, the minimum outlet temperature at the Steam EGE shall be generally about 20°C higher than the saturated steam temperature, which means that to go below about 180°C should not be operationally feasible. In fact, a lower difference value between exhaust gas outlet and saturated steam temperature will involve an increase of dimensions, weight, and counter pressure.

As foresaid it would be possible for the User to define a two-stage EGE, the first stage being a Steam EGE for saturated steam production and the second stage being a HW EGE for hot water heating using the residual heat from the exhaust gas at the outlet of the first stage. In this case the outlet temperature at the HW EGE shall not be affected by any limitations due to the operating values of the saturated steam.

Nevertheless, there is still a main technical limit to the outlet temperature at both the Steam and HW EGE and this is represented by the sulfur acid corrosion which depends on the percentage of sulfur present in the burnt fuel. According to state-of-the-art, thereby considering adoption of standard materials for EGE and stack pipes and continuous use of HFO/IFO with a sulfur content less than 4.5% as required by present normative, the minimum and safe outlet temperature to prevent excessive corrosion is 160°C.

The typical WHR scheme of a Diesel-Electric merchant ship is the following:

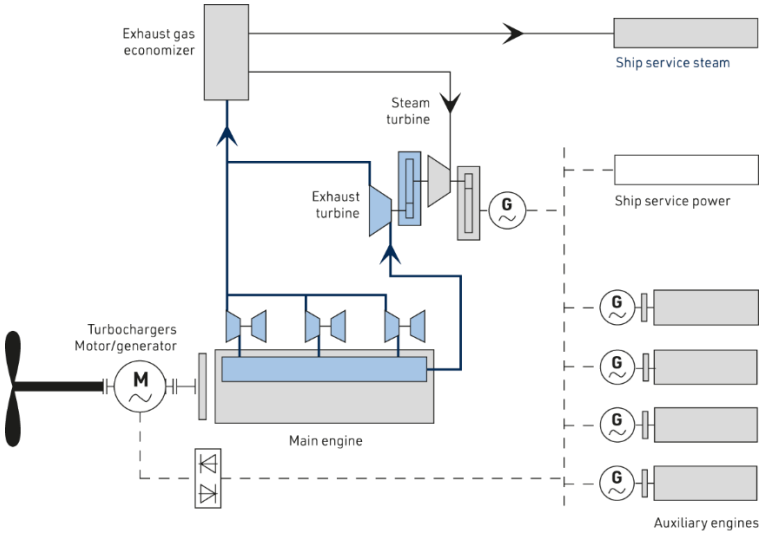

Figure 32. typical WHR scheme of a Diesel-Electric.

As aforesaid, the WHR part of the DT4GS simulator should be able to model these (and possibly other) configurations.

It must be finally considered that the necessity of reducing emissions is leading to the installation of SCR or Scrubbers before the funnels' outlet. This may pose some problems to the concomitant installation of

EG recovery units between the turbocharger outlet and the aforesaid emissions-abating devices as the resulting total counter-pressure at the turbocharger may be too high:

- Regarding SCR or Scrubbers, given the state-of-the-art of available abatement technology for exhaust gas emissions from marine DG's, a configuration with two economizers (Steam and Hot water), one SCR and one Scrubber for each DG would be not feasible since the total counter-pressure at the turbocharger would be too high.
- As an alternative to the former solution, a counter-pressure Gas Power Turbine could be installed at the outlet of each turbocharger, but the feasibility of this solution must be again checked against the total counter-pressure at the turbocharger; also, it should be also checked the possibility to further interpose Steam EGE between the turbine outlet and the SCR / Scrubber or have them in parallel with the turbine.
- In principle a counter-pressure Steam Generator could be installed at the outlet of each EGB for heat recovery in the form of electric power. However, this would require the industrial availability of a high-temperature EGB able to produce saturated steam at much higher operating pressures (at least 15 bar) and thence temperatures (indicatively about 240°C) than those of the state-of-the-art EGB. Note that such steam temperature increase implies a consequent reduction in the heat recovered from the exhaust gas. It should also be noted that, if implemented, the Steam Generator would replace the ordinary EGB to serve the steam users as its output steam flow would have pressure / temperature values similar to those of an ordinary EGB.
- On the other hand, because the exhaust gas temperature at the outlet of the high-temperature EGB would be much higher than usual, a HW EGE could be utilized to recover the residual heat from these hot exhausts.

The WHR simulator will feature a built-in library of the functional blocks of the different equipment and systems typically present in a generic CHCP Plant of a merchant / cruise vessel.

In general, these blocks will pertain to three main categories:

- Generation units
    - Diesel Engines
    - Alternators
- Recovery units
    - Heat Recovery Units
    - Electric Recovery Units
- Users
    - FW Users
    - CW Users
    - Steam Users
    - Electric Users

Generation and Recovery units will be modelled in terms of input/output mass/energy flow based on characteristic parameters and functional curves implemented in look-up tables, which could be accessed and modified by user, whereas Users units will be only modelled as input variables in terms of User-given request of fresh water / chilled water / saturated steam / electric power.

The following Thermal Power Recovery Unit will be included in the system library:

- Steam Economizers
- HW Economizers
- Evaporators

- Heat Exchangers for Heating / Re-Heating / Pre-Heating of FW
- Absorption / Adsorption Chillers Units

The following Electric Power Recovery Unit will be included in the system library:

- Organic Rankine / Kalina Cycle Units
- Steam Power Turbines
- Gas Power Turbines

The following operational conditions shall also be defined for each simulation:

- Engine Room temperature
- Sea water temperature
- Type of fuel / Sulphur content of fuel / Specific calorific power of fuel

The final output of the WHR simulator will be the FOC reduction resulting from the intended WHR Plant with respect to the baseline configuration.

The Energy Efficiency of a given WHR configuration shall be determined based on the estimated FOC reduction with respect to the baseline configuration, as per the recovery breakdown below:

- Saturated Steam generation
- Fresh Water generation
- Chilled Water generation
- Electric Power generation

Eventually, the following guiding principles will apply:

- the FOC reduction resulting from any electric power recovery will be estimated as the equivalent FOC that would be needed by the GenSet to produce the same electric load at the given operating conditions.
- the FOC reduction resulting from thermal power recovery in favour of Electric Heaters will be estimated based on the amount of electric power which would be needed by the Electric Heaters to provide the same heat.
- the FOC reduction resulting from thermal power recovery in favour of OFB will be estimated as the equivalent FOC which would be needed by the OFB to produce the corresponding amount of steam.
- the FOC reduction resulting from the use of Evaporators will be estimated based on the amount of electric power which would be needed by the RO Plant to provide the same amount of FW.
- the FOC reduction resulting from the use of ACU will be estimated based on the electric power that would be needed by the HVAC Chillers to produce the corresponding amount of CW.

9 Life Cycle Assessment Model

Sustainability in ship operations in terms of energy efficiency and the emissions impact on the environment constitute a major concern in the maritime industry. The various scenarios investigated through different LCA techniques aim to provide a systematic analysis that helps to identify, quantify, interpret, and evaluate the environmental impact of different mitigation strategies through the vessel's life. This section aims to investigate LCA in the maritime sector by a different dynamic perspective, coupling data driven methodologies with existing marine engineering theory. Conventional studies and frameworks found in pertinent literature about LCA in the maritime industry, consider the vessel as an interactive entity with its environment, described by a multitude of variables each one affecting the stages in a vessel's life from a different aspect. These stages correspond mainly to 1) the shipbuilding stage, 2) ship operation including major maintenance activities, 3) and finally the stage of ship dismantling/recycling. Initial studies on the subject focused on partitioning this entity in sub-systems describing different parts of the vessel like (machinery, equipment for cargo etc.). They also attempt to define the distribution boundaries of the control variables as well as the indicators, for each vessel empirically, a process highly subjective, that eventually results in non-optimal strategies in terms of financial and environmental efficiency.

This approach aims to present a holistic updated view on LCA in the maritime sector by utilizing a vast amount of data and exploiting a **digital replica (digital twin)** of the vessel, to construct **dynamically,** tailor made **optimum** control variables and KPIs for each LCA scenario, as well as assessing and adapting these scenarios through simulation models, as the life of the vessel progresses.

9.1 Existing LCPA Tool (Design & Retrofitting/Operation/Recycling)

DANAOS has accumulated the past few years a versatile legacy from participating in several EU projects related to LCA analysis and design optimization. Our aim is to appropriately exploit this heritage to facilitate in the progression of the project as far implementation is concerned, as well as to use it as a vantage point to set the benchmarking criteria, to transcend and extend beyond current trends and existing SOTA solutions.

The sections that follow are devoted in outlining the main modules of a LCA toolkit, the control variables as well as the KPIs utilized to assess alternative designs or retrofitting solutions for a particular vessel, in the context of HOLISHIP EU project GA: 689074. The exact calculation of the variables utilized to assess the **financial** and **environmental** impact, of different scenarios does not belong in the scope of this deliverable.

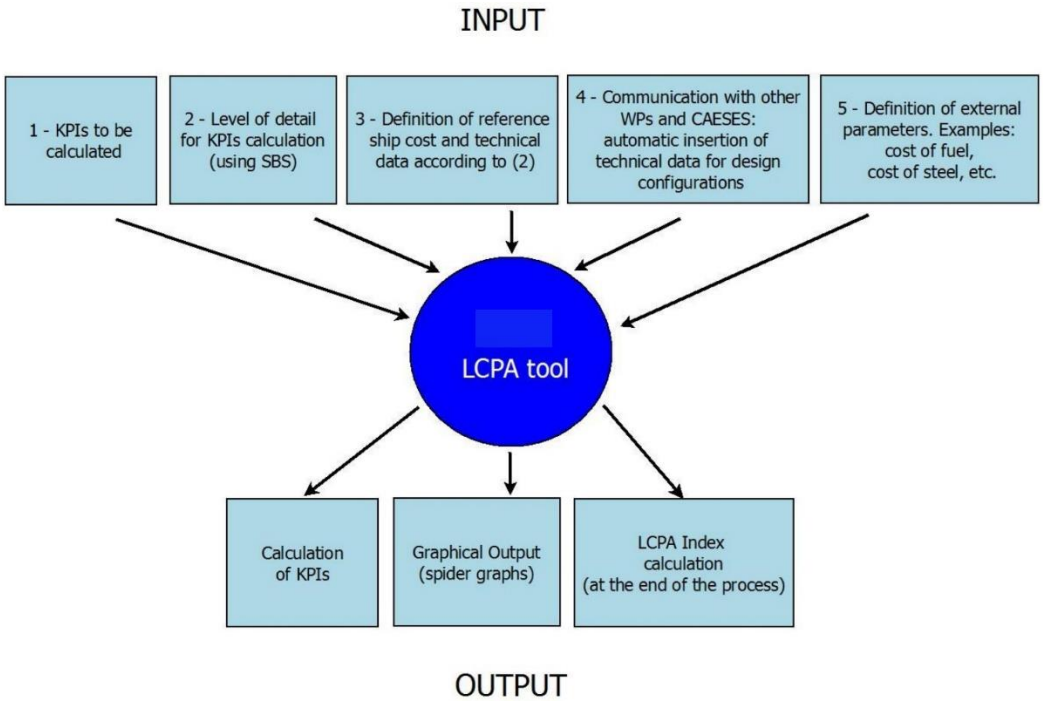

Figure 33. Main building blocks of LCA tool

KPIs to be calculated

In this part of the tool, the user will be able to select which KPIs is interested in for the analysis (Table 7). Moreover, the weight of each KPI for the LCPA Index calculation is to be assigned. Depending on the KPIs selected, certain data are required to run the analysis. The system shall be able to recognize which data shall be inserted or neglected.

Table 7. Selection of KPIs

Data collection	Selection	Weight	Total weight
1. BLD	yes	0.20	1.00
2. CAPEX	no	-	
3. OPEX	yes	0.20	
4. M&R	no	-	
5. AAC	yes	0.20	
6. RFR	no	-	
7. NPV	no	-	
8. AAB	yes	0.40	
9. EBITDA	no	-	
10. ROIC	no	-	
11. EEDI	yes	0.60	1.00

12. NOx	no	-	
13. SOx	no	-	
14. CED	yes	0.40	
15. PM	no	-	
LCC	yes	0.50	**1.00**
LCA	yes	0.50	

Level of detail for KPI calculation

The collection of data has been based on the Ship Breakdown Structure (SBS) of these two voices. The SBS will be also used to define the items modelled in the LCPA structure. Depending on the level of detail specified, different amount of data is requested.

Definition of Reference ship cost and technical data

Here technical and cost data of the reference ship will be inserted. This ship will be the reference for the evaluation of costs and emissions for the new design configuration. During the analysis of KPIs in previous phases of the project, it has been assessed that Building Cost and Opex are the two pillars to evaluate the economic performance of a vessel. Data should be received from ACs and other design WPs (e.g., WP4 LLs).

Automatic insertion of data for new design configurations

In this section, similarly as for reference ship data, technical data of the new ship are inserted, based on the SBS. Costs data are not required in this section (except for few voices if they are known). Costs are calculated through an extrapolation of the reference ship values, developed from statistical data and physical considerations. New technical data should come from ACs and other design WPs (e.g., WP4 LLs).

Definition of external parameters

External parameters are not directly affected by ship design
Examples: fuel cost, steel cost, shipyard indirect costs, etc.
External parameters should be kept constant when assessing all design configurations
In other situations, it could be interesting to assess how KPIs vary when external parameters change for the same ship (example variation of fuel cost, steel cost, etc.).

LCPA Tool

This part is the core of the tool. It is where technical data of the new ship design are used to predict costs (through Cost Estimating Relationships, CERs) and emissions through the life cycle of the ship. The model of the ship will be built in the three phases of her life cycle:

Phase 1: Design and Construction
Phase 2: Ship operation
Phase 3: Disposal/Recycling

This procedure shall be done for both the reference ship and new design configurations.

KPIs to be calculated and LCPA Index calculation

Based on the selection of KPIs in the first module of the tool and calculation of costs and emissions in the LCPA structure, KPIs can be calculated for all ship configurations analysed. After the collection of all KPIs,

coefficients can be defined and the LCPA Index can be assessed for each ship configuration, obtaining the best design. It is important to highlight that this procedure is subjective, because KPIs selection and weight of coefficients totally depend on the user. Moreover, only cost and emissions are evaluated, while other aspects of the ship (such as safety) are not implemented in the current version of the tool.

Input data – Reference scenario

Here the input data of the reference ship are collected. To facilitate the utilization of the sheet, a legend in terms of different colours has been created:

Table 8. Legend of data typologies

Legend
Design parameters
External parameters
SBS costs
insert datum
datum already inserted above
automatically calculated
do not fill

The first three rows in Table 8 describe the type of parameters which can be inserted in the sheet. These are:

Design parameters: technical data of the ship; these directly depend on the design of the ship and they are not influenced by external factors

External parameters: they do not depend on the design of the ship directly.

SBS costs: costs for each significant item of the Ship Breakdown Structure.

The last four rows in Table 1 explain how the user shall use the cell. There are four options:

Insert datum: in these cells, the user shall insert a datum of the ship

Datum already inserted above: useful datum is recalled (copied) from another cell of the spreadsheet where it has been already inserted for some other reason

Automatically calculated: the value in this cell is automatically calculated by the spreadsheet

Do not fill: (self-explaining), some cells in the new configuration ship calculations are empty due to technicalities related to the use of excel

After the legend, the main general technical data of the reference ship should be inserted (Table 9):

Table 9. Main technical data

Ship type
Deadweight - DWT [t]
Lightweight - LWT [t]
Operational Speed [kn]
Length between perpendiculars - Lbp [m]
Breadth - B [m]
Draft - T [m]
Block Coefficients - Cb
Gross Tonnage - GT [tons]
Depth - D [m]
Hull height H [m]
Wet Surface [m2]
Number of main shafts/propeller
Total propulsion power [kW]
Total electrical power [kW]
Machinery density [% surface occupied]
Lifetime (years)
Discount rate [%]

In some cells, there is already a list of data which can be used by the designer to select the option required. This happens for example when the ship type is specified.

After this section, data definition is based on the SBS. Each 1st level voice (KPI) is therefore divided in different parts according to what is defined in the SBS. Analysing the Building Cost, the sheet is organized as follows:

LEVEL		inserted	calculated	level
1	1. Building Cost (w/o 1.5) [€]		-	2
	DWT [t]	81700		
	Cubic number [m3]	194346		
	Operational speed [kn]	24.5		

In this case, technical data are automatically inserted (grey cells). The selection of level on the right side is referred to the calculation of cost data for the new configuration ship and for the insertion of data in

this sheet. In fact, it could happen that the designer is not interested in a detailed analysis of the building cost; therefore, it is not necessary to insert detailed data in this case. Level 1 means that the level one voice of the SBS will be calculated for that KPI. If level 2 is selected, the tool shall be able to calculate the level 1 voice from the calculation of level 2 voices. The same thing happens with the calculation of level 2 cost voices, with the possibility to choose between level 2 and 3.

It is important to initiate data insertion at the higher level of detail. Due to the structure of the calculation module, it is also required to insert data for lower levels of detail.

If level 2 is selected, data for level 2 voices of SBS shall be inserted. In this summary, only the structure cost will be shown. The data required to evaluate the structure cost are defined as follow:

		inserted	calculated	level					
2	1.1 Structure Cost [€]			2					
2a	LWT [t]								
2b		Type	Cost/tonne [€/t]	tonnes [t]	Cost of material [€]	Producibility	Work-hours/tonne [h/t]	Cost of Work-hour [€/h]	Cost of work [€]
	Material 1	Steel, σy = 235 MPa							
	Material 2								
	Material 3								
	Material 4								
	Total (or average)				0				0

Figure 34. Structure cost, data insertion

Input data – New design configuration

Here the input data of the reference ship are collected. However, cost values shall not be usually inserted, since they will be evaluated through calculation. The main structure of this sheet is identical to "Sheet 1: Input data – Reference Ship".

One of the differences (as concerns the SBS voices analysed) is that work hours per tonne values in this sheet are calculated based on the producibility of that material as follow:

Calculation of new values (Financial assessment)

In this layer of the tool, costs related to the new design configuration are assessed, based on data which have been previously inserted. Coefficients for formulation are not always specified inside the text and can be changed by the user. In the majority of cases analysed, coefficients have been determined using a physical and theoretical approach. Values should generally be validated for a more precise result.

The developed procedure works well and smoothly if the "topology" and systems on board do not change significantly from reference ship to new design configurations analysed. In case deep modifications are proposed, it is better to define a new reference ship for a new design investigation.

1. Building Cost (BLD) [€]

1.1 Structure cost (STR)

1.2.1 Main Engines and 1.2.2 Electricity Generators

1.2.3 Power transmission

1.2.4 Propeller

1.2.5 Steering system

1.2.6 Boilers/Heat Recovery system

1.2.7 Manoeuvring system

1.3 Auxiliaries and Outfittings (A&O) cost

1.3.1 Electricity distribution

1.3.2 Engine's aux. system:

1.3.3 Fire-fighting/safety systems

1.3.4 Anchoring

1.3.5 Bildge system

1.3.6 Ballast system

1.3.7 Painting and coatings

1.4 Systems for Payload

1.5 Shipyard indirect costs

2. CAPEX

3.OPEX and Revenues

3.1 Operating Costs

3.1.2 Crew wages

3.1.3 Stores

3.1.4 Lubricants

3.1.5 Administration & Management

3.2 Voyage Costs

3.2.1 Fuel Consumption

3.2.3 Port Charges

3.2.5 Tugs for Manoeuvring

3.2.4 Canal dues

3.3 Costs related to Payload

3.5 (4.) Maintenance & Repair (M&R)

3.5.1 Operational Maintenance

3.5.2 Scheduled dry dock

3.6 Insurance

3.6.1 Hull and Machinery

3.6.2 P&I

Fuel Consumption for LCA

In this layer of the tool, CO_2, SOx and NOx yearly emission values are determined based on the amount of fuel used. Two different procedures can be adopted to determine this value. The one concerns calculating FOC from reported operational data inserted in the variables definition layer of the tool or by incorporating SFOC and Power values for each operating condition.

After this, depending on the type of fuel and systems used on board, values for kgCO_2, kgSOx, kgNOx per ton of fuel should be inserted. In this way it is possible to evaluate the following values:

- **Kg_{CO_2} / year**
- **Kg_{SOx} / year**
- **Kg_{NOx} / year**

which will be used to calculate EEDI, SOx emission and NOx emission KPIs.

LCPA structure, Time Integration graphs and KPIs for LCPA Index

In this part of the tool the SBS cost voices are shown for both reference ship and new design configuration. With this way it is possible to analyse and outline the differences between the two scenarios.

This module entails a graph of cost and revenues in operational phase for both reference ship and new design configuration. KPIs are calculated for reference ship and new design configuration. After this, KPIs coefficient are evaluated:

Depending on the parameter taken into account, coefficients can be defined as follow. It is important to remind that this procedure has been developed to compare design configurations and not to assess economic and environmental performances of a single vessel.

- Earnings parameters (such as NPV, AAB)

They reach their optimum when the parameter reaches the higher value; therefore, it is possible to rank them comparing their maximum; a non-dimensional coefficient for the i-th scenario can be evaluated as:

$$0 \leq c_i^{NPV} = 1 - \frac{NPV_{max} - NPV_i}{NPV_{max} - NPV_{min}} \leq 1$$

The coefficient is always defined between zero and one, even if some or all solutions are negative (loss of capital). There is always a solution with coefficient equal to zero and another one with coefficient equal to one.

- Cost parameters (such as CAPEX, OPEX):

They reach their optimum when the parameter reaches the minimum value; therefore, it is possible to rank them comparing their minimum; a non-dimensional coefficient for the i-th scenario can be evaluated as:

$$0 \leq c_i^{OPEX} = 1 - \frac{OPEX_i - OPEX_{min}}{OPEX_{max} - OPEX_{min}} \leq 1$$

Again, the coefficient is always defined between zero and one. There is always a solution with coefficient equal to zero (worst) and another one with coefficient equal to one (best).

- Environmental parameters (such as CED)

They can be treated similarly as costs, since the optimum solution is the minimum one:

$$0 \leq c_i^{CED} = 1 - \frac{CED_i - CED_{min}}{CED_{max} - CED_{min}} \leq 1$$

Environmental parameters (such as EEDI) could have a maximum limit given by regulations. In this case, the solutions with $KPIi > KPI_{lim}$ shall not be considered in the calculation process.

Defining coefficients in this way, it is not possible to calculate some of them when there is only one solution (i.e., $NPV_{max}=NPV_{min}$). This happens because reference solutions (minimum and maximum) depend on the configurations analysed. If denominator is equal to zero, that is a certain KPIs for different solutions is the same, that KPI should not be considered in the decision-making process, since it does not influence the final result.

In order to keep track of economic and environmental performances, two different coefficients (LCC Index and LCA Index) can be calculated before merging them in a unique LCPA Index. In this way, during the merge, relative weights of Indexes can vary according to the designer point of view. Weights are defined in a table in this spreadsheet. This can be formulated as follows:

$$I_{LCC} = \sum_{i=1}^{N_{LCC}} f_{i,LCC} * c_{i.LCC} \leq 1 \quad ; \quad where: \quad \sum_{i=1}^{N_{LCC}} f_{i,LCC} = 1$$

$$I_{LCA} = \sum_{i=1}^{N_{LCA}} f_{i,LCA} * c_{i.LCA} \leq 1 \quad ; \quad where: \quad \sum_{i=1}^{N_{LCA}} f_{i,LCA} = 1$$

Finally, a global LCPA Index is calculated:

$$I_{LCPA} = f_{LCC} * I_{LCC} + f_{LCA} * I_{LCA} \quad ; \quad where: \quad f_{LCC} + f_{LCA} = 1$$

Another advantage of this method is the possibility to give different weights to KPIs in the decision-making process, as well as increase or decrease the influence of LCC or LCA in the final assessment according to the desire of ship owners and shipyards. On the other hand, the freedom to assign weight at all stage of the process has a strong influence on final results obtained. Increasing the influence of a KPI could mean that a design has a better performance, while this could be not true with other weights assigned.

For a correct visualization of spider graph results, the user should select coefficients of interest modifying graph data selection. In data collection table, for a correct calculation of coefficients, do not leave empty columns; if few configurations are analysed, filled the las columns with result of one solution. In this way, the spider graph can be visualized correctly.

10 Conclusions

Operational performance measures may be classified into four main areas [65]:

- Power plant and auxiliaries: Engine corrosion and oil deposits
- Propeller efficiency: Affected primarily through propeller blade roughness and damage
- Hull resistance: Affected by mechanical, chemical and biological deterioration of the hull
- Navigation, steering and routing: Speed, displacement, trim, plus dynamic effects of ship motions, steering and weather.

The interactions between the above measures are complex. For instance, the ship's fuel consumption, rpm, draught, degradation of systems (engine, hull, propeller) and the environmental conditions are linked in a manner that is not immediately clear due to the often non-linear relationships between the various elements. This necessitates the multitude of engineering analysis and simulation models that incorporate physics ('white box'), empirical measurements ('grey box') (as well as pure data driven ('black box') elements.

The assessment and reduction of fuel consumption in the maritime industry are crucial endeavours in the pursuit of a more sustainable and efficient shipping sector. This deliverable has explored a comprehensive approach to achieve fuel efficiency by incorporating various methodologies and models across different aspects of ship operations.

By adopting effective assessment of ship's consumption based on white and grey box approach, it has been possible to address voyage optimization strategies such as route planning, weather routing, and the implementation of just-in-time model, ship operators can optimize fuel consumption by taking advantage of favourable conditions and minimizing idle time. These practices not only reduce operational costs but also contribute to minimizing environmental impact.

The integration of hull and robotics inspection models plays a vital role in maintaining optimal ship performance. Regular inspections using advanced technologies allow for the timely detection and resolution of potential issues, ensuring that ships operate at peak efficiency. This proactive approach reduces fuel consumption caused by drag and mechanical inefficiencies, ultimately leading to substantial energy savings.

Condition-based monitoring, enabled by sensor technologies and data analysis, offers valuable insights into a ship's performance and allows for proactive maintenance. By identifying and addressing equipment malfunctions or performance deviations promptly, fuel-consuming inefficiencies can be mitigated, optimizing operational efficiency and reducing the overall fuel consumption of the vessel.

The use of energy simulators provides a powerful tool for ship operators to evaluate and analyse different energy management strategies. Through simulations, operators can identify the most fuel-efficient operating parameters, optimizing energy consumption and reducing the environmental impact of ship operations. This informed decision-making process facilitates the implementation of sustainable practices and the reduction of fuel consumption.

Eventually, the life cycle assessment model enables a comprehensive evaluation of a ship's environmental footprint throughout its entire life cycle. By considering all stages, from raw material extraction and ship construction to operation, maintenance, and end-of-life disposal, stakeholders can identify opportunities for improvement and implement sustainable practices that minimize fuel consumption and environmental impact.

In conclusion, the methods and models discussed in this deliverable provide a holistic approach to assessing and reducing fuel consumption in ships. By integrating navigation management, hull and robotics inspection, condition-based monitoring, energy simulation, and life cycle assessment, ship operators can enhance fuel efficiency, reduce environmental impact, and optimize operational performance. Embracing the models and workflows described in this deliverable under the DT framework that is developed in DT4GS will contribute towards a more sustainable and economically viable future, fostering a greener and more efficient global shipping sector.

References

1. Cipollini, F., Oneto, L., Coraddu, A., Murphy, A. J., & Anguita, D. (2018). Condition-based maintenance of naval propulsion systems with supervised data analysis. Ocean Engineering, 149, 268-278. [2] Sang, Y. (2018). Parameter Identification, Simulation, Linearization and Validation of a Ship Propulsion System (Doctoral dissertation, Delft University of Technology).
2. Greene, W., Ramsey, J. S., Leeb, S. B., DeNucci, T., Paris, J., Obar, M., ... & McCoy, T. J. (2005, February). Non-intrusive monitoring for condition-based maintenance. In American Society of Naval Engineers Reconfigurability and Survivability Symposium (Vol. 11).
3. Witten, I. H., Frank, E., & Hall, M. A. (2005). Practical machine learning tools and techniques. Morgan Kaufmann, 578.
4. Wynn, D. C., & Clarkson, P. J. (2018). Process models in design and development. Research in Engineering Design, 29, 161-202.
5. Haranen, M., Pakkanen, P., Kariranta, R., & Salo, J. (2016, April). White, grey and black-box modelling in ship performance evaluation. In 1st Hull performance & insight conference (HullPIC) (pp. 115-127).
6. Coraddu, A., Oneto, L., Baldi, F., & Anguita, D. (2015, May). Ship efficiency forecast based on sensors data collection: Improving numerical models through data analytics. In OCEANS 2015-Genova (pp. 1-10). IEEE.
7. Bakker, M. (2021). A Reference-based Design Approach: in Preliminary Ship Design.
8. Ahlgren, F., & Thern, M. (2018). Auto machine learning for predicting ship fuel consumption. In ECOS 2018-the 31st International Conference on Efficiency, Cost, Optimization, Simulation and Environmental Impact of Energy Systems, 17-21 June, 2018, Guimarães.
9. Martelli, M., Faggioni, N., & Donnarumma, S. (2022). A time-domain methodology to assess the dynamic positioning performances. Ocean Engineering, 247, 110668.
10. Martelli, M., Faggioni, N., & Berselli, G. (2019). Fuel saving in a marine propulsion plant by using a continuously variable transmission. Proceedings of the Institution of Mechanical Engineers, Part M: Journal of Engineering for the Maritime Environment, 233(4), 1007-1021.
11. Altosole, M., Campora, U., Figari, M., Laviola, M., & Martelli, M. (2019). A diesel engine modelling approach for ship propulsion real-time simulators. Journal of Marine Science and Engineering, 7(5), 138.
12. Holtrop, J., & Mennen, G. G. J. (1978). A statistical power prediction method. International shipbuilding progress, 25(290).
13. Holtrop, J., & Mennen, G. G. J. (1982). An approximate power prediction method. International Shipbuilding Progress, 29(335), 166-170.
14. International Organization Standardization, n.d. ISO 15016, 2015. - Ships and Marine Technology – Guidelines for the Assessment of Speed and Power Performance by Analysis of Speed Trial Data.
15. Lyu, X., Tu, H., Xie, D., & Sun, J. (2018). On resistance reduction of a hull by trim optimization. Brodogradnja: Teorija i praksa brodogradnje i pomorske tehnike, 69(1), 1-13.
16. Labanti, J., Islam, H., & Guedes Soares, C. (2016). CFD assessment of Ropax hull resistance with various initial drafts and trim angles. Maritime Technology and Engineering, 3, 325-332.
17. Campbell, R., Terziev, M., Tezdogan, T., & Incecik, A. (2022). Computational fluid dynamics predictions of draught and trim variations on ship resistance in confined waters. Applied Ocean Research, 126, 103301.

18. Zwart, RH. Trim optimization for ships in service: A grey-box model approach using operational voyage data. MSc Thesis. 2020; Delft University of Technology.
19. MariEMS - Improving Models for Marine EnviRonment Services – Chapter III - https://ec.europa.eu/programmes/erasmus-plus/project-result-content/5f1405e1-a87d-4e8d-9f0e1ed40773d1fa/Chapter%203%20%20Trim%20optimisation%2C%20Hull%20and%20propeller%20condition.pdf
20. Barnitsas, M. M., Ray, D., & Kinley, P. (1981). KT, KQ and efficiency curves for the Wageningen B-series propellers. University of Michigan.
21. Sheng, W., & Liu, X. (2006). A genetic k-medoids clustering algorithm. Journal of Heuristics, 12, 447-466.
22. Hartigan, J. A., & Wong, M. A. (1979). A k-means clustering algorithm. Applied statistics, 28(1), 100-108.
23. Liang, Y., & Wang, L. (2020). Applying genetic algorithm and ant colony optimization algorithm into marine investigation path planning model. Soft Computing, 24, 8199-8210.
24. He, Z., Liu, C., Chu, X., Negenborn, R. R., & Wu, Q. (2022). Dynamic anti-collision A-star algorithm for multi-ship encounter situations. Applied Ocean Research, 118, 102995.
25. Singh, Y., Sharma, S., Sutton, R., & Hatton, D. (2017). Optimal path planning of an unmanned surface vehicle in a real-time marine environment using a dijkstra algorithm. In Marine Navigation (pp. 399-402). CRC Press.
26. Zaccone, R., & Martelli, M. (2018, October). A random sampling based algorithm for ship path planning with obstacles. In Proceedings of the International Ship Control Systems Symposium (iSCSS) (Vol. 2, p. 4).
27. Kang, Y. T., Chen, W. J., Zhu, D. Q., Wang, J. H., & Xie, Q. M. (2018). Collision avoidance path planning for ships by particle swarm optimization. Journal of Marine Science and Technology, 26(6), 3.
28. Liang, Y., & Wang, L. (2020). Applying genetic algorithm and ant colony optimization algorithm into marine investigation path planning model. Soft Computing, 24, 8199-8210.
29. Zaccone, R. (2021). COLREG-compliant optimal path planning for real-time guidance and control of autonomous ships. Journal of Marine Science and Engineering, 9(4), 405.
30. Zaccone, R., Martelli, M., & Figari, M. (2019, June). A colreg-compliant ship collision avoidance algorithm. In 2019 18th European Control Conference (ECC) (pp. 2530-2535). IEEE.
31. Enevoldsen, T. T., & Galeazzi, R. (2021). Grounding-aware RRT∗ for Path Planning and Safe Navigation of Marine Crafts in Confined Waters. IFAC-PapersOnLine, 54(16), 195-201.
32. Zaccone, R., Figari, M., Altosole, M., Ottaviani, E., Soares, C., & Santos, T. (2016, December). Fuel saving-oriented 3D dynamic programming for weather routing applications. In Proceedings of the 3rd International Conference on Maritime Technology and Engineering, MARTECH (pp. 183-189).
33. Zaccone, R., Ottaviani, E., Figari, M., & Altosole, M. (2018). Ship voyage optimization for safe and energy-efficient navigation: A dynamic programming approach. Ocean engineering, 153, 215-224.
34. Just In Time Arrival Guide Barriers and Potential Solutions, GloMEEP Project Coordination Unit (IMO), (2020 UK).
35. Hakim, M. L., Nugroho, B., Nurrohman, M. N., Suastika, I. K., & Utama, I. K. A. P. (2019). Investigation of fuel consumption on an operating ship due to biofouling growth and quality of anti-fouling coating. *IOP Conference Series: Earth and Environmental Science*, *339*(1). https://doi.org/10.1088/1755-1315/339/1/012037
36. United Nations. (2015). *Paris Agreement*. https://doi.org/10.4324/9789276082569-2

37. IMO. (2020). Fourth IMO GHG Study 2020 Full Report.
38. Demirel, Y. K., Turan, O., & Incecik, A. (2017). Predicting the effect of biofouling on ship resistance using CFD. Applied Ocean Research, 62, 100–118. https://doi.org/10.1016/j.apor.2016.12.003
39. Schultz, M. P. (2007). Effects of coating roughness and biofouling on ship resistance and powering. Biofouling, 23(5), 331–341. https://doi.org/10.1080/08927010701461974
40. Abarzua, S., & Jakubowski, S. (1995). Biotechnological investigation for the prevention of biofouling . I . Biological and biochemical principles for the prevention of biofouling. 123, 301–312.
41. IMO, GEF, & UNDP. (2022). Biofouling Management for Recreational Boating: Recommendations to Prevent the Introduction and Spread of Invasive Aquatic Species.
42. Song, C., & Cui, W. (2020). Review of Underwater Ship Hull Cleaning Technologies. Journal of Marine Science and Application, 19(3), 415–429. https://doi.org/10.1007/s11804-020-00157-z
43. Degiuli, N., Farkas, A., Martić, I., & Grlj, C. G. (2023). Optimization of Maintenance Schedule for Containerships Sailing in the Adriatic Sea. Journal of Marine Science and Engineering, 11(1). https://doi.org/10.3390/jmse11010201
44. Tadros, M., Vettor, R., Ventura, M., & Guedes Soares, C. (2022). Assessment of Ship Fuel Consumption for Different Hull Roughness in Realistic Weather Conditions. Journal of Marine Science and Engineering, 10(12). https://doi.org/10.3390/jmse10121891
45. Oliveira, D., Larsson, A. I., & Granhag, L. (2018). Effect of ship hull form on the resistance penalty from biofouling. Biofouling, 34(3), 262–272. https://doi.org/10.1080/08927014.2018.1434157.
46. Schultz, M. P., Walker, J. M., Steppe, C. N., & Flack, K. A. (2015). Impact of diatomaceous biofilms on the frictional drag of fouling-release coatings. Biofouling, 31(9), 759–773. https://doi.org/10.1080/08927014.2015.1108407
47. Uzun, Dogancan & Demirel, Yigit & Coraddu, Andrea & Turan, Osman. (2019). Time-dependent biofouling growth model for predicting the effects of biofouling on ship resistance and powering. Ocean Engineering. 191. DOI: 10.1016/j.oceaneng.2019.106432.
48. Kerr, A., Hodgkiess, T., Cowling, M.J., Beveridge, C.M., Smith, M.J., Parr, A.C.S., 1998. A novel technique to prevent bacterial fouling, using imposed surface potential. J. Appl. Microbiol. 85 (6), 1067–1072.
49. Dickon Howell & Brigitte Behrends (2006) A review of surface roughness in antifouling coatings illustrating the importance of cutoff length, Biofouling, 22:6, 401-410, DOI: 10.1080/08927010601035738.
50. Candries, M., 2001. Drag, Boundary Layer and Roughness Characteristics of Marine Surfaces Coated with Antifoulings. University of Newcastle Upon Tyne, Newcastle.
51. Lehaitre, M., Delauney, L., Compere, C., 2008. In: Babin, M., Roesler, C.S., Cullen, J.J. (Eds.), Real-time Coastal Observing Systems for Marine Ecosystem Dynamics and Harmful Algal Blooms: Theory, Instrumentation and Modelling. Unesco Publishing.
52. Cargo hold cleaning: Why it matters. (2018, November 12). SAFETY4SEA.
53. Han, G., Li, J., Chen, Y., Wang, S., & Chen, H. (2023, January 3). Dynamic Modeling and Motion Control Strategy of Cable-Driven Cleaning Robot for Ship Cargo Hold. Journal of Marine Science and Engineering, 11(1), 87. https://doi.org/10.3390/jmse11010087.
54. J-P. Merlet, Parallel Robots, Kluwer publishers, Dordrecht, Holland, 2000.
55. D. Daney and I.Z. Emiris, Robust Parallel Robot Calibration with Partial Information, In Proc. IEEE International Conference in Robotics and Automation (ICRA), 2001, Seoul, S. Korea, pp. 3262--3267.

56. R. Chellal, L. Cuvillon and E. Laroche, "A Kinematic Vision-Based Position Control of a 6-DoF Cable-Driven Parallel Robot," in Cable-Driven Parallel Robots, Bd. 32, Springer International, 2015, pp. 213-225.
57. Kaklis, Dimitrios Varlamis, I., Giannakopoulos, G., Spyropoulos, C., Varelas, T.J., 2022b. Online training for fuel oil consumption estimation: A data driven approach.
58. S. Siami-Namini, N. Tavakoli, and A. S. Namin, "A comparison of arima and lstm in forecasting time series," in 2018 17th IEEE ICMLA. IEEE, 2018, pp. 1394–1401.
59. Kaklis, D., Giannakopoulos, G., Varlamis, I., Spyropoulos, C.D., Varelas, T.J., 2019. A data mining approach for predicting main-engine rotational speed from vessel-data measurements, in: Proceedings of the 23rd International Database Applications & Engineering Symposium, pp. 1–10.
60. J. H. Friedman, "Multivariate adaptive regression splines," The annals of statistics, pp. 1–67, 1991.
61. S. Hochreiter and J. Schmidhuber, "Long short-term memory," Neural computation, vol. 9, no. 8, pp. 1735–1780, 1997.
62. Kaklis, D., Eirinakis, P., Giannakopoulos, G., Spyropoulos, C., Varelas, T.J., Varlamis, I., 2022a. A big data approach for fuel oil consumption estimation in the maritime industry, in: 2022 IEEE Eighth International Conference on Big Data Computing Service and Applications (BigDataService), IEEE. pp. 39–47.
63. IMO. Guidelines and relevant information under MARPOL Annex VI. Note: Guideline 2014 MEPC 866, 30/01/17, pp 136-137 for conversion factors from fuel consumption to CO_2 emissions. 2017.
64. Kaklis, Dimitrios, Takis J. Varelas, Iraklis Varlamis, George Giannakopoulos, Pavlos Eirinakis, Constantine Spyropoulos, 2023. "From STEAM to Machine: Emissions control in the shipping 4.0 era" The 8th International Symposium on Ship Operations, Management & Economics (SOME), 9-12
65. Reid, RE. A Condition and Performance Monitoring System with Application to U.S. Navy Ship Operations. November 1985 https://doi.org/10.1111/j.1559-3584.1985.tb01876.x